AN ABSTRACT OF THE THESIS OF

Yuanhua Shen for the degree of Master of Science in Forest Products presented on November 2, 1995. Title: Evaluation of Creep Behavior of Structural Lumber in a Natural Environment

Signature redacted for privacy.

Abstract approved: _____

Rakesh Gupta

In order to describe long term creep behavior of structural lumber in a natural environment, a bending test with twenty Douglas-Fir beams subjected to a constant load was set up in an open shed in the Forest Research Laboratory at Oregon State University. Deflections of the beams were measured along with daily fluctuations in temperature and relative humidity. An existing five-element creep model was used to predict the creep strain and compared to the experimental data. The model did not predict creep behavior of structural lumber in a natural environment. The general observations showed that stiffness of the beams has a strong influence on the magnitude of creep strain, and the creep strain closely follows the fluctuations in air temperature. The mechano-sorptive creep strain in this experiment is likely to be the shrinking and swelling on the surfaces of the beam and is not tied to the moisture content (MC) of the entire beam, which changed very little over a one year period. Four-element Burger model and power law empirical model were modified to include the stiffness of the beams and air temperature effects. Both models fit the experimental data very well.

Evaluation of Creep Behavior of Structural Lumber in a Natural Environment

by

Yuanhua Shen

A THESIS

submitted to

Oregon State University

in partial fulfillment of
the requirements for the
degree of

Master of Science

Presented November 2, 1995
Commencement June 1996

Master of Science thesis of Yuanhua Shen presented on November 2, 1995

APPROVED:

Signature redacted for privacy.

Major Professor, representing Forest Products

Signature redacted for privacy.

Chair of Department of Forest Products

Signature redacted for privacy.

Dean of Graduate School

I understand that my thesis will become part of the permanent collection of Oregon State University libraries. My signature below authorizes release of my thesis to any reader upon request.

Signature redacted for privacy.

Yuanhua Shen, Author

ACKNOWLEDGEMENTS

I would like to express my sincere thanks to professor Rakesh Gupta, my major advisor. With his beneficial instruction, continuous encouragement and support, this program was able to be completed. I also want to thank professor Thomas H. Miller Department of Civil Engineering, my minor advisor, professor James B. Wilson Department of Forest Products, and professor Goran Jovanovic Department of Chemical Engineering, who served on my committee, and enthusiastically provided their valuable advises to the research. Special acknowledgment to professor Kenneth J. Fridley Department of Civil Engineering, Washington State University, Pullman, WA, as his former studies are the basis for this investigation, and his initial suggestions led the experiment to be more successful. My sincere appreciation is also extended to professor Mike Milota Department of Forest Products for his help on measuring moisture content, and to Valerie Eskelsen, David LaFever, Rand Sether, Milo Clauson and Milan Vatovec, for their assistance in setting up the experiment. The most beneficial tutoring for data logger programming and advise for electrical sensor selection from Mr. Dick Holbo are highly appreciated. I would also like to thank Dr. Robert Ethington, former head of the Department of Forest Products, who offered me the opportunity to pursue my Master's degree in the Department of Forest Products at Oregon State University.

The most important acknowledgement must go to my family. My father, Weihong Shen, and my mother, Zhusheng Teng, have consistently encouraged and supported me to obtain success. My wife, Hongya Chen, and daughter, Aili Shen, have always brought me family warmth and care, although Aili has from time to time during this work not seen much of daddy.

TABLE OF CONTENTS

TABLE OF CONTENTS (Continued)

LIST OF FIGURES

LIST OF FIGURES (Continued)

LIST OF FIGURES (Continued)

LIST OF TABLES

EVALUATION OF CREEP BEHAVIOR OF STRUCTURAL LUMBER IN A NATURAL ENVIRONMENT

I. INTRODUCTION

Wood, as one of the most commonly used construction materials, exhibits notable creep behavior under sustained loads. Creep behavior is defined as the time-dependent deformation exhibited by a material under a constant load (Bodig and Jayne 1982). Figure 1-1 shows a load-time function and a deformation-time function for a simply supported beam under a constant load P. The beam deforms instantaneously when the load is applied, and continuously deforms when the load is held over time. The portion after the instantaneous deformation is termed as creep.

It has been verified that creep behavior of wood has significant effects on the safety and serviceability of wood structures over their design life (Philpot and Rosowsky 1992). Creep of wood members may produce largely irrecoverable deformation, which could eventually result in failure. And the sustained load which causes wood members to fail doesn't have to be larger than the ultimate static load (Schaffer 1972). Both the National Design Specification (NDS) for Wood Construction, and the American Society for Testing and Materials (ASTM), have recommended creep factors for designing wood members (NDS 1991; ASTM 1990). Studies on creep behavior of wood have been conducted for decades (Clouser 1959; Kingston and Armstrong 1951). Most early studies have focused on small, clear wood samples subjected to constant environmental conditions.

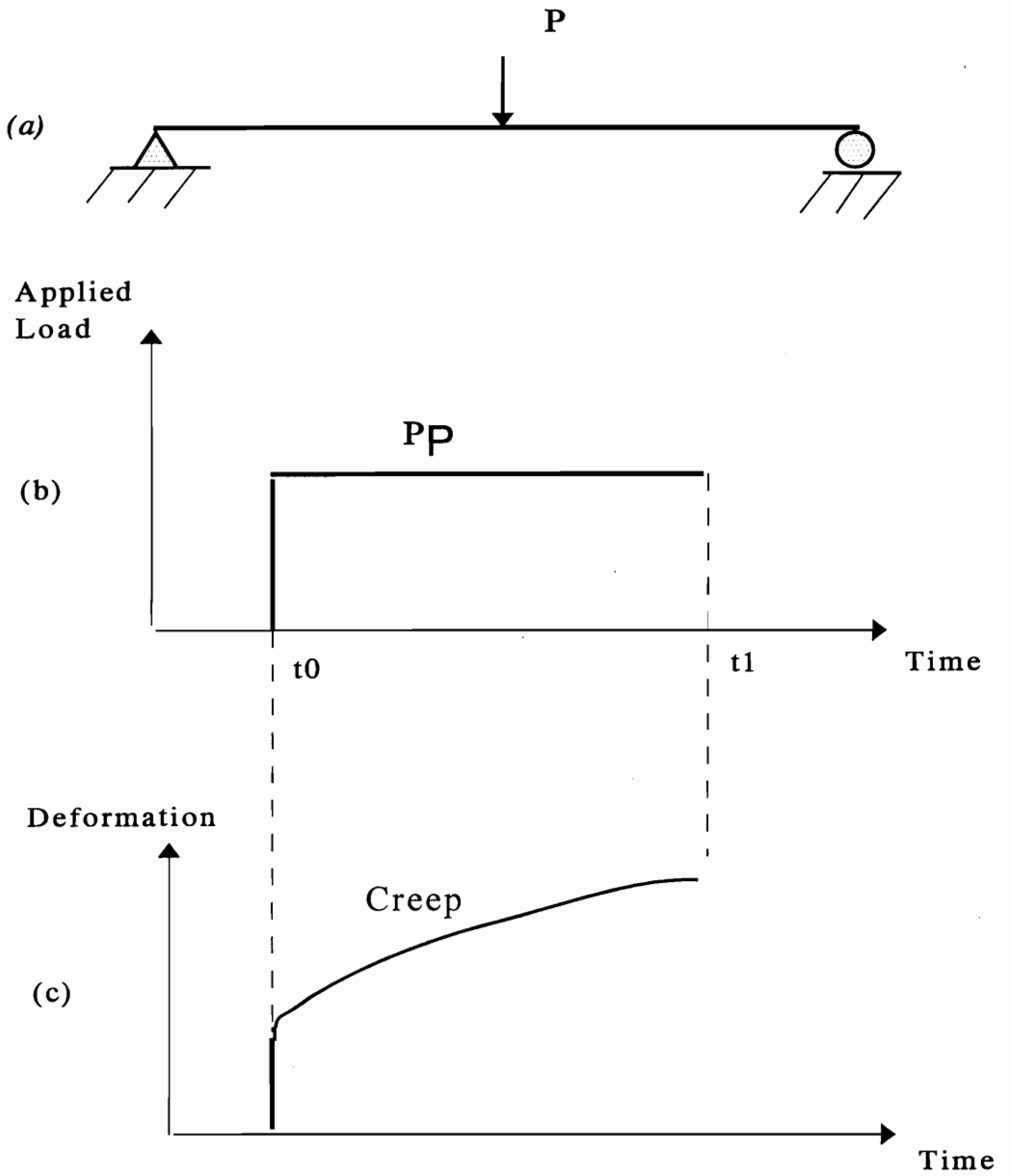

Figure 1-1 (a) Simply Supported Beam System
(b) Load-time Function
(c) Deformation-time Function
(Bodig and Jayne 1982)

However, these studies appear less useful when they are applied to practical utilization of wood, such as, full-size structural lumber used to build houses. Due to the tremendous variabilities associated with the natural defects of wood and the moisture content history, conclusions from small, clear wood samples can not be directly used to interpret behavior of structural lumber applied in a natural environment.

Therefore, more investigations (Fridley et al 1992d; Gerhards 1985, 1988; Hoyle et al 1985) on creep behavior of structural beams have been conducted. It has been discovered that the level of applied loads, time of load duration, moisture content, and temperature are the most critical factors which affect creep behavior of wood. Mechano-sorptive phenomenon has also been discovered when a large change of moisture content in wood occurred under controlled cyclic environmental conditions.

In order to describe creep behavior quantitatively, both empirical and mechanical creep models have been developed. Fridley et al. (1992d) developed a five-element creep model using creep data from commercial size beams subjected to step-constant loads in several different constant environmental conditions. The model is capable of predicting creep behavior of wood beams in controlled cyclic environmental conditions. However, there are not many studies on creep behavior of structural lumber in a natural environment, and neither are there models to predict it.

The main objectives of this study are:

(1) To evaluate creep behavior of structural lumber in a natural environment;

(2) To modify an existing model or develop a new model to describe creep behavior of structural lumber in a natural environment.

II. LITERATURE REVIEW

It has been shown in the literature (Bodig and Jayne 1982; Hoyle et al 1986; Leicester 1971; Gerhards 1985; Fridley et al 1992d) that creep behavior of wood is affected by the level of applied loads, and the ambient environment. Also, creep can be described using both empirical and mechanical models. Each of these will be discussed separately.

2.1 Load Effects

Researchers have found that creep increases with increasing time and with increases in the applied loads (Clouser 1959; Kingston and Armstrong 1951; Bodig and Jayne 1982; Gerhards 1985, 1988, 1991; Pentoney and Davidson 1962; Szabo and Ifju 1970).

Kingston and Armstrong (1951) conducted creep experiments with mountain ash specimens to show the effect of constant loading on the strength and deflection of initially green wooden beams as a function of stress and time. They found that deflection increased with time, and the deflection of beams under load increases at a diminishing rate, however, if failure occurred during this period, deflection continued at an increasing rate. They also disclosed that the larger the applied load was, the faster the failure of the beams.

Gerhards (1985) evaluated the time-dependent deflections of Douglas-Fir 2 by 4 beams tested at three different constant load levels for up to 220 days. He found that the ratio of total deflection to assumed elastic deflection increases with time and also increases when the level of stress increases.

2.2 Hygrothermal Effects

Wood is highly hygroscopic, and any variation in humidity and temperature will affect its moisture content. Because wood properties change with moisture content, several investigators have reported that creep behavior of wood is related to environmental changes (Armstrong and Kingston 1962; Davidson 1962; Fridley et al 1992a, 1992b, 1992c, 1991, 1990a, and 1990b; Hoyle et al 1986; Mohager and Toratti 1993; Molinski and Raczkowski 1988; Pozgaj 1982; Raczkowski 1969; Ranta-Maunus 1975).

Hoyle et al (1986) conducted a creep experiment with 3.5-in. by 3.5-in. Douglas fir beams as specimens. The experiment lasted for about seven weeks under conditions of cyclic relative humidity at 70°F, and with varied environmental equilibrium moisture content (EMC) from 7% to 20% for periods of 24 and 168 hours, respectively. They found that creep for cycled specimens greatly exceeded creep for uncycled specimens.

A similar result has also been obtained by Fridley et al (1991, 1992b). They tested 2 by 4 Douglas fir lumber in bending at relative humidities of 35%, 50%, and 95% with a constant temperature of 73°F, and found a trend toward shorter times-to-failure at higher moisture contents subjected to equal mechanical stress ratios. Then, they conducted the same experiment under two cyclic relative humidity environments: 35% to 95% on 24 and 96 hour cycles with a constant temperature of 73°F. The results indicated a trend toward shorter times-to-failure in cyclic relative humidity conditions compared to constant relative humidity conditions.

Before presenting moisture effects , Fridley et al. (1990a, 1990b) had also performed an experiment on thermal effects on load-duration behavior of lumber. They discovered that as the temperature was increased, the beam failure time was shorter for equal levels of mechanical stress.

2.3 Mechano-Sorptive Effects

In addition to the hygrothermal effects, wood properties are also affected by nonlinear interaction of applied stress and changing moisture content in wood, which are so called mechano-sorptive effects.

Szabo and Ifju (1970) tested 144 small yellow poplar beams under conditions of moisture adsorption and desorption over a period of 10 days. The experimental results showed that the rate of creep in wooden beams under constant load was highest during periods of moisture adsorption and desorption. They further found that the creep component of the total strain in beams under conditions of adsorption was higher than that of beams in desorption.

Leicester (1971) found that the increase in deflection was due more to the change in moisture content than to the passage of time, during the drying of initially green beams under load.

Hoffmeyer (1989, 1990, 1993) conducted two experiments. One included mechano-sorptive bending creep tests using clear wood. Another included an analysis of the longitudinal shrinkage/swelling of structural timber which had earlier been subjected to a mechano-sorptive duration of load experiment. It was found that the intensity of slip planes known as the minute compression failures of

the cell walls, had a linear relationship with creep. In other words, creep is reflected as failures of the cell walls in the micro-structure of wood.

Ranta-Maunus (1990) concluded in the analysis of stresses in timber during long-term loading that the creep rate was higher at the surface layer of timber than in the middle of the cross-section, due to the larger variation of moisture content at the surface.

The creep results of commercial size lumber creep-tested under a controlled cyclic environment, predicted by a five-element model (Fridley et al. 1992d), shows that the creep strain produced by the mechano-sorptive effects is much larger than that from other effects.

Mohager and Toratti (1993) presented long term creep and recovery test results of wood under a constant bending load and subjected to relative humidity cycling. The results showed that the mechano-sorptive deformation was not recoverable, and increased in magnitude when the load duration was increased.

2.4 Creep Models

In addition to studies on the load and environmental effects to creep, investigators have also developed a number of models to describe creep phenomenon quantitatively. In general, there are two types of creep models (Holzer et al 1989), the empirical models and the mechanical models.

Empirical models are obtained by fitting mathematical equations to experimental data (Clauser 1959; King 1961; Bach and Pentoney 1968; Schniewind and Barrett 1972; Hoyle et al. 1985; Gressel 1984; Gerhards 1985). The so-called

power law is the most commonly used empirical equation for creep strain and is shown as follows:

$$\varepsilon(t) = \varepsilon_e + bt^n \quad \ldots\ldots (2\text{-}1)$$

where $\varepsilon(t)$ = total creep strain at time t; ε_e = elastic strain; b, n = model constant.

Mechanical models are composed of springs and dashpots, which are used to simulate the creep behavior of wood (Grossman and Kingston 1954; Davidson 1962; Bhatnagar 1964; Ylinen 1965; Senft and Suddarth 1971; Leicester 1971; Mukudai 1983a, 1983b; Mukudai and Yata 1986, 1987, 1988; Fridley et al 1992d). The most widely applied mechanical model is the Burger body, which is composed of a Maxwell and a Kelvin body in series, shown in Figure 2-1 (Bodig and Jayne 1982).

The corresponding mathematical expression for the Burger model is:

$$\varepsilon(t) = \frac{\sigma}{K_e} + \frac{\sigma}{K_k}\left[1 - \exp\left(-\frac{K_k t}{\mu_k}\right)\right] + \frac{\sigma t}{\mu_v} \quad \ldots\ldots (2\text{-}2)$$

where, σ = the applied stress; K_e = the Hookean spring constant associated with elastic deformation (i.e., modulus of elasticity); K_k and μ_k = the Hookean spring constant and viscosity of the Newtonian dash pot, respectively, of the Kelvin element, and μ_v = the viscosity of the Newtonian dashpot associated with unrecoverable strain.

The empirical models can work well over time domains, whereas, the mechanical models are only valid over the time span for which the parameters are

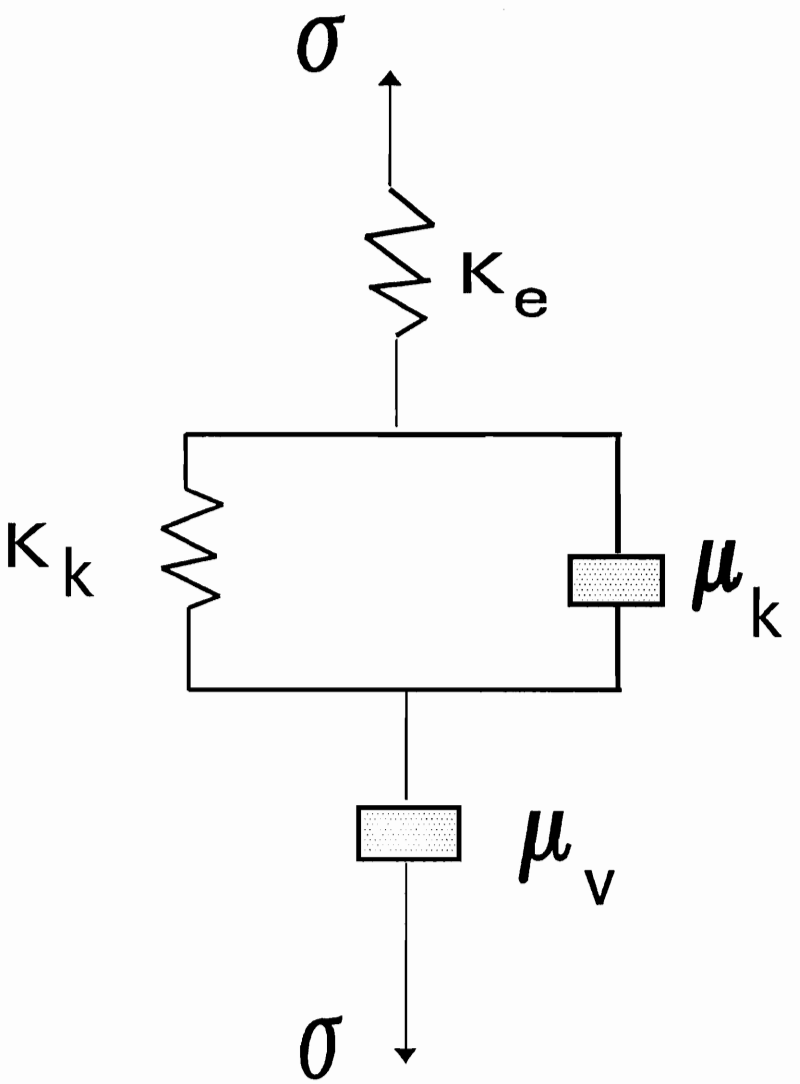

Figure 2-1 The Burger Model (Bodig & Jayne 1982)

determined (Holzer et al. 1989). Also, the empirical models are applicable to only constant-load histories (Gerhards 1985; Hoyle et al 1985, 1986).

2.4.1 Models for small and clear samples

Wood is a biological material with large variabilities. In order to exclude the natural defects of wood, such as knots, irregular grain, and pitch pockets, early investigators preferred to use small, clear wood samples in their studies.

Schniewind and Barrett (1972) conducted several creep experiments under a controlled environment, with small and clear samples with different grain angles. They used a power law to fit the experimental data, and found that there were more differences between experimental data and the fitted results by plotting relative instead of total creep. They suggested a series of exponential terms might be more suitable for tests extending over a longer time.

Senft and Suddarth (1971) used the four-element Burger model and the three-element model (a Kelvin body plus an elastic spring) to describe creep responses for small specimens of Sitka spruce under a constant environment. They discovered that the three-element model fit short-term creep data accurately, but for time periods of 24 hours or longer, they suggested the use of the four-element model, particularly at higher stress levels.

2.4.2 Models for structural lumber

Since the study results of creep from small and clear wood samples can not be used directly for full-size beams, more investigations on creep behavior of full-size structural lumber have been conducted.

2.4.2.1 Constant environmental conditions

Hoyle et al (1985) used a power law to predict the creep responses of 4-in. by 4-in. Douglas-Fir beams under four constant levels of stress, at 12% moisture content. They found that a power law did describe primary creep (the creep region in which the rate of deformation is decreasing) during the first 400 hours of sustained load, and relative creep (creep without portion of elastic deformation) was nearly independent of stress level. They also found that relative creep was larger for the beams with lower modulus of elasticity.

Gerhards (1985) had Douglas-Fir 2-in. by 4-in. beams creep-tested at three different constant load levels for up to 220 days, and used a power law to model creep. He found that the results from the power law model showed that relative creep rate for lumber was less than the relative creep rate for small clear wood specimens.

2.4.2.2 Controlled cyclic environmental conditions

Under controlled cyclic temperature and relative humidity conditions, a large change of moisture content in wood takes place, and creep of wood will be largely contributed by mechano-sorptive deformation (Leicester 1971; Fridley et al. 1992d)

Leicester (1971) developed a first approximation rheological model for mechano-sorptive deflection by tests on small messmate stringybark beams. The model is composed of two elements in series, illustrated in Figure 2-2 (Leicester 1971).

Functions associating an elastic component Δ_e and a mechano-sorptive component Δ_m with the load parameter P are presented below (Leicester 1971):

$$\Delta=\Delta_e+\Delta_m \quad \ldots\ldots (2\text{-}3)$$

$$\Delta_e=KP \quad \ldots\ldots (2\text{-}4)$$

$$-\frac{d\Delta_m}{dm}=Pf(m) \quad \ldots\ldots (2\text{-}5)$$

where, Δ=total deflection; m = the average moisture content of the beam; K = a constant and f(m) = a function of moisture content. Deformation described by equation (2-5) is termed as irrecoverable mechano-sorptive deformation. The results from the experiment illustrated that during the initial drying about 85% of the total deformation was attributable to the first approximation rheological model.

2.4.3 A five-element creep model

Fridley et al. (1992d) presented a five-element model, which was based on the four-element Burger model with a fifth mechano-sorptive element added. Figure 2-3 shows the mechanical structure of the five-element model. The model was developed based on creep experiments of 2-in. by 4-in. Douglas-Fir specimens subjected to constant and step-constant loads, under several constant environmental conditions and controlled cyclic environmental conditions. During the experiments, since either temperature or relative humidity was cycled while the other was held constant, and the cycle was up to 96 hours, a large change of moisture content was

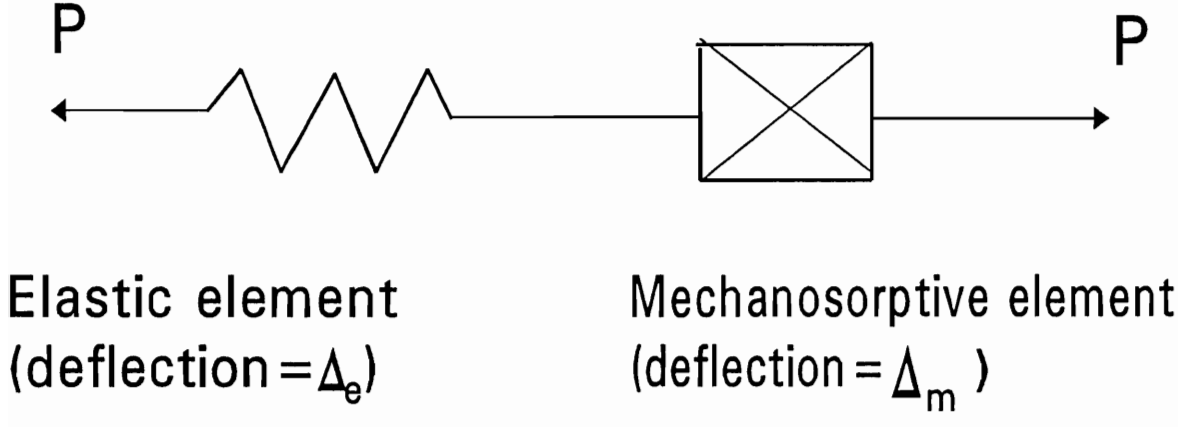

Figure 2-2 A First Approximation Rheological Model (Leicester 1971)

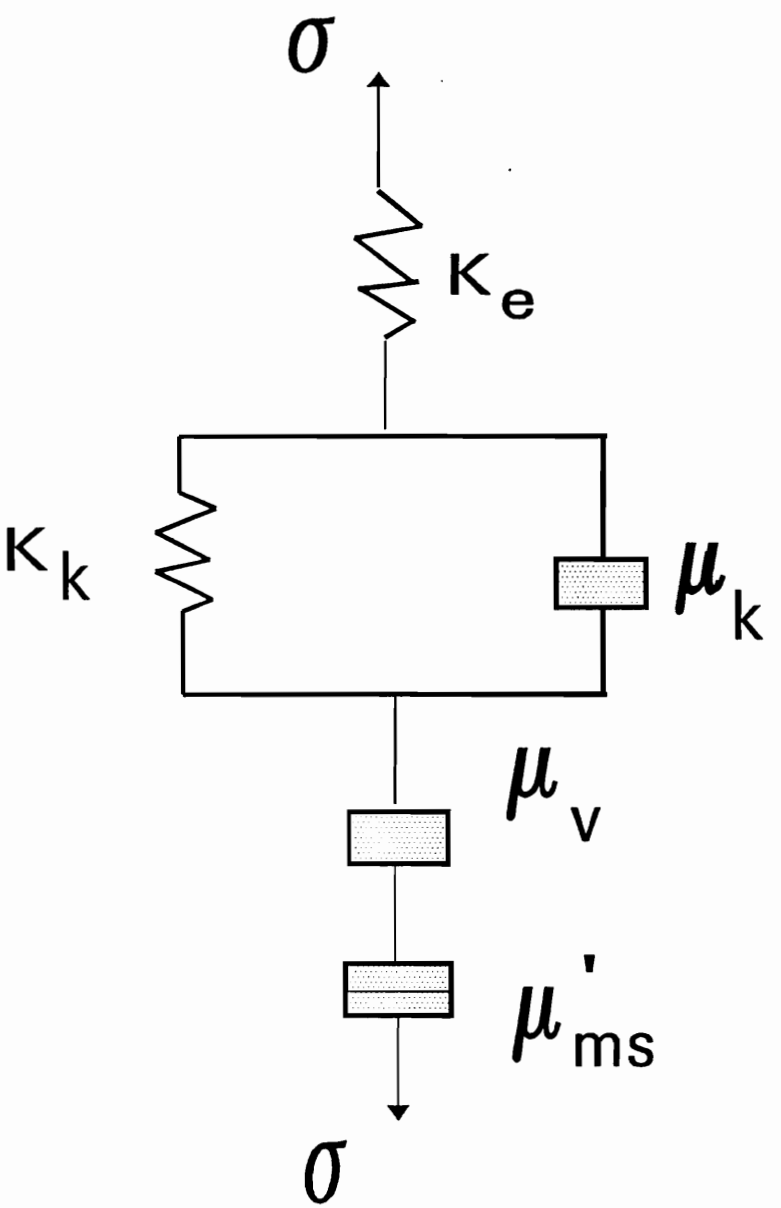

Figure 2-3 The Five-Element Model (Fridley et al. 1992d)

observed to take place in the wood. Mechano-sorptive deformation, therefore, became the dominant contributor to the time-dependent deformation.

The five-element creep model (Fridley et al.1992d) was capable of predicting load and environmental effects, as well as mechano-sorptive effects stochastically for the first two stages of creep behavior. The function for the total strain, $\varepsilon(t)$, at time t, under a constant stress, σ, is as follows:

$$\varepsilon(t) = \frac{\sigma}{K_e} + \frac{\sigma}{K_k}[\,1 - \exp\,(-\frac{K_k t}{\mu_k})\,] + \frac{\sigma t}{\mu_v} + \frac{\sigma}{\mu'_{ms}}|\Delta w|[\,1 - \exp\,(-B_w t)\,] \quad \ldots\ldots (2\text{-}6)$$

where, K_e =the Hookean spring constant associated with elastic deformation(i.e., modulus of elasticity); K_k and μ_k =the Hookean spring constant and viscosity of the Newtonian dash pot, respectively, of the Kelvin element; μ_v=the viscosity of the Newtonian dashpot associated with unrecoverable strain; μ'_{ms}=a constant with units of force per unit area, estimated using an iterative best-fit procedure, and determined as 3.78×10^6 psi for the mean value; $\Delta w = w_e - w_i$, w_e= the eventual equilibrium moisture content in the new environment, w_i = the initial moisture content in the original environment; B_w = constant associated with the time required to achieve moisture equilibrium. B_w is dependent on the size of the member and can vary if the change in moisture content is positive or negative. For example, moisture absorption and desorption can occur at different rates and B_w should reflect this fact. However, B_w is assumed constant for simplicity in modeling. Determined experimentally, B_w is 7.85×10^{-5} min^{-1}.

The four Burger model parameters, K_e, K_k, μ_k, and μ_v were modified to include moisture and temperature effects, using the following equations:

$$K_e(w, \theta) = K_{e_0}(1 + D_1 w + D_2 w^2 + D_3 \theta + D_4 \theta^2) \ldots\ldots (2\text{-}7)$$

$$K_k(w, \theta) = K_{k_0}(1 + D_5 w + D_6 w^2 + D_7 \theta + D_8 \theta^2) \ldots\ldots (2\text{-}8)$$

$$\mu_k(w, \theta) = \mu_{k_0}(1 + D_9 w + D_{10} w^2 + D_{11} \theta + D_{12} \theta^2) \ldots\ldots (2\text{-}9)$$

$$\mu_v(w, \theta) = \mu_{v_0}(1 + D_{13} w + D_{14} w^2 + D_{15} \theta + D_{16} \theta^2) \ldots\ldots (2\text{-}10)$$

$$w = \frac{M - M_0}{M_0} \ldots\ldots (2\text{-}11)$$

$$\theta = \frac{T - T_0}{T_0} \ldots\ldots (2\text{-}12)$$

where K_{e0}, K_{k0}, μ_{k0}, and μ_{v0} = the model parameters in the reference condition (i.e., $w = \theta = 0$); D_1---D_{16}=model constants; w = a relative moisture content factor; M = the actual moisture content; M_0 = a reference moisture content; θ = a relative temperature factor; T = the actual temperature; and T_0=a reference temperature.

The mechano-sorptive element was based on the assumption of a function related to the time rate of change of the moisture content factor as a predictor of mechano-sorptive creep effects. The function is shown as follows:

$$d\varepsilon_{ms} = \frac{\sigma}{\mu_{ms}} = \frac{\sigma |dw|}{\mu'_{ms}} \quad \ldots\ldots (2\text{-}13)$$

where $d\varepsilon_{ms}$ = the rate of mechano-sorptive strain ; dw = the rate of change in the moisture factor with units of inverse time; μ_{ms}=the viscosity of the mechano-sorptive element; μ'_{ms}=a constant with units force per unit area. It was assumed that the viscous parameter would have the following relationship with the moisture factor:

$$\mu_{ms} = \frac{\mu'_{ms}}{|dw|} \quad \ldots\ldots (2\text{-}14)$$

To apply (2-13), a function for the average moisture content factor of a specimen following an abrupt change in the surrounding environment was assumed:

$$w(t) = w_e + (w_i - w_e) \exp(-B_w t) \quad \ldots\ldots (2\text{-}15)$$

where w(t) = the average moisture content factor of the member at a time t following the environmental change; w_e= the eventual equilibrium moisture content in the new environment; w_i= the initial moisture content in the original environment; and B_w = constant associated with the time required to achieve moisture equilibrium. The derivative of (2-15) with respect to time is:

$$dw(t) = B_w(w_e - w_i)\exp(-B_w t) \ldots\ldots (2\text{-}16)$$

For a constant load, (2-13) could be integrated as follows to yield the total mechano-sorptive stain, ε_{ms}:

$$\varepsilon_{ms}(t) = \frac{\sigma}{\mu'_{ms}} |\Delta w|[1 - \exp(-B_w t)] \ldots\ldots (2\text{-}17)$$

where $\Delta w = w_e - w_i$.

So far, a creep experiment of full-size structural beams has not been conducted under a natural environment. It is the intention of this study to carry out this experiment and evaluate creep behavior of full-size structural lumber under a natural environment.

III. MATERIALS AND METHODS

3.1 Specimens

Twenty, No.2 grade, Douglas-Fir beams (1.5-in. by 3.5-in. by 8-ft.), specially selected from a local lumber mill (Frank Lumber Co., Mill City, Oregon), are used as specimens for the creep test. The original length of all the beams was 14 feet. The beams were then cut into 8-foot long specimens with the worst defect within the load span. The MOE of all the specimens was measured both in edge-wise (E_e) and flat-wise (E_f) static bending. The dynamic MOE (E_c) for all specimens was also measured using a Metriguard Model 340 E-computer, and the specific gravity of each specimen was also obtained from the E-computer output. All measurements were taken when the specimens were at 11% moisture content. The basic properties and characteristics of all specimens, such as dimensions, modulus of elasticity (MOE), specific gravity, and critical defects are listed in Table 3-1.

The specimens were sorted into five test groups from A to E based on their modulus of elasticity (MOE) and specific gravity. There are four specimens in each group. Within each group, specimens have similar ranges of MOE and specific gravity. Group A has the lowest MOE, and group E has the highest MOE.

One extra specimen is used for determining moisture content. All specimens were initially conditioned (20°C and RH 69%) to 11% moisture content.

Table 3-1 Initial Parameters of Specimens

Group	Specimen Number	Width (in.)	Depth (in.)	Length (ft.)	Modulus of Elasticity(10^6psi)			Weight (lbs.)	MC (%)	Specific Gravity	Defects in Load Span
					Ef.	Ee.	Ec.				
	02A1	1.505	3.511	8.0	1.28	1.07	1.42	8.973	11	0.491	CK
	01A3	1.509	3.516	8.0	0.98	0.97	1.10	7.231	11	0.395	CK
A	03A4	1.513	3.508	8.0	1.22	0.95	1.39	9.017	11	0.496	BEK
	04A5	1.489	3.457	8.0	1.23	0.93	1.33	8.179	11	0.446	CEK
	17B2	1.513	3.538	8.0	1.32	0.98	1.50	8.708	11	0.481	TEK
	19B3	1.506	3.519	8.0	1.43	1.19	1.51	9.237	11	0.506	CEK
B	18B4	1.502	3.511	8.0	1.38	1.21	1.45	8.620	11	0.468	CK
	20B5	1.519	3.520	8.0	1.46	1.30	1.51	8.267	11	0.444	CK
	13C1	1.516	3.530	8.0	1.71	1.47	1.89	9.854	11	0.593	CK
	14C2	1.514	3.529	8.0	1.56	1.15	1.70	9.766	11	0.537	CEK
C	16C4	1.512	3.515	8.0	1.50	1.65	1.59	9.237	11	0.505	CK
	15C5	1.517	3.530	8.0	1.56	1.27	1.64	9.083	11	0.487	CK
	05D2	1.512	3.515	8.0	1.90	1.89	1.96	9.877	11	0.528	NONE
	06D3	1.505	3.517	8.0	1.83	1.42	1.98	10.317	11	0.566	BEK
D	07D5	1.518	3.537	8.0	1.79	1.35	2.08	10.163	11	0.557	BEK
	08D8	1.521	3.510	8.0	1.81	1.68	2.10	9.832	11	0.536	CK
	09E2	1.508	3.515	8.0	2.31	1.71	2.57	10.979	11	0.603	CK(hole)
	10E3	1.509	3.515	8.0	2.18	1.96	2.37	10.053	11	0.552	BEK
E	11E4	1.518	3.515	8.0	2.15	1.61	2.52	10.670	11	0.592	TEK(hole)
	12E7	1.526	3.539	8.0	2.06	1.53	2.26	10.406	11	0.564	CEK

MOE = Modulus of Elasticity; Ef = Flatwise MOE; Ee = Edgewise MOE; Ec = Dynamic MOE;
MC = Moisture Content; CK = Centerline Knot; BEK = Edge Knot at both compression and tension zones;
CEK = Edge knot at compression zone; TEK = Edge knot at tension zone.

3.2 Applied Load

In order to observe long term creep behavior of wood under a natural environment, the applied constant loads, under a condition of two equal loads applied symmetrically on a beam, were chosen at a low level. The applied loads for all the specimens were determined in terms of a deflection limits of L/360 (where L= the span) using the following equation (Western woods use book 1973):

$$P=\frac{24EIL}{360\,a(3L^2-4a^2)} \quad \ldots\ldots (3\text{-}1)$$

Where, P = half of the total load applied; L = 7 feet span; a = 2.5 feet from the load point to the nearest support; E = 1,600,000 psi (NDS 1991); I = 5.359 $in.^4$ (moment of inertia). This equation yields a total load of 182 lbs. However, due to the limitation of the capacity of loading equipment, we chose 150-pound of total load as the applied load in the experiment for every specimen. The average applied stress level is about 6% of modulus of rupture (MOR) (Wood Handbook 1987). Since MOR for each specimen is not available, the applied stress level (percentage of the ultimate strength) may be different for each specimen due to the variation in MOR. All dead loads weighed 75 pounds each and were made by filling gravel into laminated plastic vinyl cylindrical containers.

3.3 Sensors

Three different types of sensors are used for taking all measurements in the experiment. Twenty deflection sensors, linearly variable resistors, are used to

measure deflections for all the specimens. The linearity of the sensors has been calibrated by measuring the voltage from the two ends of the resistors under a normal room temperature before they are used in the experiment. Five measurements were taken for each sensor by changing the length of the resistor. The linear relationship between the voltage and the length of the resistor is calculated using the five measured data for each sensor. The calibration coefficients for each sensor are listed in Table 3-2.

Table 3-2 Calibration Coefficients for Deflection Sensors

Specimen	Coefficient (10^{-4}, mV/in)	Specimen	Coefficient (10^{-4}, mV/in)
01A3	2.704	11E4	2.706
02A1	2.726	12E7	2.773
03A4	2.707	13C1	2.706
04A5	2.726	14C2	2.677
05D2	2.728	15C5	2.759
06D3	2.740	16C4	2.743
07D5	2.730	17B2	2.709
08D8	2.702	18B4	2.710
09E2	2.706	19B3	2.761
10E3	2.716	20B5	2.734

However, this type of sensor is somewhat sensitive to temperature changes, and it may not be suitable for using under an uncontrolled environment. A detail description on how the sensor affects the accuracy of deflection measuring was presented in Appendix C.

An Omega Engineering LCCA-25 (OMEGA) load cell is used to monitor the change of weight of the moisture content sample beam. According to the

calibration certificate issued by the company, the load cell has a full scale output of 3.000 mV/V, and a capacity of 25 lbs. The operating temperature range is from 0° to 66° C.

A Campbell Scientific, Inc. HMP-35C temperature and relative humidity probe (Campbell Scientific, Inc.) is used to detect the temperature and relative humidity of the ambient environment. According to the calibration certificate issued by the company, the measurement range for the relative humidity sensor is from 0 to 100% with accuracy from +/- 1% to +/- 3%; for the temperature sensor, the working range is from -40 to 60° C with accuracy from +/- 0.5° C to +/- 0.4° C. The operating temperature for the relative humidity sensor is from -20 to 60° C.

In order to determine how temperature on the surface of the specimen varies with respect to air temperature, two thermocouples were attached to the top and bottom of the moisture content sample beam.

3.4 Method

The experiment was conducted under a shed outside the Forest Research Laboratory (FRL) at Oregon State University. The schematic of the set-up with one beam is shown in Figure 3-1. A picture of the set-up is shown in Figure 3-2. A Campbell Scientific Inc. 21X Micrologger is used to record all data taken by the sensors during the experimental period. The load cell and the temperature and relative humidity probe are connected directly to the data logger. Due to the insufficient number of channels on the data logger, a multiplexer is also used to

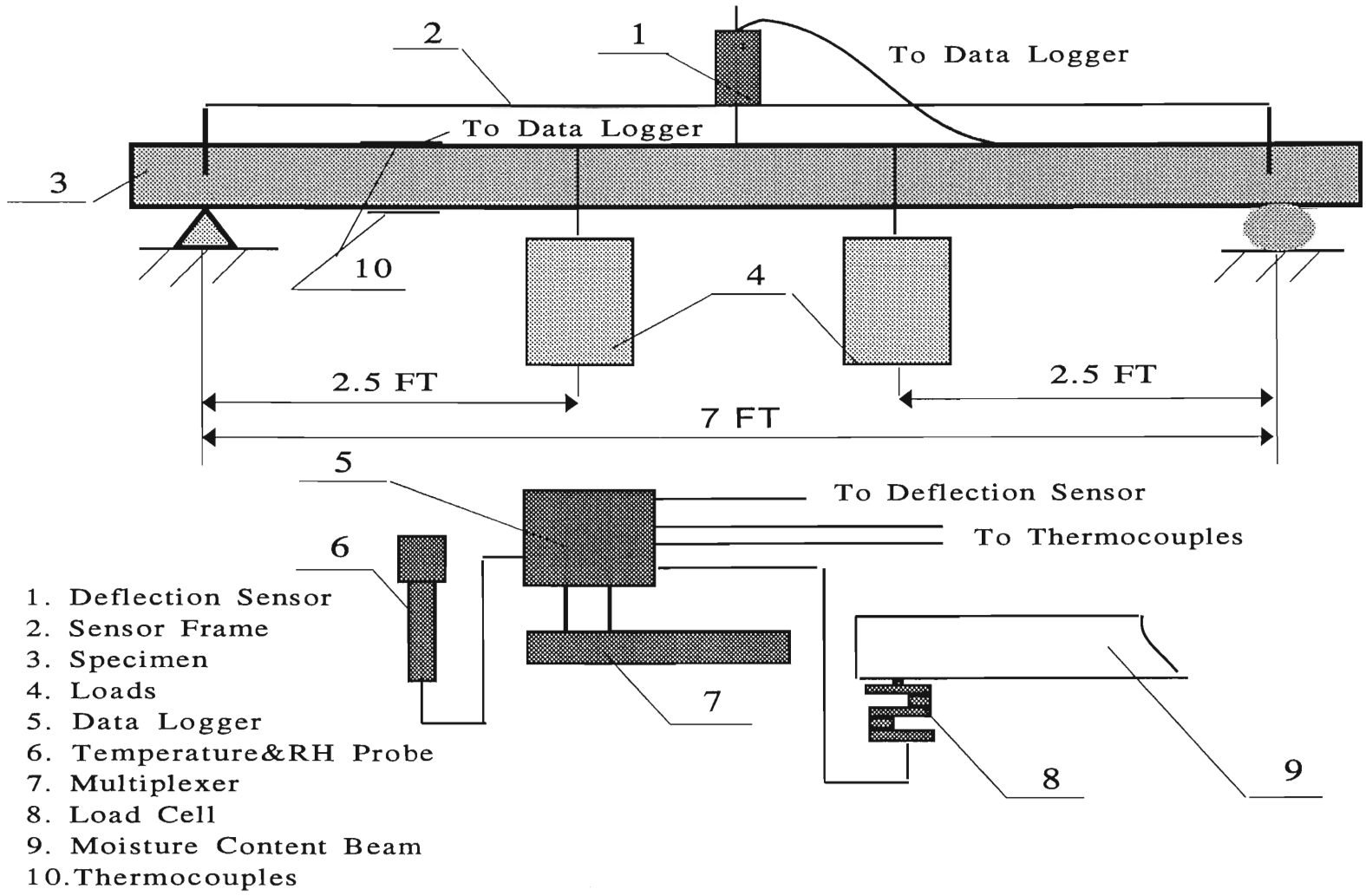

Figure 3-1 Creep Experiment Set-Up (Schematic)

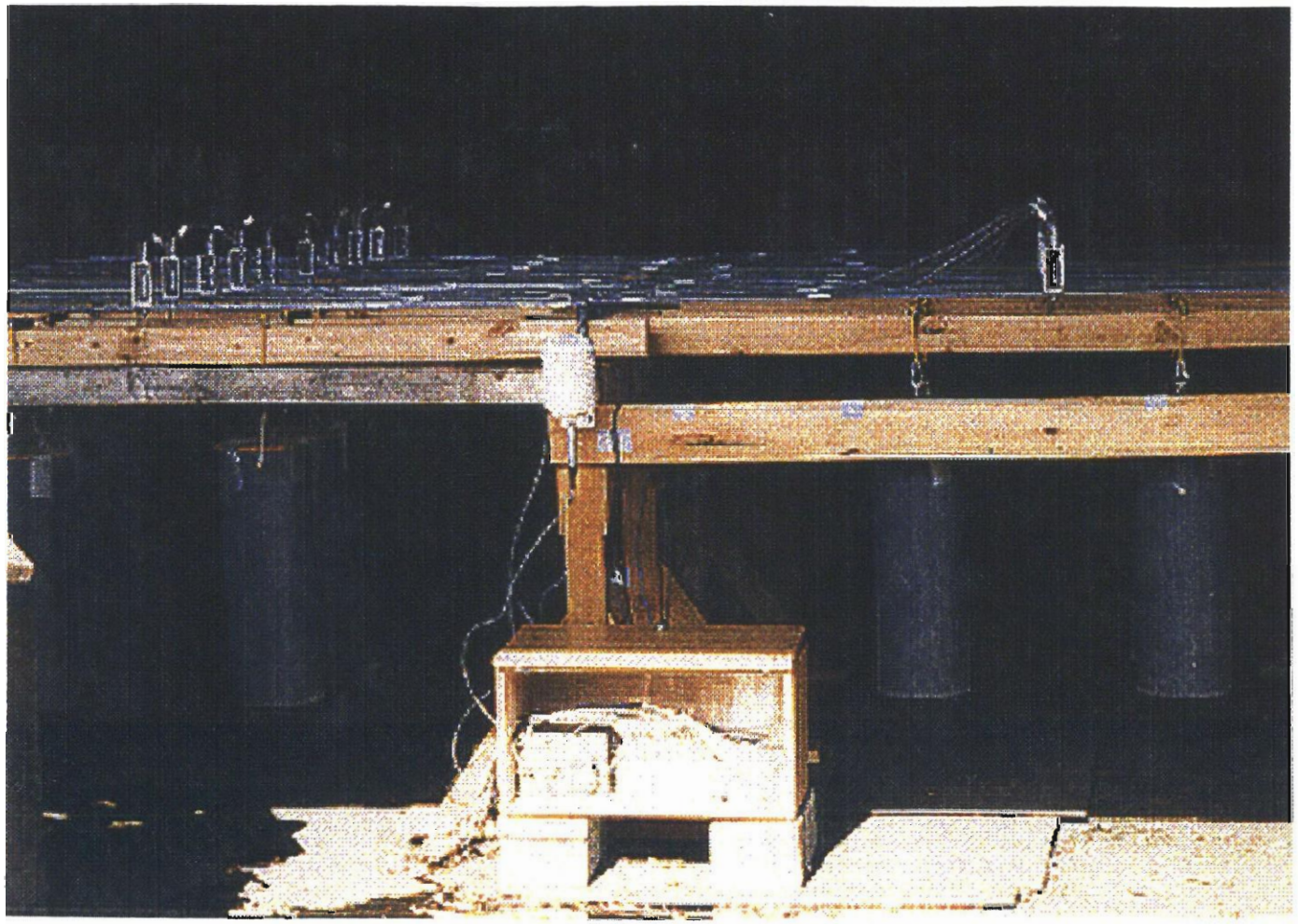

Figure 3-2 Creep Experiment Set-Up

connect the twenty deflection sensors with the data logger. The data logger was programmed before being used in the experiment. All programs for the data logger are listed in Appendix A.

All twenty one specimens have been weighed and were assumed to have the same moisture content (11%) as the controlled room (20°C and RH 69%) before they were taken to the experimental location. A hydraulic pallet truck was used to load the specimens one by one. The initial deflection readings were taken every second, and this reading condition lasted for an hour after loading for every specimen had been completed. Then, the deflection readings were taken once every hour. The recorded data were down-loaded using a portable computer every two weeks. Temperature, relative humidity, and weight of the moisture content beam can be directly read from the data logger. The experiment is still continuing, but this thesis presents data from April 1994 to June 1995 for about 10,000 hours.

IV. DATA ANALYSIS

4.1 Deflection and Strain Calculation

The raw data from the deflection sensors, recorded by the data logger, were the voltages. They were converted into deflections (in inches) using calibration coefficients listed in Table 3-2.

Creep behavior is generally described using strain in most previous research efforts. Deflections, in this study, are very small due to the low level of applied load. Figure (4-1) shows the deformed shape of a simply supported beam subjected to two symmetric loads. The deformation from the applied-load point to the support is assumed to be a straight line. And the deformed shape between the two applied loads is a section of a circle due to the pure bending condition imposed. Figure (4-1) is a description of the experimental situation. According to Kassimali (1993), the longitudinal normal strain (for small θ) is given by:

$$\varepsilon = -\frac{y}{\rho} \quad \ldots\ldots (4-1)$$

where, ε = normal strain under pure bending; y = 1.75 in. (the distance from the neutral surface); ρ = radius of curvature. Based on Figure (4-1), δ can be determined as:

$$\delta = 30 * \tan\theta + \rho * (1 - \cos\theta) \quad \ldots\ldots (4-2)$$

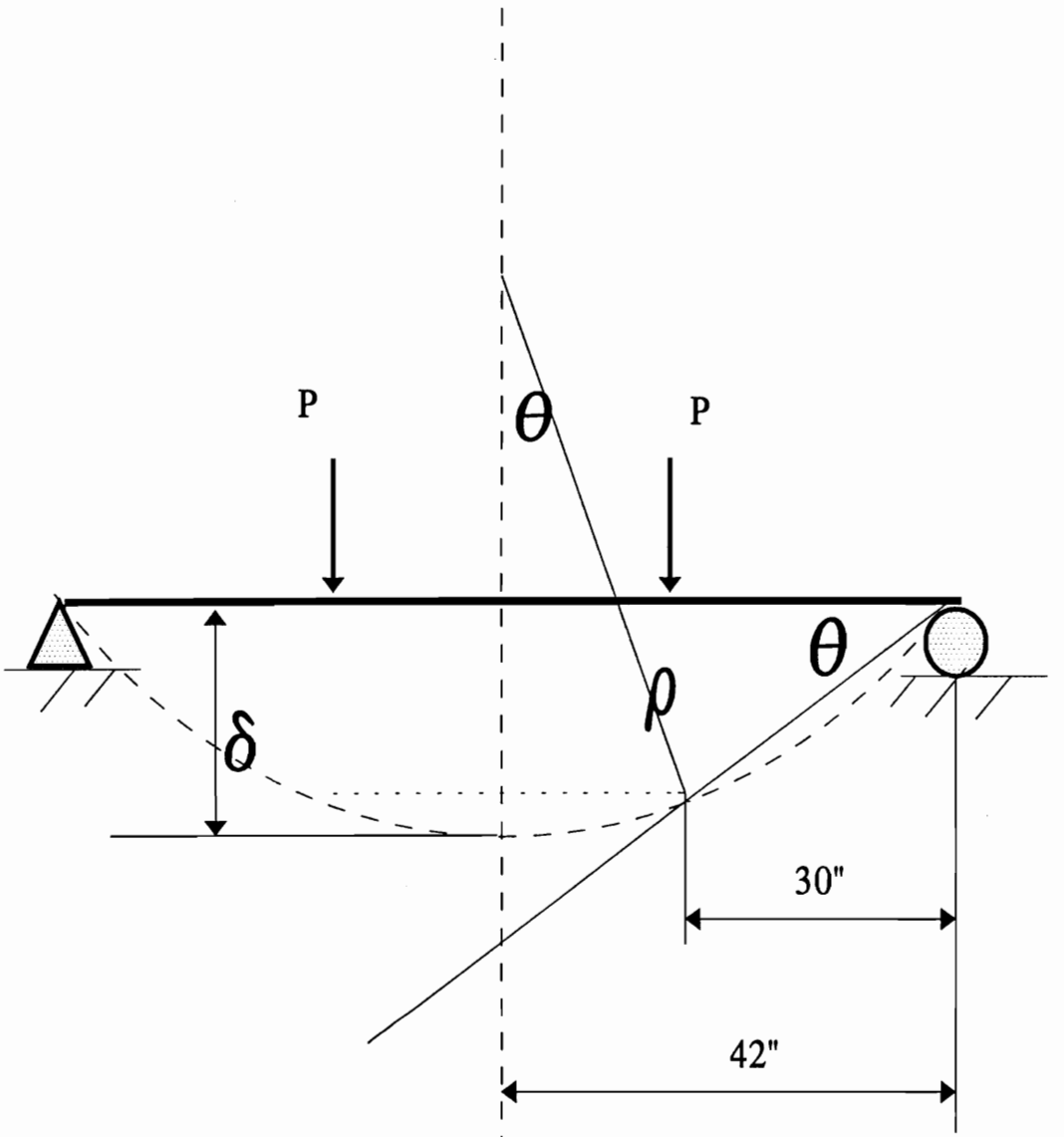

Figure 4-1 Geometrical Relationship
between Deflection and Curvature

$$\tan\theta = \frac{12}{\rho * \cos\theta} \quad \ldots\ldots (4\text{-}3)$$

as θ is small, $\cos\theta \approx 1$,

$$\rho \approx \frac{360}{\delta} \quad \ldots\ldots (4\text{-}4)$$

Using equations (4-1) to (4-4), the following linear relationships between strain, ε, and deformation, δ, is derived:

$$\varepsilon \approx 0.0049 * \delta \quad \ldots\ldots (4\text{-}5)$$

This linear relationship is used for all conversion between strain and deformation in the following data processing. The total strain therefore is obtained from the recorded deflection using equation (4-5).

4.2 Data Reduction

There are twenty-four deflection measurements per specimen for each day, as reading are taken every hour. In order to process the data using QuattroPro (Burns 1993) and not lose any characteristic points, the twenty-four points were reduced to four points for each specimen every day, using the following rules.

Two points were selected based on the corresponding daily maximum and minimum temperature. The other two points were selected from the daily maximum and minimum measurements of deflection. Table 4-1 shows the full data

and Table 4-2 shows the corresponding reduced data for one beam for one day. Figure 4-2 shows time-dependent deflection curves for one month of data in full, reduced and moving average status.

It is observed from Figure 4-2 that the curve of the reduced data is completely identical to that of the full data. The 14-point moving average curve based on the reduced data shows a smoother curve and the same trend as the full data curve. Therefore, the data reducing rules and the moving average method were applied for all data processing and plotting thereafter.

4.3 Creep Strain

Creep strain is obtained using what total strain minus elastic strain. The elastic strain is calculated from the recorded deflection at three seconds after a specimen is loaded, using the linear relationship between deformation and strain (equation 4-5). According to Bodig and Jayne (1982), elastic strain occurs instantaneously as the load is applied. In this experiment, however, there was a time difference between the two loads being applied on the beam. This time difference will delay the specimens to reach the elastic deformation under the full load.

A power law (equation 2-1) is introduced to fit the data showing average creep behavior of the nineteen specimens under a natural environment, in order to determine maximum creep strain under an average condition for each specimen. The data for one of the specimens was somehow misrecorded. The sample was therefore excluded from the experiment.

Table 4-1 One Day Full Data

Time(hrs)	Deflection in mV	Temperature(°C)	RH%
1	3545	24.46	35.10
2	3545	23.72	37.45
3	3545	22.72	40.20
4	3545	21.51	43.71
5	3546	20.19	48.78
6	3546	18.30	56.58
7	3548	16.94	64.28
8	3559	16.85	66.30
9	3563	16.70	67.14
10	3563	16.67	68.87
11	3568	16.82	69.59
12	3568	16.21	71.10
13	3568	13.72	77.70
14	3548	11.73	83.50
15	3501	11.35	85.80
16	3509	16.32	70.90
17	3509	22.38	49.94
18	3510	21.15	52.71
19	3509	22.13	48.99
20	3509	23.16	45.99
21	3507	24.63	41.24
22	3488	25.97	37.35
23	3479	26.91	34.33
24	3479	27.79	30.47

The procedure for fitting a power law function is as follows:

The power law (equation 2-1) can be linearized through a logarithmic transformation so that b and n can be determined using the linear regression program in Quattro Pro (Burns 1993).

Table 4-2 One Day Reduced Data

Conditions	Time(hrs)	Deflection in mV	Temperature(°C)	RH%
Max. Deflections	13	3568	13.72	77.70
Min. Temperature	15	3501	11.35	85.80
Min. Deflections	23	3479	26.91	34.33
Max. Temperature	24	3479	27.79	30.47

$$\ln(\varepsilon_t - \varepsilon_e) = \ln(b) + n * \ln(t) \ldots\ldots (4-6)$$

$$Y = A + BX \ldots\ldots (4-7)$$

where, ε_t = total creep strain at time t; ε_e = elastic strain (at three seconds); b, n = model constants; Y = dependent variable = $\ln(\varepsilon_t - \varepsilon_e)$; X = independent variable = ln(t); A = intercept = ln(b); B = slope = n.

When the constants, b and n, are obtained using the regression procedures, average creep strain of beams under a natural environment is calculated using the power law. In addition, the deformation of every specimen under the constant load condition is also calculated using the following equation (4-8). The MOE values used in equation (4-8) are the E_e value from Table 3-1.

$$\delta = \frac{Pa}{24EI}(3L^2 - 4a^2) \ldots\ldots (4-8)$$

where, P = 75 lbs., half of the total load applied; L = 7 feet span; a = 2.5 feet from each load point to the nearest support; E = E_e from Table 3-1; I = 5.359 $in.^4$ (moment of inertia).

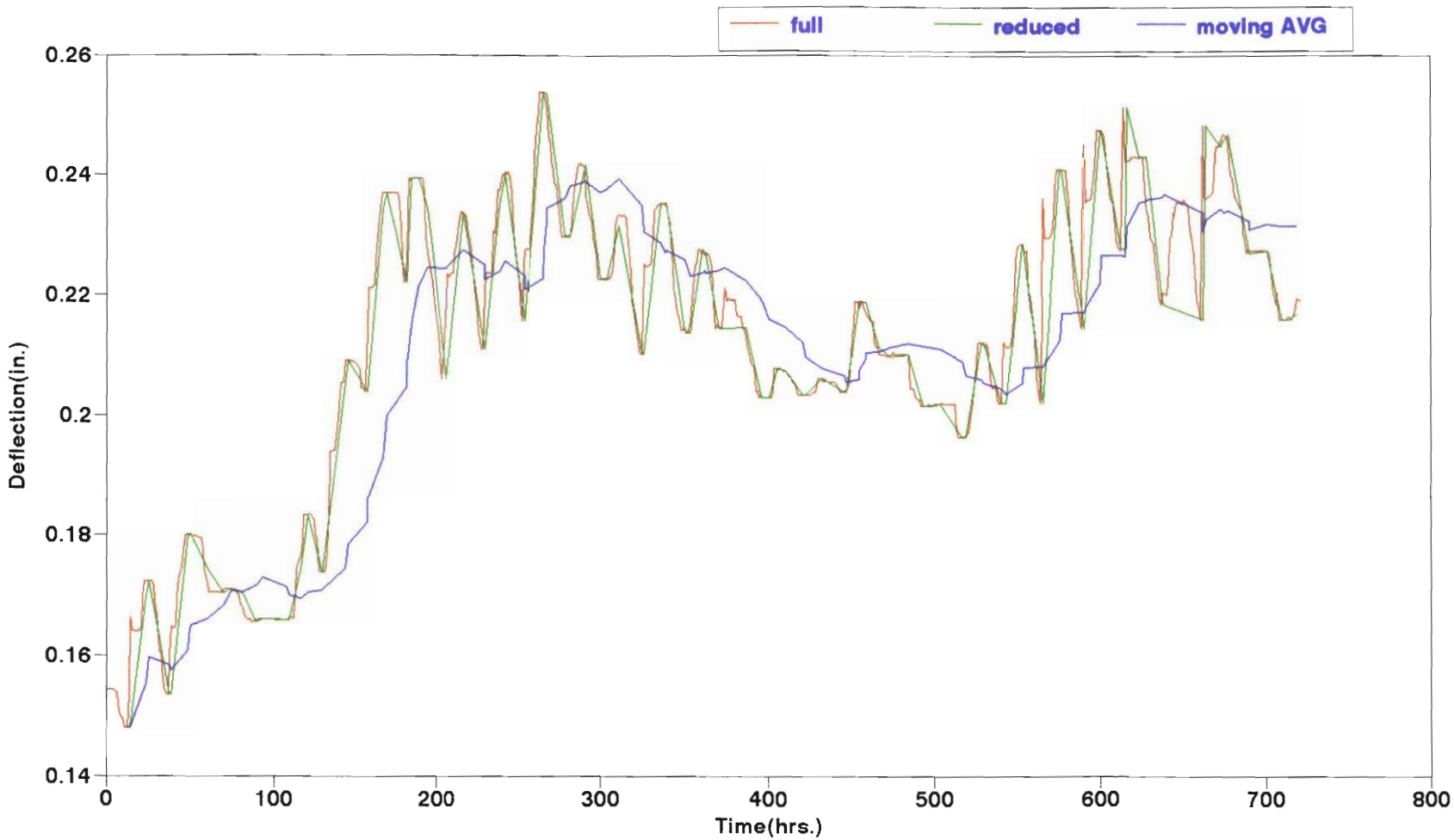

Figure 4-2 One Month Data Comparison

A brass bar in deflection sensors and a steel frame supporting the sensor will expand and contract due to temperature changes, which may affect the accuracy of deflection data. The influence of the expansion and contraction of all metal parts had negligible effects on deflection measurements. Detailed calculations for expansion and contraction of all metal parts are given in Appendix C.

4.4 Moisture Content

It was assumed that the moisture content of all the specimens is the same as that of the moisture content sample beam. Moisture content of the sample beam is calculated using the following equation:

$$M_t = \frac{W_t - W_{od}}{W_{od}} * 100\ \% \quad \ldots\ldots (4\text{-}9)$$

where, M_t = moisture content at time t; W_{od} = oven-dry weight of the beam obtained using the previous moisture content data in the conditioned room; W_t = weight of the beam at time t. W_{od} is calculated using the following equation:

$$W_{od} = \frac{W_0}{1 + M_0} \quad \ldots\ldots (4\text{-}10)$$

where, W_0 = weight of the moisture content sample beam at the controlled room condition (20° C, RH 69%); M_0 = 11%, moisture content of the sample beam at the controlled room, which was determined using the method recommended by ASTM D 4442 (ASTM 1990).

V. MODELLING

5.1 Five-Element Creep Model

A five-element creep model developed by Fridley et al (1992d) is used to predict creep behavior of structural lumber in a natural environment. As introduced in Section 2.4, the five-element creep model is composed of a Burger model and a mechano-sorptive element. This model can be used to predict load and environmental effects, as well as mechano-sorptive effects to the primary and secondary creep behavior. For a constant load, the model is expressed as equation (2-6).

The parameters, K_e, K_k, μ_k, and μ_v, are calculated using equations (2-7) to (2-12). The reference condition in this study is the environmental condition in the conditioned room (20° C, RH 69%). The actual moisture content is calculated using equation (4-8). The actual temperature is directly read from the temperature and relative humidity probe.

Since experimental data in a constant environment is not available in this study, the reference parameters and the constants in the above equations were chosen exactly the same as Fridley's (Fridley et al. 1992d), except for K_{e0}, which is the edge-wise MOE measured at 20°C and RH 69% using the static method. The mechano-sorptive constants, $\mu'_{ms} = 3.78 \times 10^6$ psi and the constant, $B_w = 7.85 \times 10^{-5}$ min^{-1} were also taken from Fridley et al. (1992d). The parameters for the reference condition, K_{e0}, K_{k0}, μ_{k0}, and μ_{v0}, were determined by Fridley et al. (1992d), using the experimental data under the constant environment(i.e. 73°F and

50% RH). The mean values of the four parameters are listed as follows:

$$K_{e0} = 1.84 \times 10^{6} \text{ psi.}$$

$$K_{k0} = 3.87 \times 10^{6} \text{ psi.}$$

$$\mu_{k0} = 6.57 \times 10^{10} \text{ psi.-min.}$$

$$\mu_{v0} = 7.49 \times 10^{14} \text{ psi.-min.}$$

Equation (2-6) and the above constants are used to predict creep strain of structural lumber in a natural environment.

5.2 Four-Element Model

The Burger model, equation (2-2) has been successfully used for predicting creep behavior of wood (Ylinen 1965, Senft and Suddarth 1971, Gressel 1984, Hoyle et al 1985, 1986, Fridley et al 1992d). However, all these applications for the Burger model were conducted under either constant or controlled environment. Since overall moisture content of the specimen has changed little during fourteen months in this study, the mechano-sorptive element in Fridley's model based on large moisture content change may not predict creep in a natural environment. In addition, creep behavior observed in this study is influenced by both ambient temperature and MOE. Therefore, a four-element model with MOE and temperature effects is developed based on the Burger model. The mathematical expression of the four-element model is as follows:

$$\varepsilon(t) = Q*\{\frac{\sigma}{K_e} + \frac{\sigma}{K_k}*[\,1-\exp(-\frac{K_k*t}{\mu_k})\,] + \frac{\sigma*t}{\mu_v}\}. \quad .....(5-1)$$

$$Q = \frac{reference\ \ MOE}{Actual\ \ MOE}. \quad .....(5-2)$$

where $\varepsilon(t)$ = total strain at time t; Q = MOE factor; Actual MOE = E_e values in Table (3-1); σ = the applied stress; K_e =the Hookean spring constant associated with elastic deformation(i.e., modulus of elasticity); K_k and μ_k =the Hookean spring constant and viscosity of the Newtonian dash pot, respectively, of the Kelvin element; μ_v=the viscosity of the Newtonian dashpot associated with unrecoverable strain.

The reference MOE in equation (5-2) is based on the average value of the edge-wise MOE, E_e, of all specimens listed in Table (3-1). Specimen 07d5 is chosen as the reference sample with the reference MOE = 1.35 x 10^6 psi, which is closest to the average MOE of all specimens.

However, if the four parameters, K_e, K_k, μ_k, and μ_v, are constant, the prediction will be a smooth exponential curve. The temperature fluctuations are added into the model to adjust K_e, K_k, μ_k, and μ_v for the temperature effects based on the following equations:

$$K_e(\alpha) = K_{e0}*(1+q_1*\alpha+q_2*\alpha^2) \quad .....(5-3)$$

$$K_k(\alpha) = K_{k0}*(1+q_3*\alpha+q_4*\alpha^2) \quad .....(5-4)$$

$$\mu_k(\alpha) = \mu_{k0} * (1 + q_5 * \alpha + q_6 * \alpha^2) \ldots\ldots (5\text{-}5)$$

$$\mu_v(\alpha) = \mu_{v0} * (1 + q_7 * \alpha + q_8 * \alpha^2) \ldots\ldots (5\text{-}6)$$

where, α = a relative temperature factor, defined as follows:

$$\alpha = \frac{T - T_0}{T_0} \ldots\ldots (5\text{-}7)$$

where, T = temperature at time t; T_0 = temperature at the reference condition (RH 69%, 20°C); K_{e0}, K_{k0}, μ_{k0}, and μ_{v0} = model parameters at the average condition; q_1-q_8 = constants.

The average condition is obtained by fitting the power law, equation (2-1), to the experimental data of the reference specimen. The fitted curve is assumed as creep under the average environmental condition. The curve fitting uses equations (4-5) and (4-6) introduced in Section 4.3. Data for the first 5,000 hours is used to develop the model. The regression results show that b = 5.98 x 10^{-5}, n = 0.2. Average creep strain data, ε_{avg}, is then calculated using equation (2-1) by substituting b and n into the regression results. After that, K_{k0}, μ_{k0}, and μ_{v0}, the reference parameters, are determined using the SAS NLIN procedure (SAS 1979), with the four-element model, equation (5-1), based on the average creep strain data, ε_{avg}. The regression results for the reference parameters are listed in Table 5-1. K_{e0} is the edge-wise MOE of specimen 07d5 previously measured under the reference condition (20° C, RH 69%).

Table 5-1 Reference Parameters

Parameters	Estimate	Asymptotic Std. Error
K_{k0}	3×10^{6} psi	2.11×10^{-9}
μ_{k0}	6×10^{8} psi-hr	4.49×10^{-11}
μ_{v0}	4×10^{10} psi-hr	7.08×10^{-13}

The four model parameters, K_e, K_k, μ_k, and μ_v in equation (5-1), are substituted into equations (5-3) to (5-6). Then, the eight model constants, q_1-q_8, are determined using the SAS NLIN procedure (SAS 1979) again, with the four-element model, equation (5-1), based on the experimental data of the reference specimen, 07d5. The regression results for q_1-q_8 are shown in Table (5-2).

Table 5-2 Four-Element Model Constants

Parameters	Estimate	Asymptotic Std. Error
q_1	-0.21	0.05
q_2	0.009	0.06
q_3	0.404	0.23
q_4	4.304	0.47
q_5	-4.09	1.03
q_6	12.20	2.96
q_7	-2.12	0.15
q_8	1.32	0.18

5.3 Empirical Model

Like the Burger model, the power law, equation (2-1), is also a popularly used model in describing creep behavior of wood in a constant environment (Clauser 1959, Schniewind and Barrett 1972, Hoyle et al 1985, 1986, Gerhards 1985). The power law in this study is expressed as follows, in order to consider the temperature effects:

$$\varepsilon_r = \varepsilon_t - \varepsilon_e = Q * [\, b(\alpha) * t^{\,n(\alpha)}] \quad \ldots\ldots (5\text{-}8)$$

where, ε_r =creep strain; ε_t = total strain at time t; ε_e = elastic strain; Q = MOE factor, same as that in the four-element model (equation 5-1); b(α) and n(α) = model parameters, functions of the relative temperature factor, α, described as follows:

$$b(\alpha) = b_0 * (1 + r_1 * \alpha + r_2 * \alpha^2) \quad \ldots\ldots (5\text{-}9)$$

$$n(\alpha) = n_0 * (1 + r_3 * \alpha + r_4 * \alpha^2) \quad \ldots\ldots (5\text{-}10)$$

where, b_0 = 5.98 x 10^{-5}; n_0 = 0.2, obtained using the linear regression procedure on the reference specimen, 07d5, introduced in Section 6.2; r_1-r_4 = model constants. The model constants, r_1-r_4, are determined using the SAS NLIN procedure (SAS 1979) with the modified power law model, equation (5-8), based on the experimental data recorded from the reference specimen in a natural

environment. The regression results for r_1-r_4 are listed in Table (5-3). Again, data for the first 5,000 hours are used to develop the model.

Table 5-3 Constants for Modified Power Law

Parameter	Estimate	Asymptotic Std. Error
r_1	0.1	0
r_2	0.3	0
r_3	0.5	0
r_4	0.1	0

VI. RESULTS AND DISCUSSION

6.1 Initial Properties of the Specimens

Table (3-1) shows the MOEs, specific gravity, and dimensions of the specimens measured at 11% moisture content, as well as a description of the defects. It is shown that almost every specimen has knots within the load span. The knots are located either at the centerline or at the edges of beams. In general, the presence of the knots reduces the mechanical properties of the wood beams subjected to bending stresses (Panshin and Zeeuw 1970), and may lead to more creep strain.

It is also shown in the table that MOE and specific gravity are similar within each group, and increasing from group A to group E. The lowest specific gravity corresponds to the lowest MOE in group A, and the highest specific gravity corresponds to the highest MOE in group E.

Specific gravity is defined as a ratio of weight of the substance to the weight of an equal volume of water (Panshin and Zeeuw 1970). In general terms, the specific gravity of wood depends upon how much wood substance that certain volume of wood contains, which may relate to the size of the cells and the thickness of the cell walls. If the fibers are thick-walled and show small lumina, then the total air space is relatively small, and the specific gravity tends to be high. On the other hand, if they are thin-walled or wide-lumened, or both, the specific gravity will be low. Wood Handbook (1987) suggests that mechanical properties

within a species are linearly related with specific gravity. Therefore, MOE may also be linearly related with specific gravity.

6.2 Weather Conditions and Moisture Content

Figure (6-1) shows temperature and relative humidity conditions, as well as moisture content of the sample beam recorded over fourteen months. It is observed that temperature and relative humidity fluctuate continuously, and relative humidity always increases when the temperature drops, and vice versa. However, moisture content of the sample beam, under such environmental conditions, has only changed minimally.

This is because it takes more time for heat and moisture to transfer through wood than through air, due to the natural properties of wood and air (Wood Handbook 1987). The change in moisture content of the wood never catches up with the fluctuations in the ambient environment. In addition, the average temperature and relative humidity during the experimental period is about 15 °C and RH 70%, respectively. This average condition is close to that of the previous controlled room (20 °C, RH 69%) where specimens were stored for months before they were used in the experiment.

Two additional thermocouples were used to measure temperature on the top and the bottom surfaces of the sample beam, to observe how temperature changes on wood surface. Figure (6-2) shows temperature on both surfaces of the beam and air temperature for about three months. The three curves are virtually on top of each other, showing that temperature on both surfaces of the beam is the same

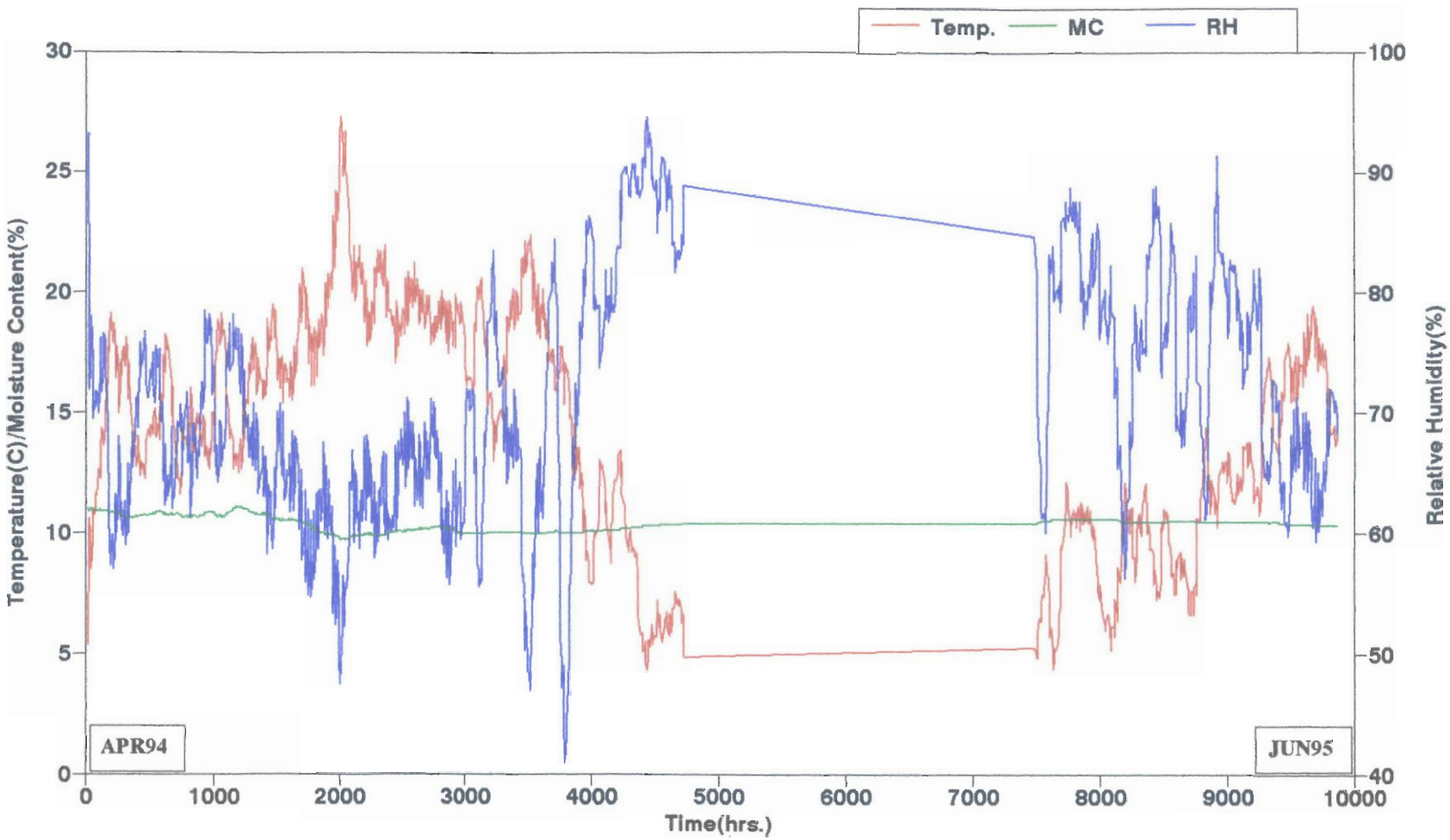

Figure 6-1 Environmental Conditions and Moisture Content

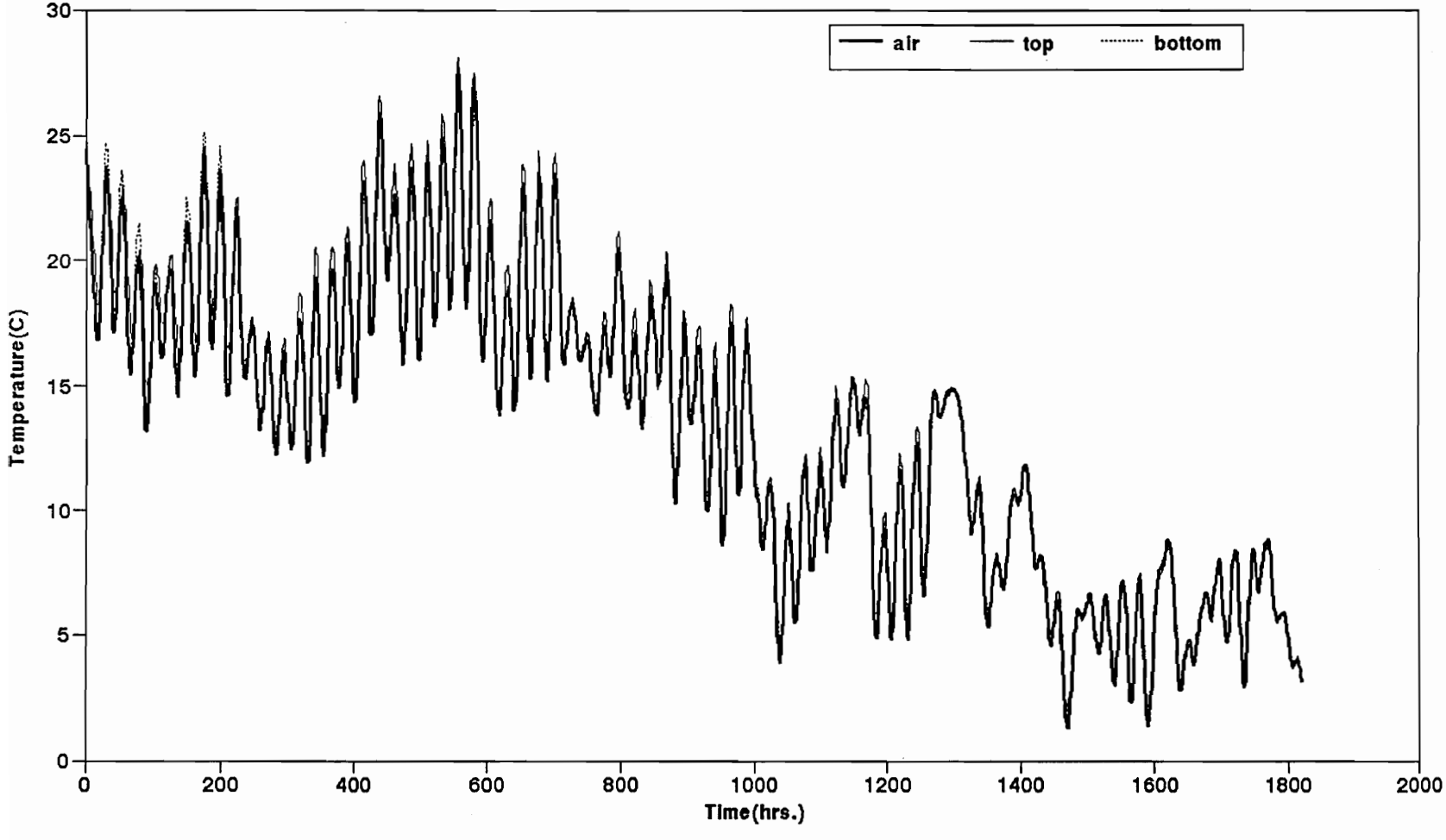

Figure 6-2 Comparison of Temperatures

as the air temperature. Therefore, air temperature is used in all further temperature related calculations and discussions.

6.3 Creep Strain vs. Modulus of Elasticity (MOE)

The creep deformations for each specimen at the 10,000th hour are listed in Table (6-1). The elastic deformation and the deformation calculated using equation (4-8) are also listed in Table (6-1) for every specimen. Some trends for the elastic deformations and the creep deformations can be observed in this table. The table shows that the experimental elastic deformation of each specimen is generally close to the theoretical elastic deformation. It has been discussed in section 4.3 that the experimental elastic deformation of each specimen is determined three seconds after the beam is loaded. Some specimens may not fully reach their elastic deformations at that time, or may start creeping. This may be one of the reasons for the differences between the experimental and the theoretical deformations. There may also be some measurement errors in determining MOE used in the calculation of the theoretical deformations.

Table (6-1) also shows that the elastic deformations decrease from group A (lowest MOE) to group E (highest MOE) as expected, as do the creep deformations (the 10,000th hour deformation). The same trend for creep strain can also be observed from Figure (6-3). This indicates that MOE affects not only the elastic deflections, but it seems that it affects creep deformations as well. It also could be due to the variation in the stress level on each specimen. Although the applied stress for each specimen is the same, 722 psi, the stress level for each specimen,

defined as the percentage of MOR, may not be the same because of the variation in MOR.

Table 6-1 Comparison of Deformations

Group Number	Specimen Number	Experimental Elastic Deformation(in.)	Theoretical Elastic Deformation(in.)	Creep Deformation(in.) at 10,000th hour
A	02A1	0.212	0.214	0.296
	01A3	0.290	0.274	0.336
	03A4	0.261	0.218	0.376
	04A5	0.282	0.242	0.540
B	17B2	0.242	0.197	0.272
	19B3	0.218	0.199	0.272
	18B4	0.213	0.210	0.220
	20B5	0.187	0.198	0.171
C	13C1	0.137	0.157	0.143
	14C2	0.164	0.175	0.293
	16C4	0.174	0.189	0.160
	15C5	0.178	0.181	0.209
D	05D2	0.148	0.154	0.156
	06D3	0.154	0.152	a*
	07D5	0.176	0.141	0.216
	08D8	0.128	0.143	0.112
E	09E2	0.116	0.117	0.117
	10E3	0.120	0.127	0.132
	11E4	0.125	0.119	0.133
	12E7	0.138	0.129	0.196

a* Data lost

In general, creep deformations of the specimens within each group are close to each other due to the consistent values of MOEs and specific gravity shown in Table (3-1). However, it is shown in Table (6-1) that specimens 04A5, 14C2,

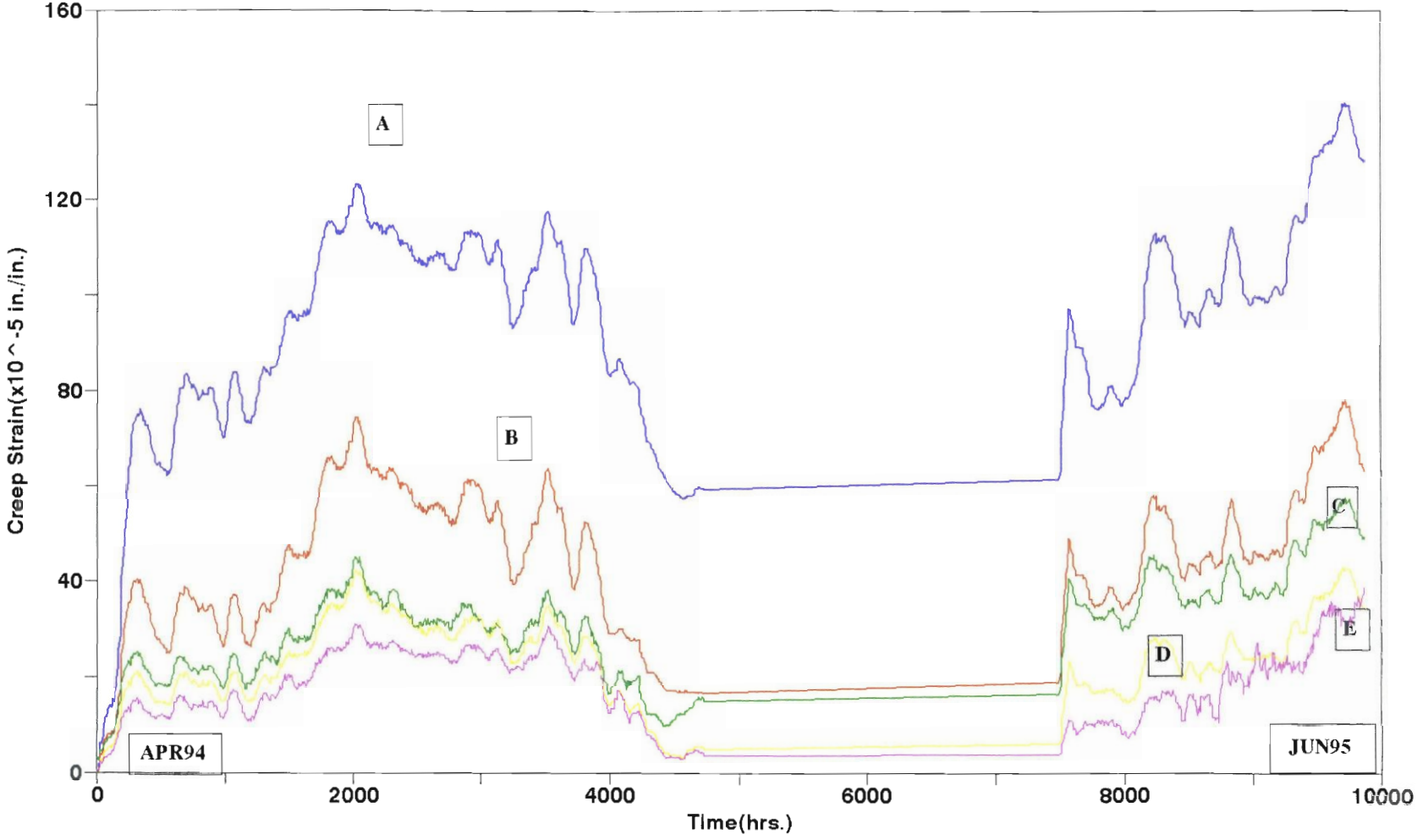

Figure 6-3 Typical Creep Strain Curves

07D5, and 12E7 have apparently higher creep strain than the others in the same group.

This may be related to the defect characteristics and MOE of each specimen. The defect characteristics of the four specimens show that the specimens have edge knots within the load span, and the knots are located at the center of the span in the compression zone, and the knots also cause cross grain all the way to the tension zone. The presence of the knots reduces the mechanical properties of the wood beams subjected to bending stresses (Panshin and Zeeuw 1970), and probably leads to more creep strain. In addition, the edge-wise MOE of the four specimens is the lowest within the group. This shows that MOE of the beam and defect location can significantly affect the creep strain.

Figure (6-3) also shows that the shape of creep strain curves is similar for the specimens from each group. The magnitude of creep strain, however, is different. It can be observed that the specimens (group A) with the lowest MOE have the highest creep strain, and the specimens (group E) with the highest MOE have the lowest creep strain. Hoyle et al (1985) conducted a creep experiment using Douglas-Fir beams of commercial size and quality under a controlled environment, and observed that creep was larger for low elastic modulus material. He further suggested that in a wider range of MOE, there should be a relationship between MOE and creep. However, in this study, these differences of creep strain between each specimen could be produced by different stress levels (percentage of ultimate strength) applied upon the specimens.

6.4 Creep Strain vs. Temperature

Figure (6-4) shows the fluctuations in air temperature along with the creep strain for one specimen from group D. The shape of the creep strain curves are similar to the fluctuations in air temperature as shown in this figure. Since the shape of the creep strain curves for all the specimens is similar (Figure 6-3), it is assumed that creep strain follows the fluctuations in air temperature for each specimen. This observation agrees with previous studies that the stiffness of wood decreases as temperature increases, based on constant moisture content (Fridley et al 1992d, Gerhards 1985, Szabo and Ifju 1970). It is seen from Figure (6-1) that moisture content of the sample beam has changed little over the fourteen-month period.

Fridley et al. (1990a) observed from their experiment, a load duration test on structural lumber under several constant levels of temperature, that creep strain increased when the temperature increased, under the same level of applied stress.

In addition, the mechanical properties of wood, based on the Wood Handbook (1987), generally decrease when heated and increase when cooled. MOE has a linear relationship to temperature under a constant moisture content and below about 150°C condition. When the temperature increases, MOE decreases linearly. As it has been discussed, creep strain increases as MOE decreases. Therefore, the air temperature may have more influence on creep behavior of full-size beams in a natural environment than moisture content, as Figure (6-1) shows that moisture content of all the beams has changed very little over the fourteen-month experimental period.

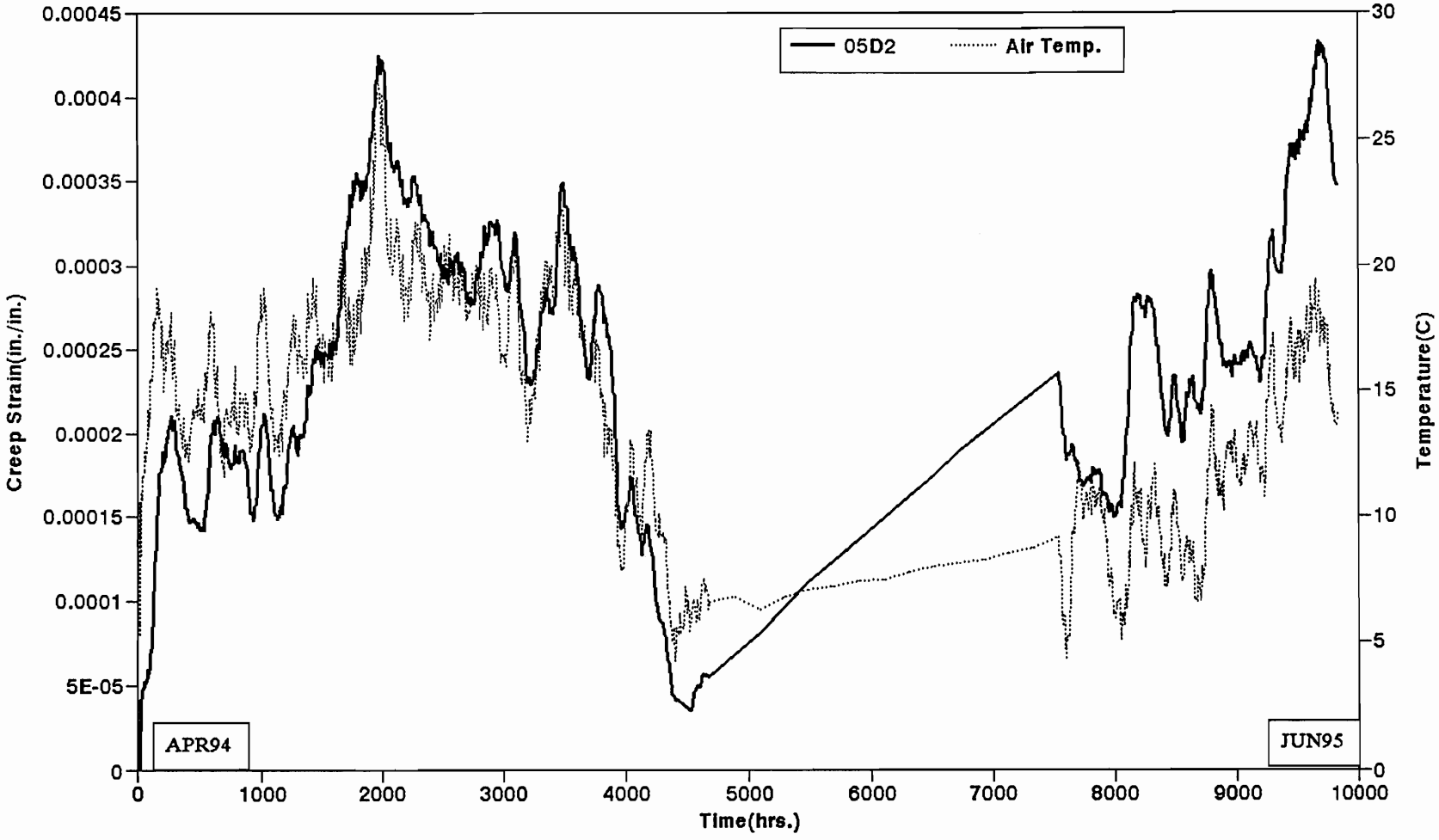

Figure 6-4 Creep Strain and Air Temperature

6.5 Mechano-Sorptive Creep Strain vs. Wood Shrinkage

As previously shown in Figure (6-2), temperature on the sample beam surfaces is nearly the same as that of the air. It is therefore inferred that moisture content on the beam surfaces changes with the ambient environment, although moisture content of the entire beam remained almost unaffected by the environment. That is, moisture content of the beam surface is in equilibrium with that of the air.

Based on the recorded temperature and relative humidity (RH) data, equilibrium moisture content (EMC) is calculated using the following equation (Wood Handbook 1987) and shown in Figure (6-5):

$$M = \frac{1800}{w}\left[\frac{KH}{1-KH} + \frac{K_1KH + 2K_1K_2K^2H^2}{1+K_1KH+K_1K_2K^2H^2}\right] \quad \ldots\ldots (6\text{-}1)$$

where $w = 330 + 0.452T + 0.00415T^2$;

$K = 0.791 + 0.000463T - 0.000000844T^2$;

$K_1 = 6.34 + 0.000775T - 0.0000935T^2$;

$K_2 = 1.09 + 0.0284T - 0.0000904T^2$.

and T = air temperature (°F); H = relative humidity (%); M = moisture content (%). It is shown in Figure (6-5) that EMC was always above actual MC in wood, and followed the fluctuations of RH in the air.

It is known that wood is dimensionally stable when the moisture content is above the fiber saturation point (about 30% MC). Wood changes dimension as it gains or loses moisture below that point. It shrinks when losing moisture from the

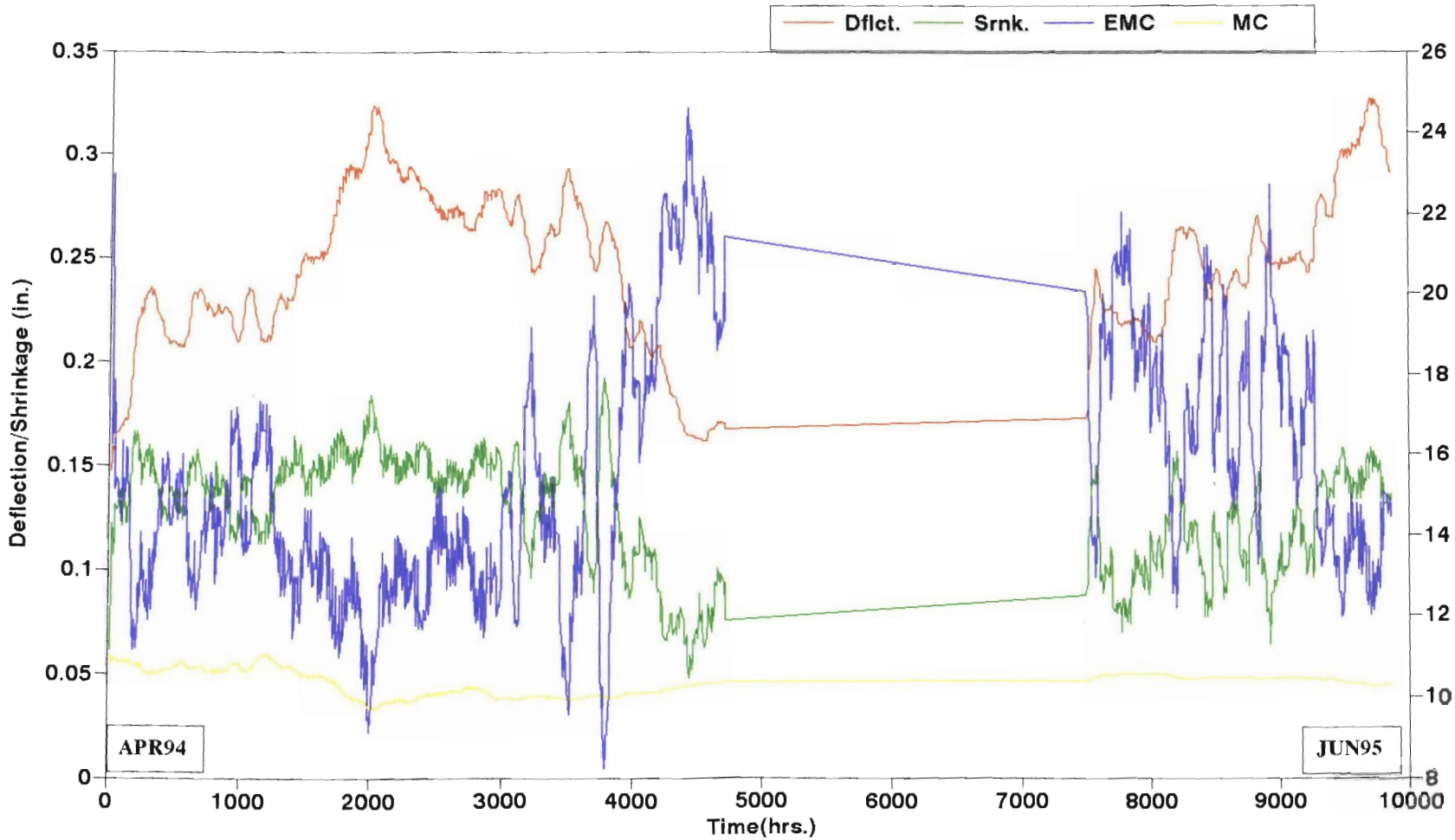

Figure 6-5 Deflection, Shrinkage, MC & EMC

cell walls and swells when gaining moisture in the cell walls. In addition, wood is an anisotropic material with respect to shrinkage characteristics. It shrinks most in the tangential direction of the annual growth rings. The shrinkage in the tangential direction is calculated using the following equation (Wood Handbook 1987):

$$S_m = S_0 [\frac{30 - m}{30}] \ldots\ldots (6\text{-}2)$$

where S_m = shrinkage from the green condition to moisture content m; S_0 = 7.6%, shrinkage value in tangential direction for Coast Douglas-fir from Wood Handbook (1987).

It is shown in Figure (6-5) that the shrinkage of the beam follows the change in the deflections of the beam, but is opposite from the fluctuations of EMC. It was observed that the deflection of the beam increased, when EMC decreased, and vice versa. That is, when the beam is in the desorption phase, the deflection increases, and when the beam is in the adsorption phase, the deflection recovers. Although overall specimen moisture content in this experiment does not change much, this phenomenon is also observed in Figures (6-1) and (6-3) where moisture content starts decreasing around 1500 hours, and the creep strain for each strain curve starts increasing. And, the reverse is true from around 2000 hours when moisture content starts increasing. This phenomenon was also observed by Lu and Erickson (1994) in their experiment under a controlled environment, and such behavior of wood was defined as mechano-sorptive creep.

The mechano-sorptive effect is usually considered to be that wood under load exhibits greater deformation when subjected to moisture content changes than

under constant humidity conditions. Lu and Erickson (1994) concluded based on their experimental results that mechano-sorptive creep of the beam in bending, was actually produced during the first desorption and adsorption cycle. With subsequent moisture content cycling, the additional creep was due to the shrinking and swelling of the beams. It was also experimentally shown in Toratti's study (Toratti 1992) that when more humidity cycles were introduced the mechano-sorptive effect decreased.

The time period for moisture cycles in Lu and Erickson's experiment (1994) was about 570 hours, and the change in moisture content for each cycle was about 10%. The dimensions of the specimen used were 0.9x0.5x18 inches. Therefore, there was enough time for such small specimens to reach equilibrium moisture content with the environment. However, it has already been discussed that moisture content of the entire beam in this study has changed very little. Only on the surface of the beam, can moisture content reach equilibrium with the environment. Therefore, the major contribution to mechano-sorptive creep in this study is from the dimensional changes of the beam.

6.6 Five-Element Model Prediction

The predictions of creep strain of structural lumber in a natural environment using a five-element model are shown in Figures (6-6) and (6-7) for one specimen from each of the A and C groups, respectively. Only the first 3,000 hours of data are used to compare model predictions with the experimental data. The predicted result is close to the experimental data for group C (Figure 6-7), but far below for

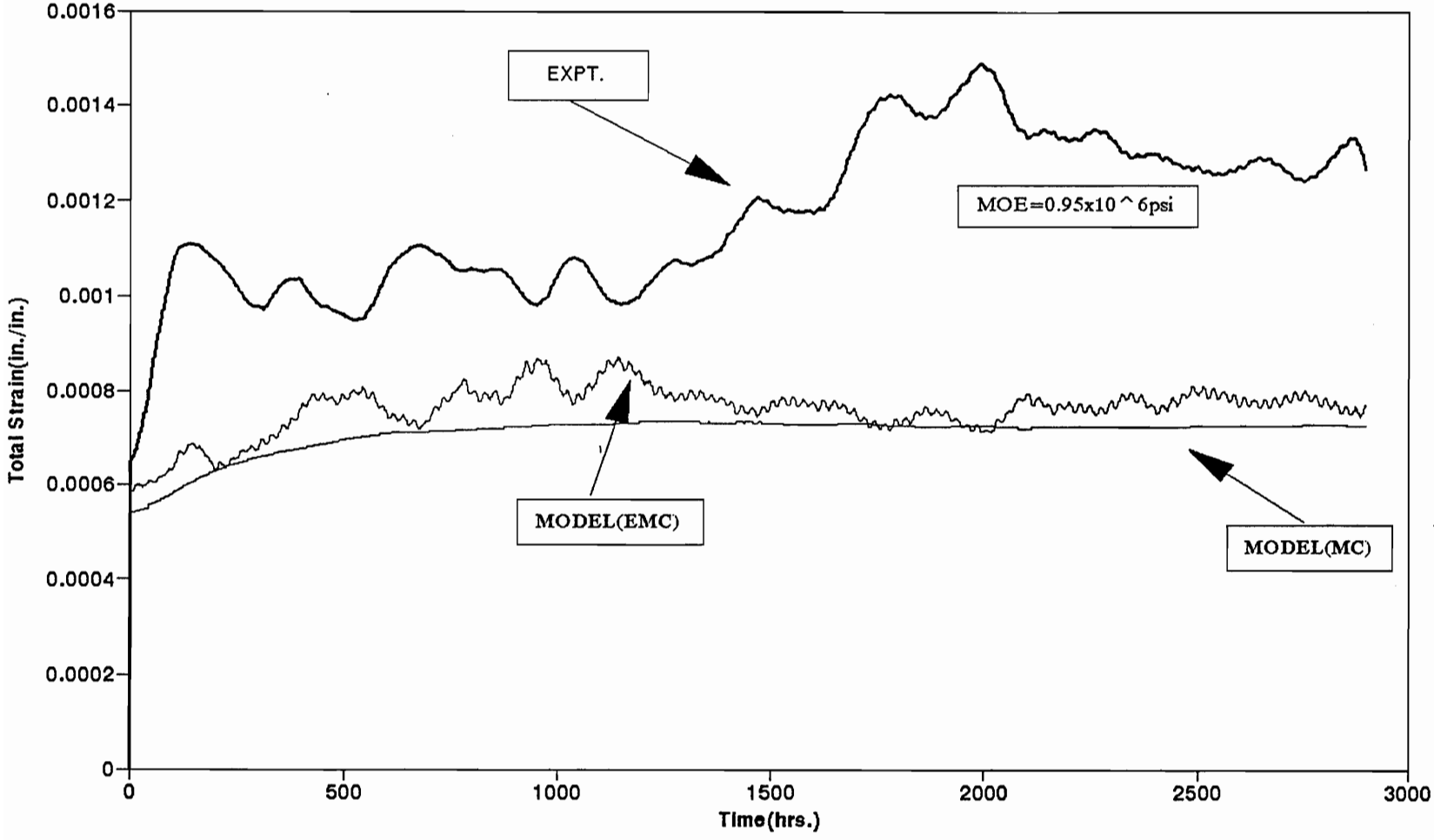

Figure 6-6 Experimental Strain (03A4) and Strain Predicted by Fridley's Model

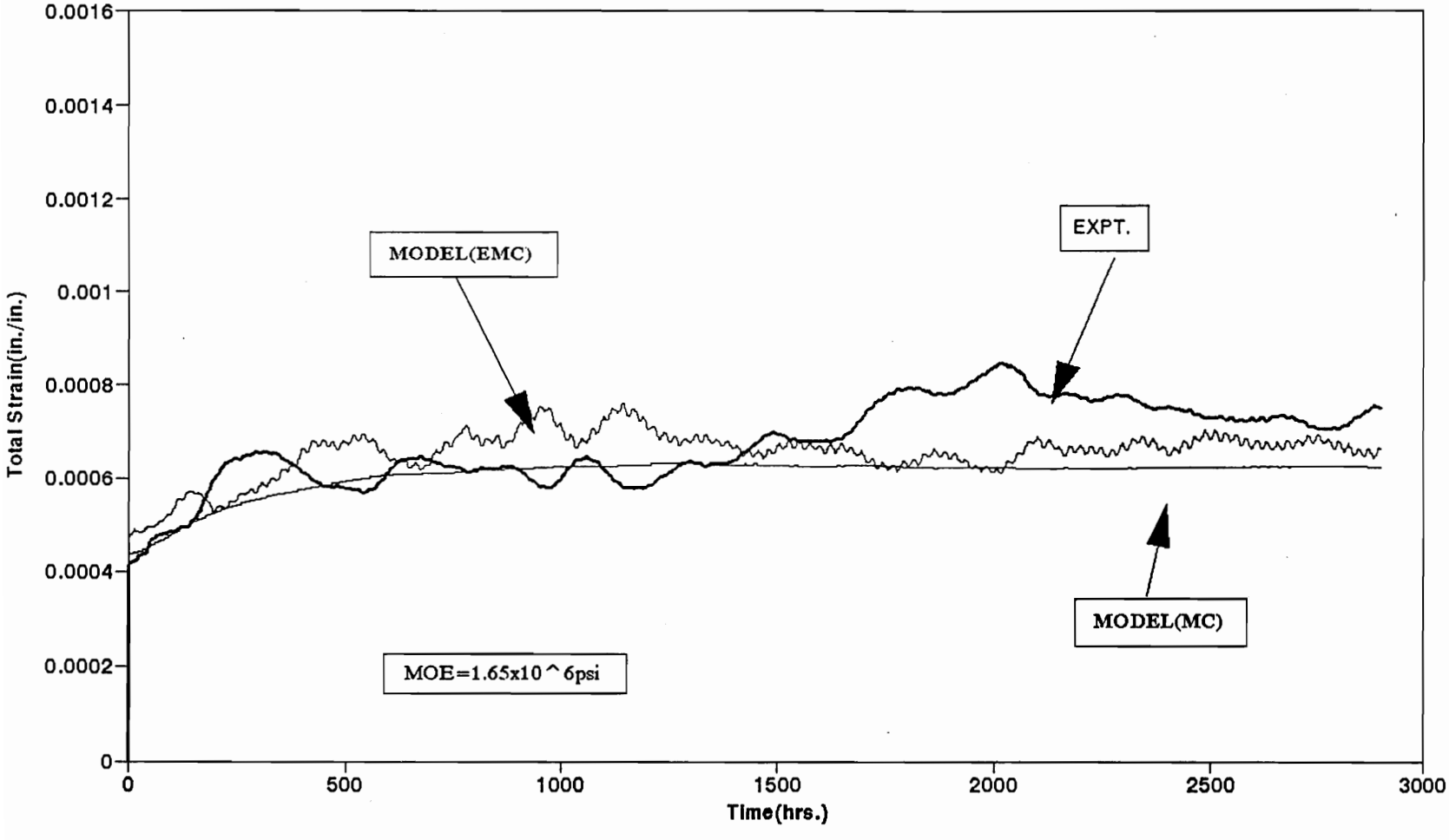

Figure 6-7 Experimental Strain (16C4) and Strain Predicted by Fridley's Model

group A (Figure 6-6). This is probably due to the difference in MOE between the two groups.

Unlike this study, in Fridley's experiment for developing the five-element model, all groups of specimens had similar values of MOE (Fridley et al. 1992d). Although MOE (K_e, the elastic spring constant) has been included in Fridley's model, it can only predict creep strain of a specimen which has a similar MOE to those used to develop the five-element model.

It has previously been discussed that creep strain is also affected by MOE. As shown in Figure (6-6), predicted strain from Fridley's model is much lower than the actual strain. This is because the MOE for group A is much lower than that used to develop this model. On the other hand, the MOE for group C is close to that for Fridley's samples, shown in Figure (6-7). Therefore, the predicted creep curve is close to the experimental creep curve.

There are two predicted curves in Figures (6-6) and (6-7), model (EMC) represents the predicted results using EMC on the beam surfaces in the mechano-sorptive element, and model (MC) represents the predicted results using MC of the entire beam in the mechano-sorptive element. It is shown that neither the model (MC) curve nor the model (EMC) curve predicts the experimental result.

It is also observed from both Figures (6-6) and (6-7) that the five-element model does not describe the fluctuations in creep strain seen in the experimental curves. It has been previously discussed that the fluctuation in creep strain is due to the shrinking and swelling of the beam which is caused by the changes of moisture content on the beam surfaces. Although the five-element model does

include the temperature effects, its contribution to the creep strain is very small. It seems that the mechano-sorptive element is only applicable to a controlled cyclic environment when there is a significant change in moisture content of the entire specimen.

The mechano-sorptive element in Fridley's model has no effects on creep strain in our experiment. After the mechano-sorptive element is removed from the five-element model, the predicted curve using the Burger model is exactly the same as the predicted curve using the five-element model, showing no mechano-sorptive effects. This is because the mechano-sorptive element is dominated by the changes of moisture content, $\Delta\omega$. As has been discussed, the overall specimen moisture content during the six months has changed little. Therefore, the mechano-sorptive creep strain has contributed little to the total creep strain.

Based on the above discussions, a creep model should include a parameter which takes MOE effects into account, so that the model can describe creep behavior of beams with different MOE.

Since the experiment in this study is conducted in a natural environment, the values for model constants, in equations (2-7) to (2-10), may not be the same as Fridley's, which were determined under either constant or controlled cyclic conditions with large changes of moisture content. This is probably the other reason why the five-element model does not predict the creep behavior of structural lumber in a natural environment.

6.7 Four-Element Model Prediction

Figure (6-8) shows the predicted creep curve using a four-element model (equation 5-1), and the experimental creep curve of the reference specimen, 07d5. Although the predicted curve does not perfectly match the experimental curve, the predicted curve reflects the fluctuation trends of the experimental curve, and is close to the experimental curve. However, the rate of strain changes is different between the experimental curve and the predicted curve. In general, the predicted creep strain changes faster than the experimental creep strain does. It has been discussed that the fluctuations in predicted creep strain are brought on by the air temperature. Therefore, the rate of the predicted curve is the same as that of the air temperature. It is known that wood responds to temperature changes slower than the air. Only the temperature changes on the surfaces of wood can catch up with the air temperature changes. This is probably the reason for the rate difference between the change of the predicted creep strain and the experimental creep strain.

Figures (6-9) to (6-26) show the predicted creep strain using the four-element model and experimental creep strain of the remaining specimens. For the predicted creep strain of all the remaining specimens, the model parameters are the same as those developed using the reference specimen, 07D5, except for the MOE factor, Q, which is determined by the ratio of the reference edge-wise MOE and the actual edge-wise MOE of each specimen. It can be observed that the predicted creep strain is close to the experimental creep strain of most specimens for the first

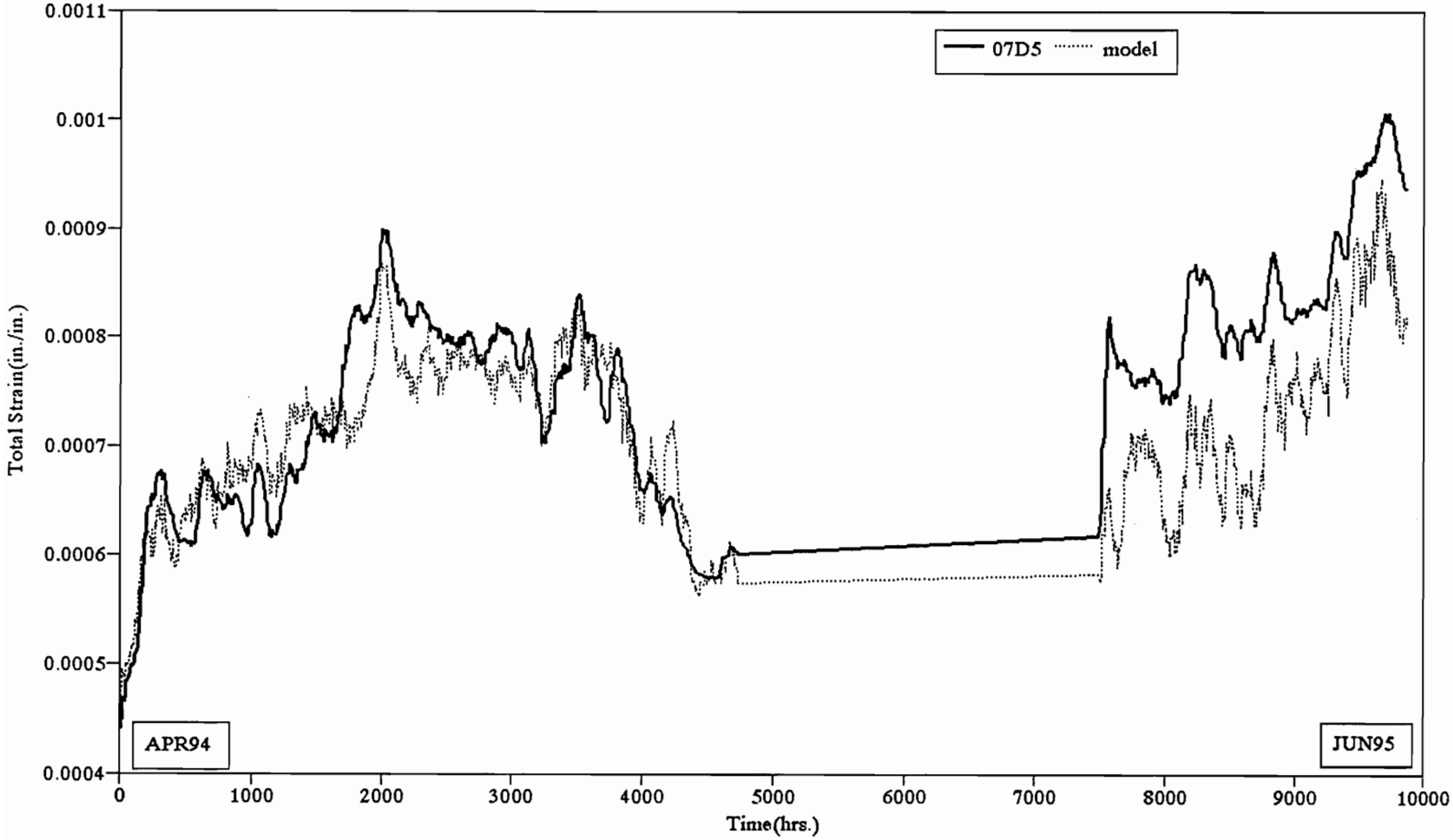

Figure 6-8 Four-Element Model Predicted for Reference Beam 07D5

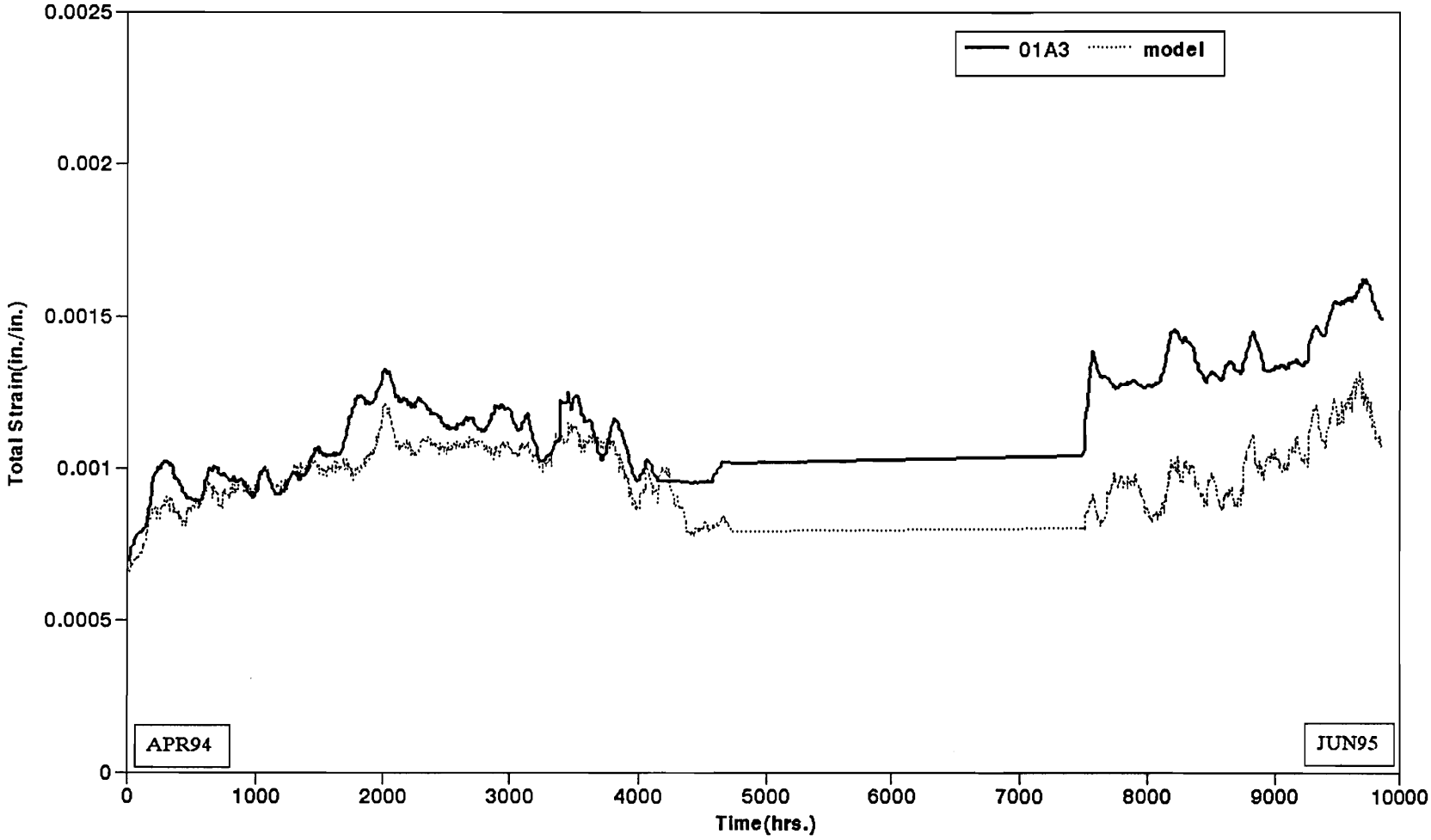

Figure 6-9 Four-Element Model Prediction for 01A3

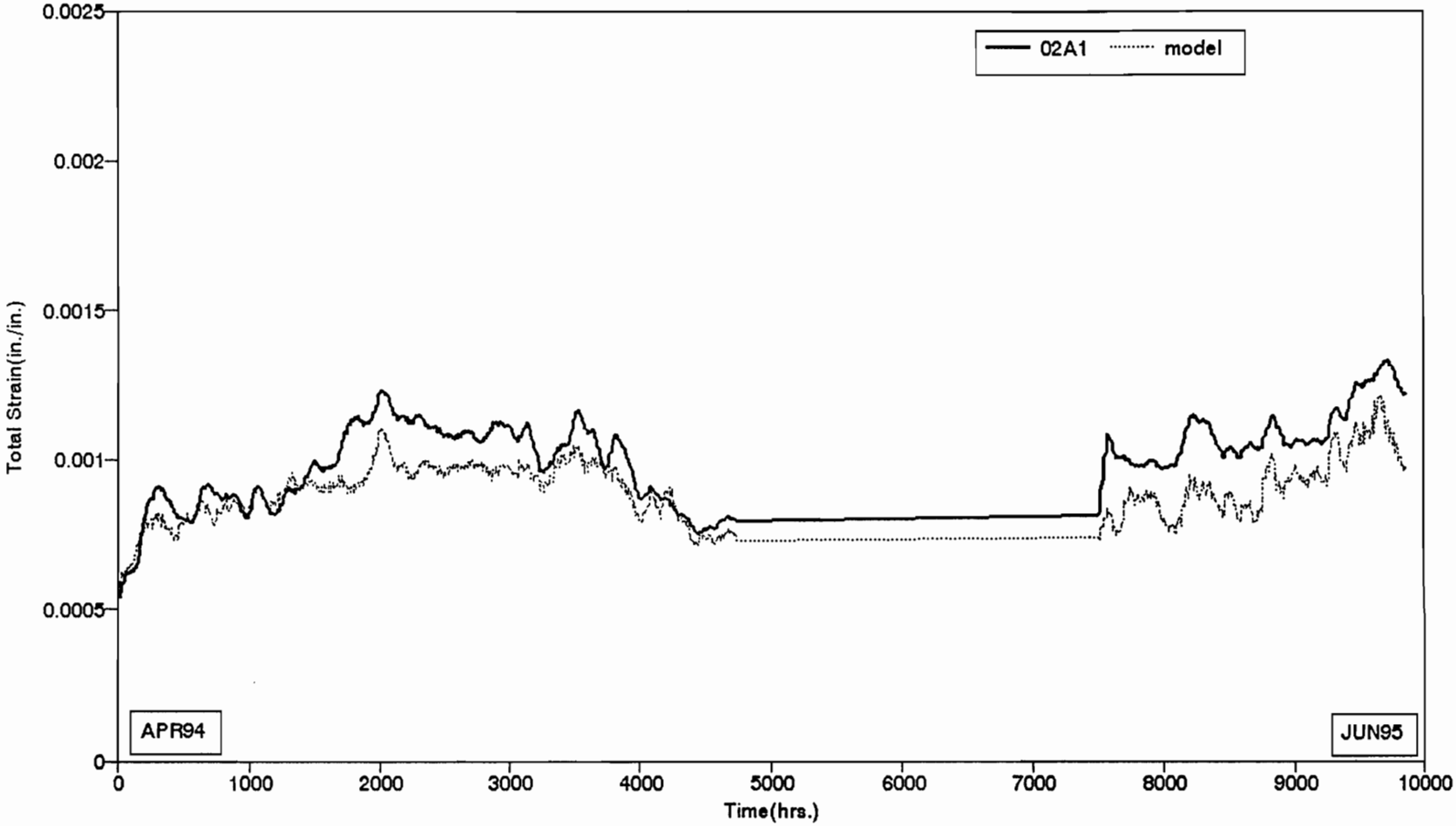

Figure 6-10 Four-Element Model Prediction for 02A1

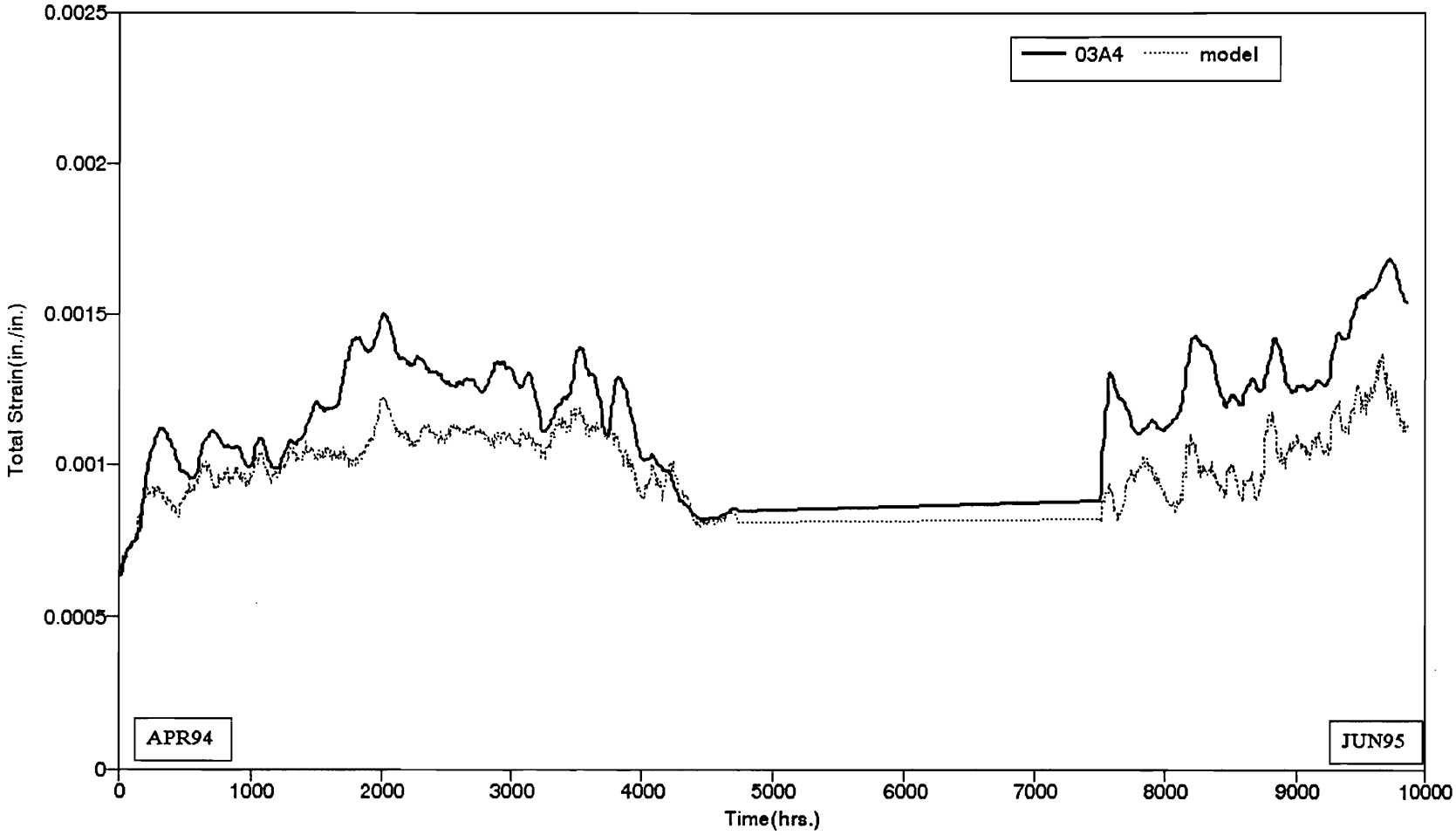

Figure 6-11 Four-Element Model Prediction for 03A4

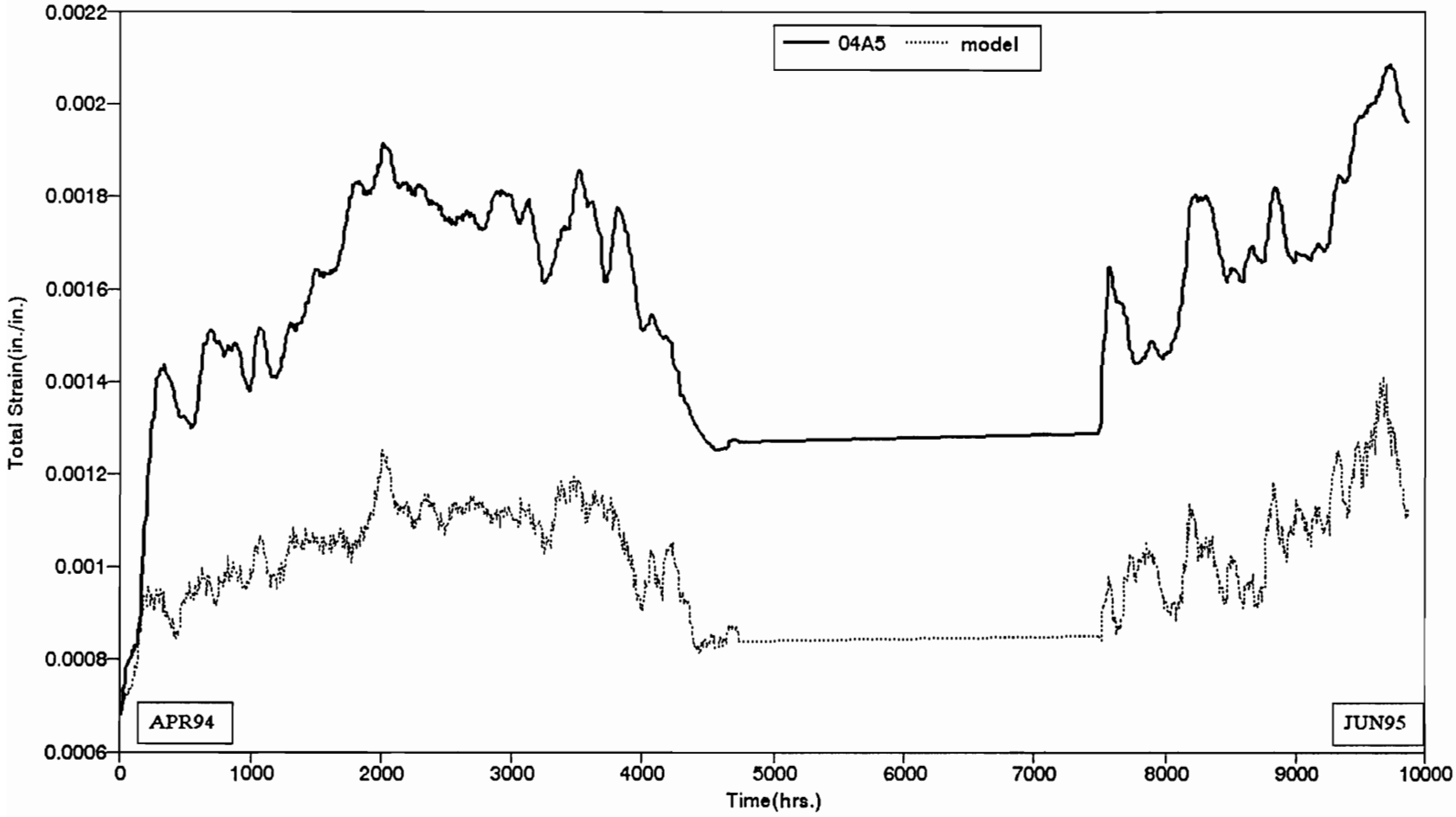

Figure 6-12 Four-Element Model Prediction for 04A5

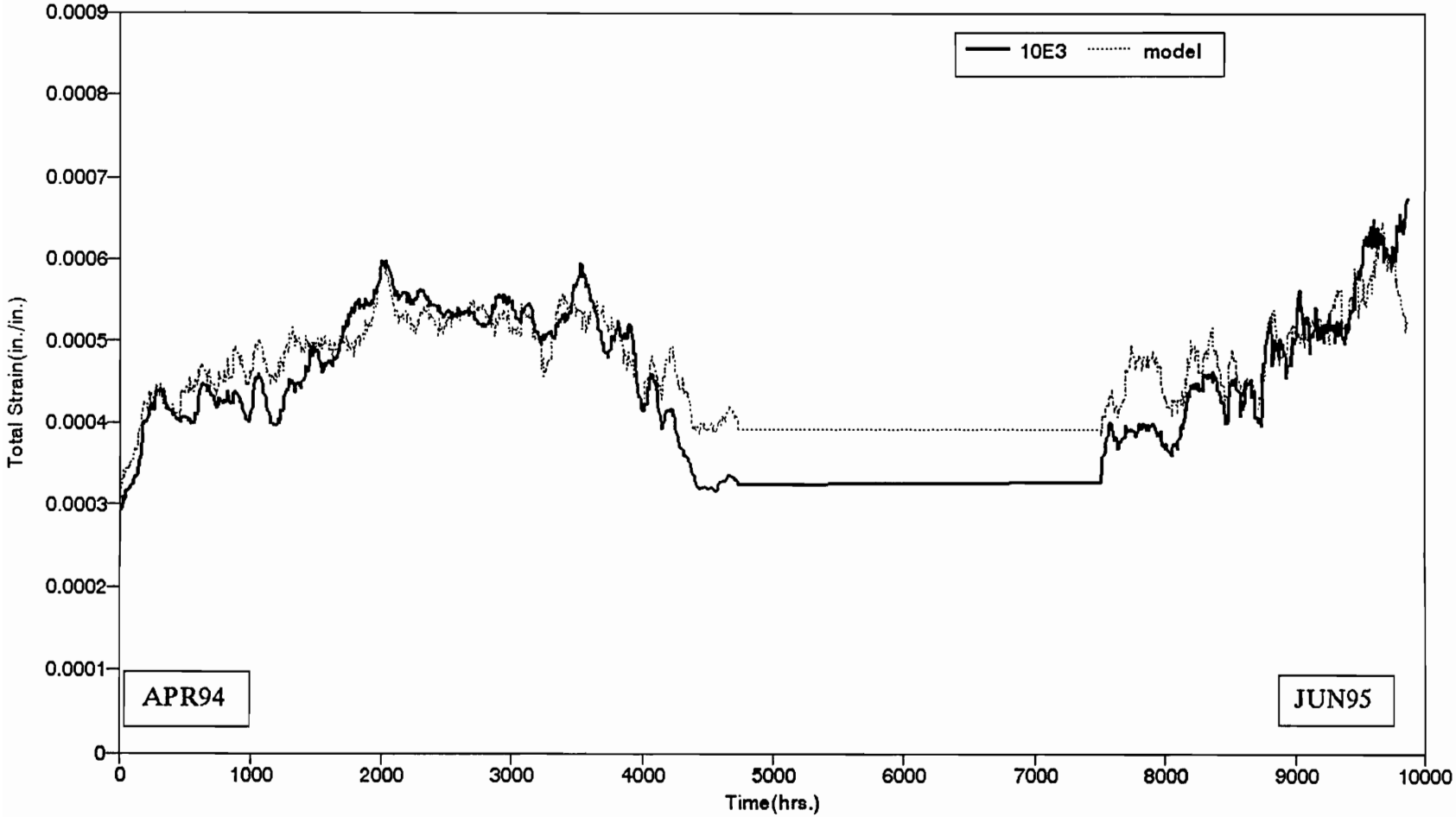

Figure 6-13 Four-Element Model Prediction for 10E3

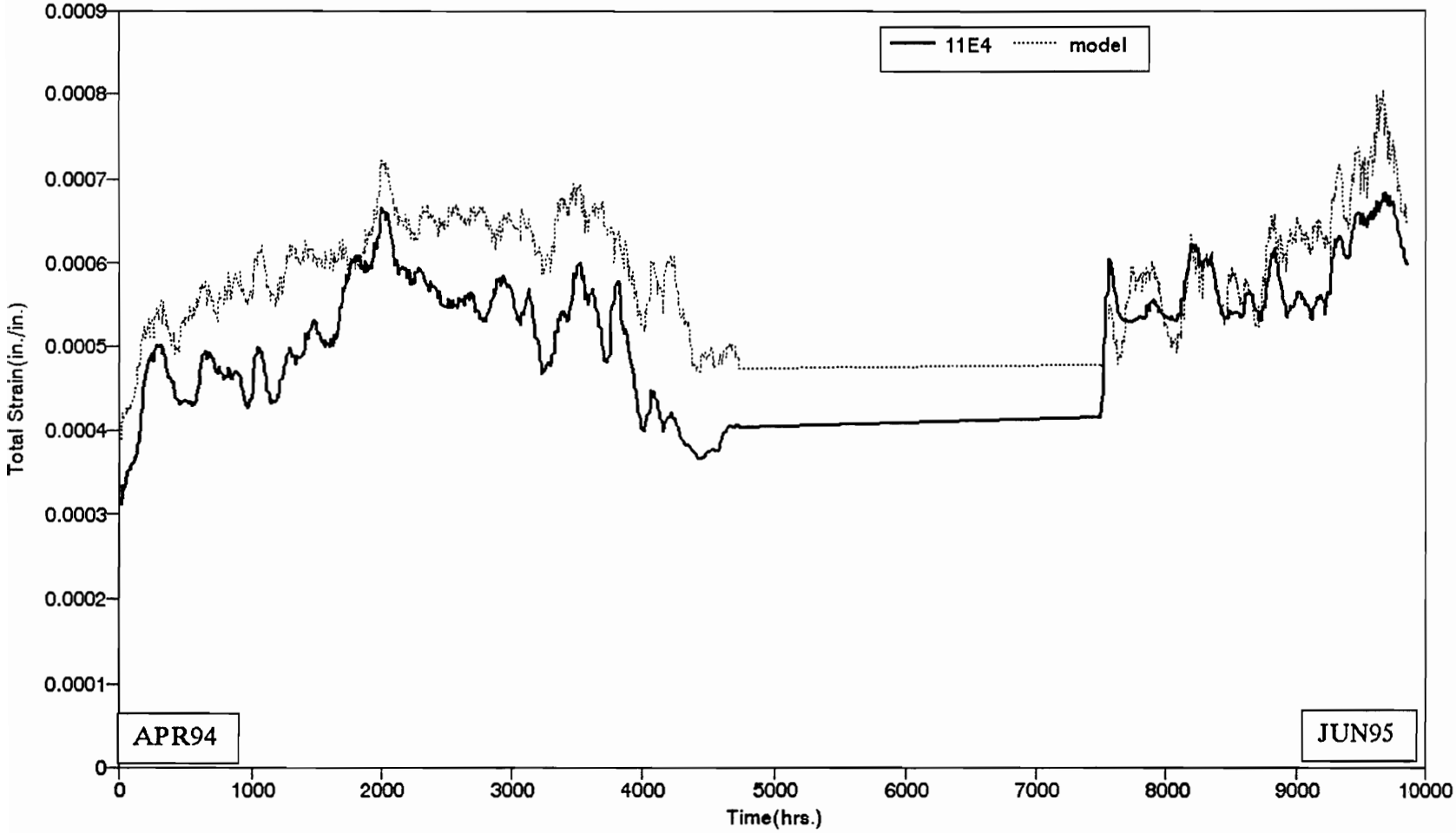

Figure 6-14 Four-Element Model Prediction for 11E4

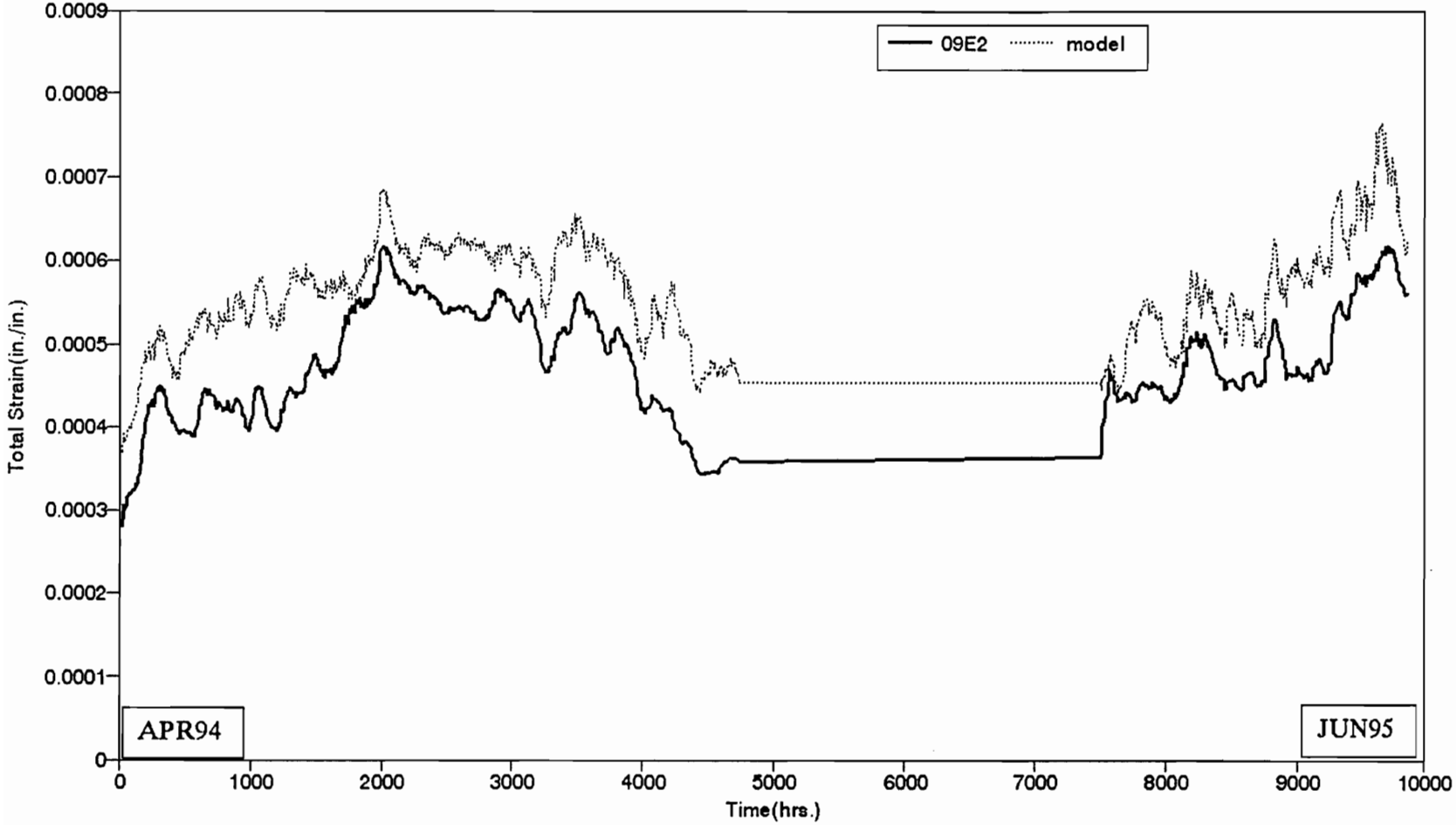

Figure 6-15 Four-Element Model Prediction for 09E2

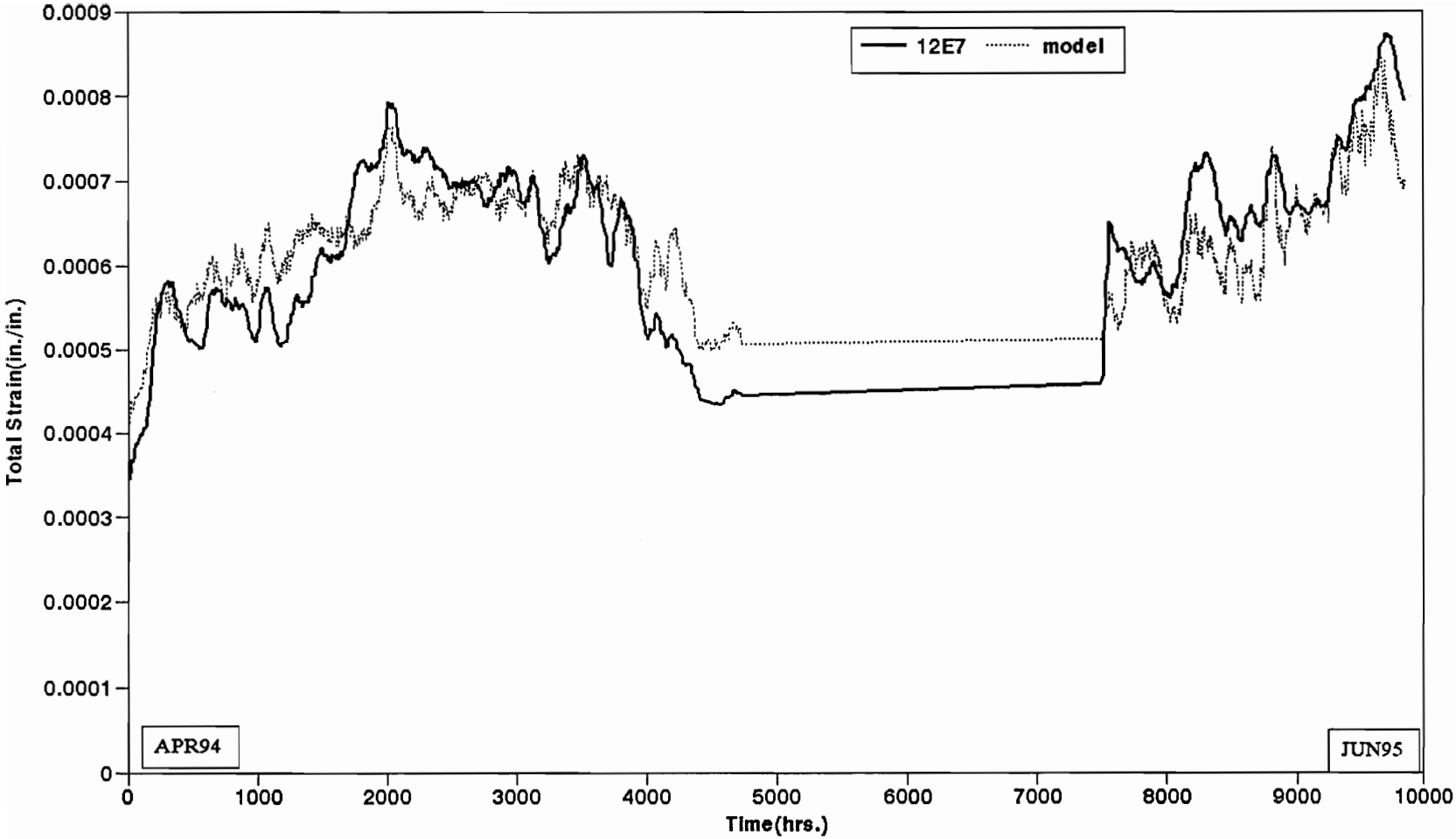

Figure 6-16 Four-Element Model Prediction for 12E7

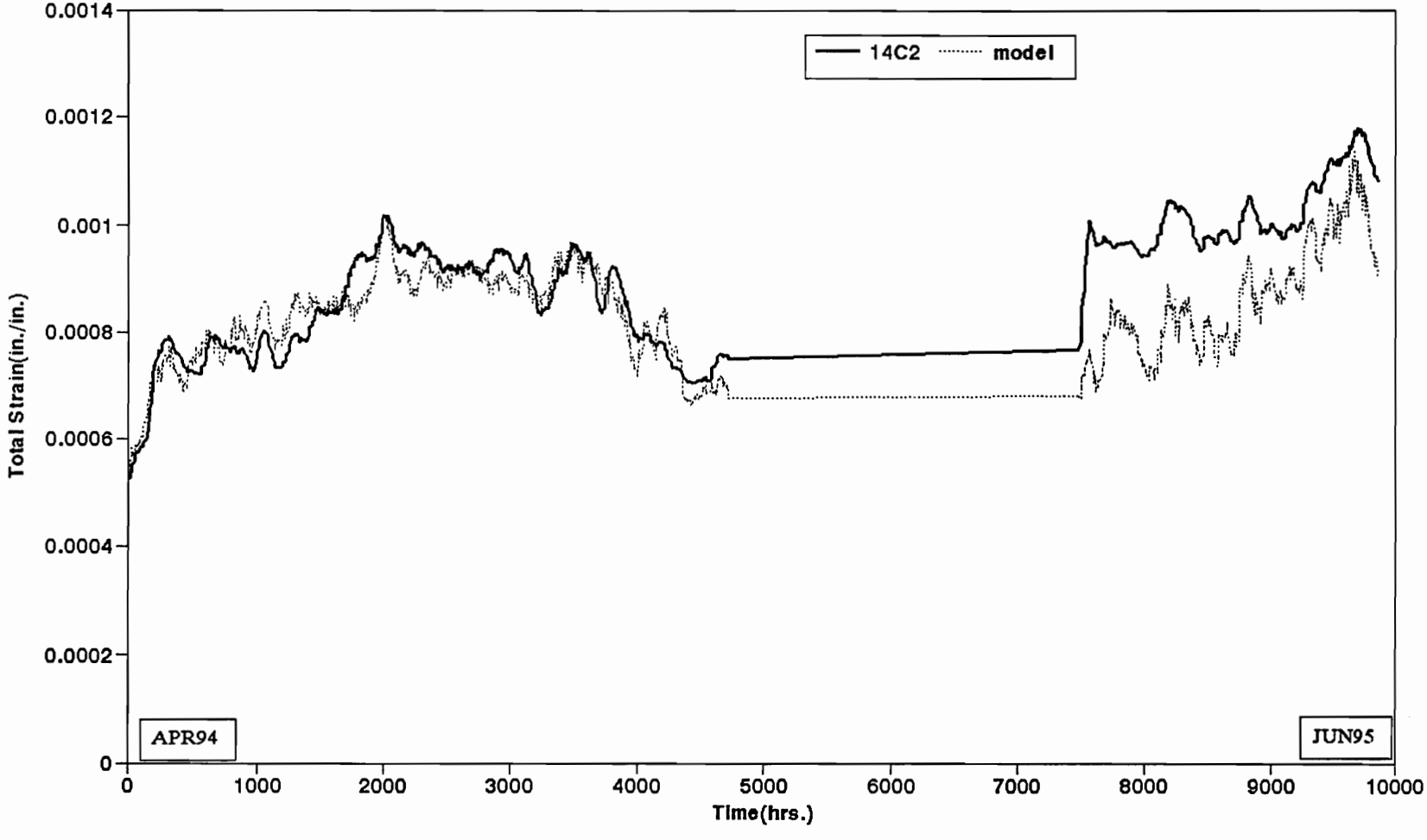

Figure 6-17 Four-Element Model Prediction for 14C2

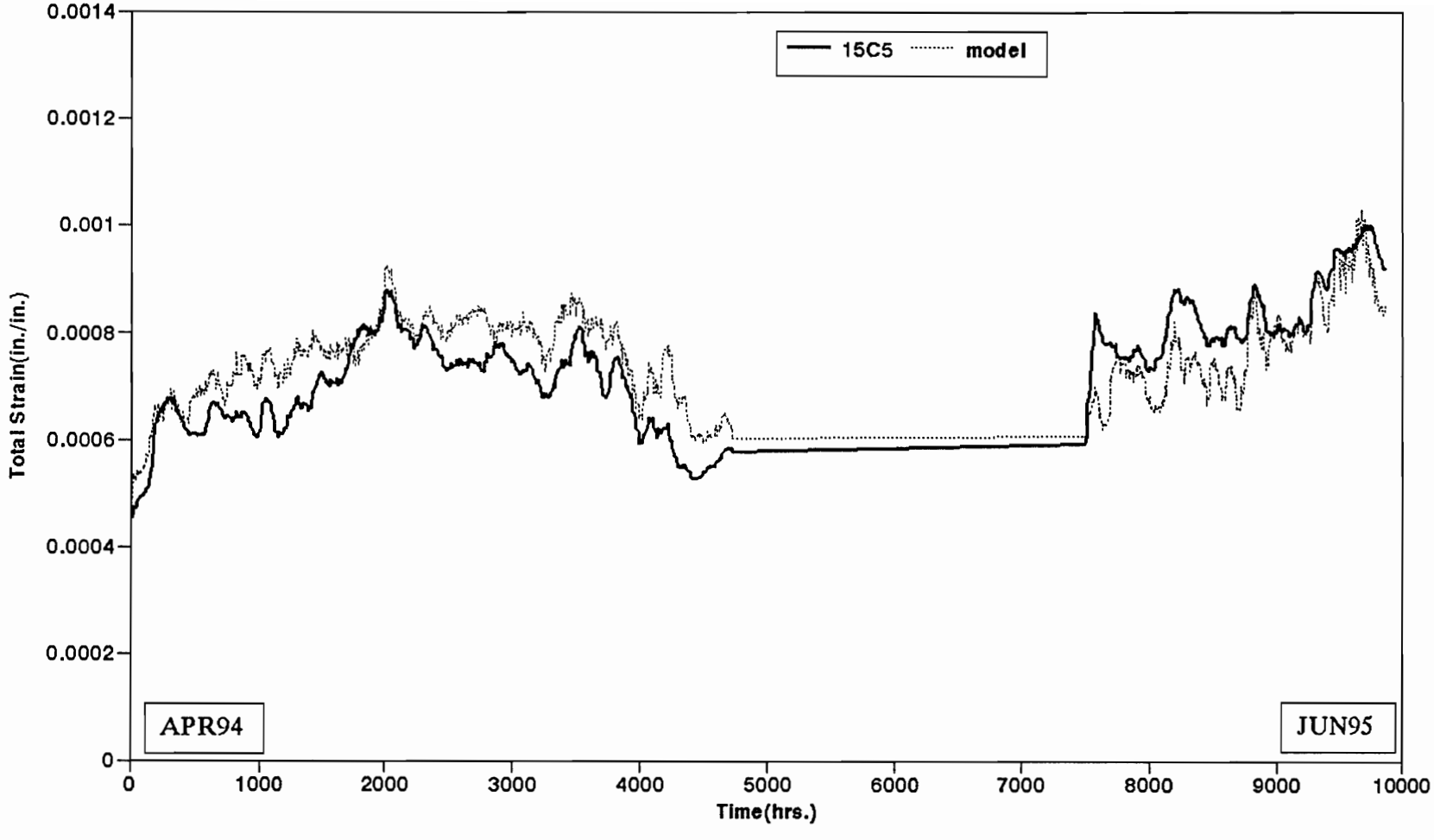

Figure 6-18 Four-Element Model Prediction for 15C5

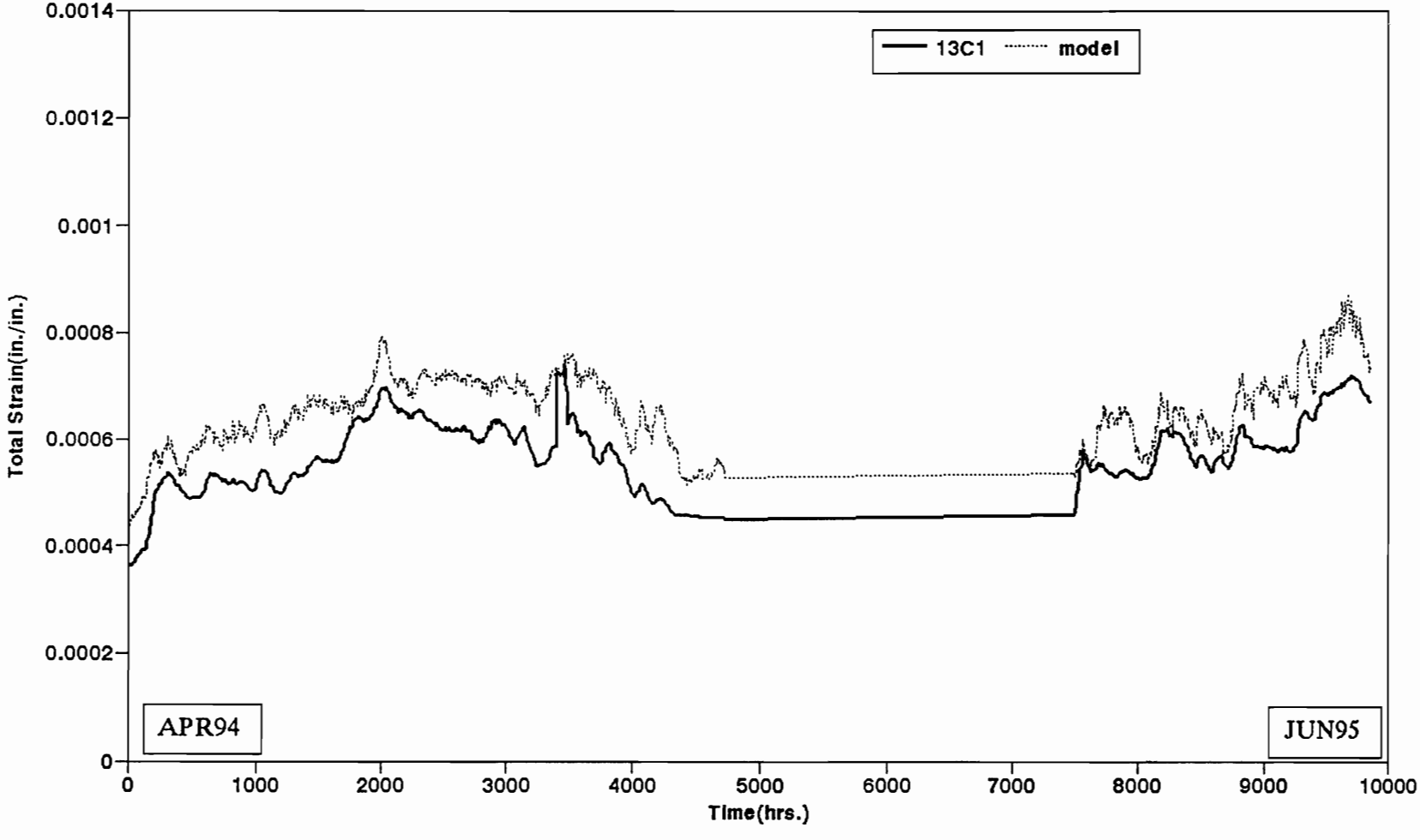

Figure 6-19 Four-Element Model Prediction for 13C1

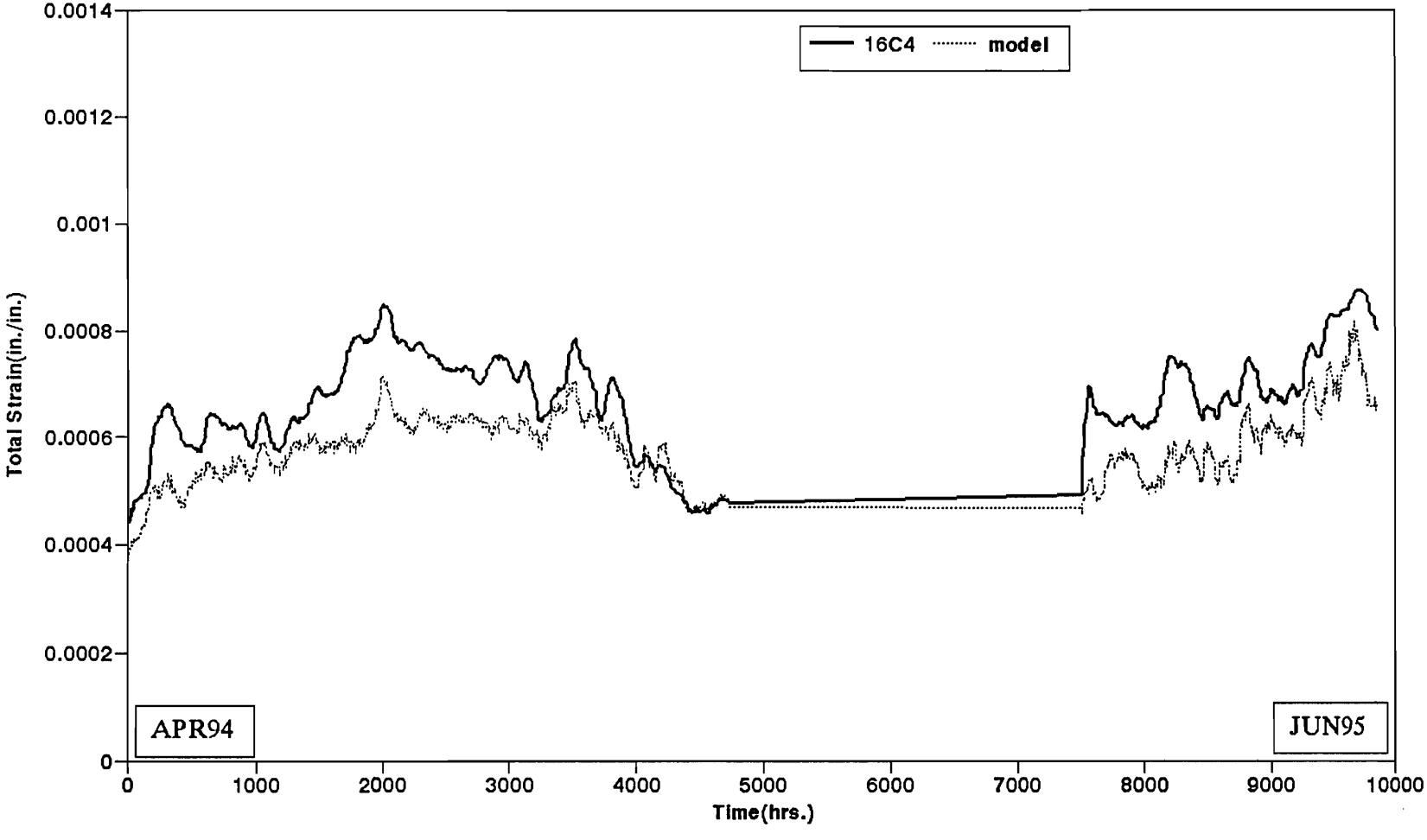

Figure 6-20 Four-Element Model Prediction for 16C4

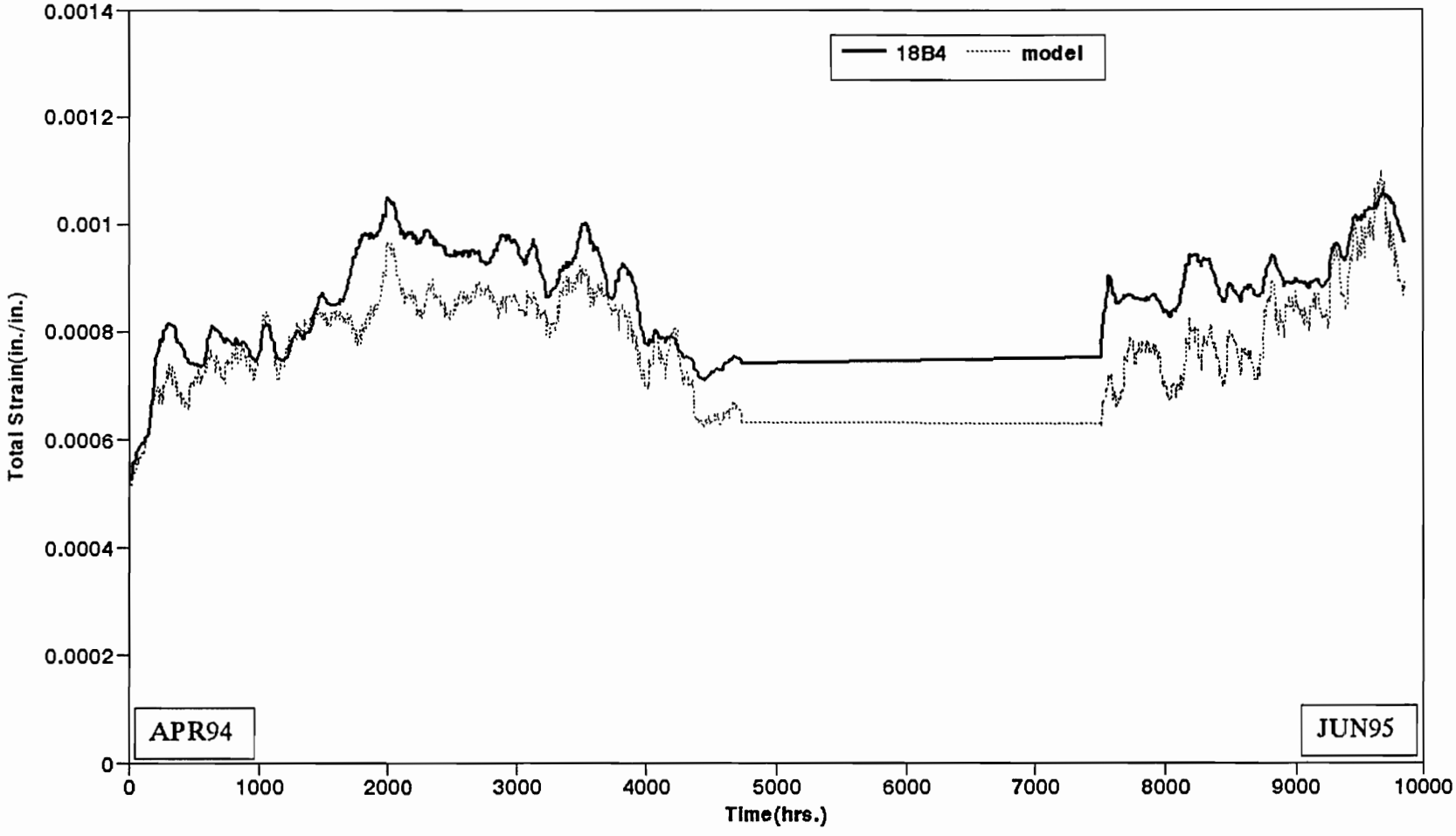

Figure 6-21 Four-Element Model Prediction for 18B4

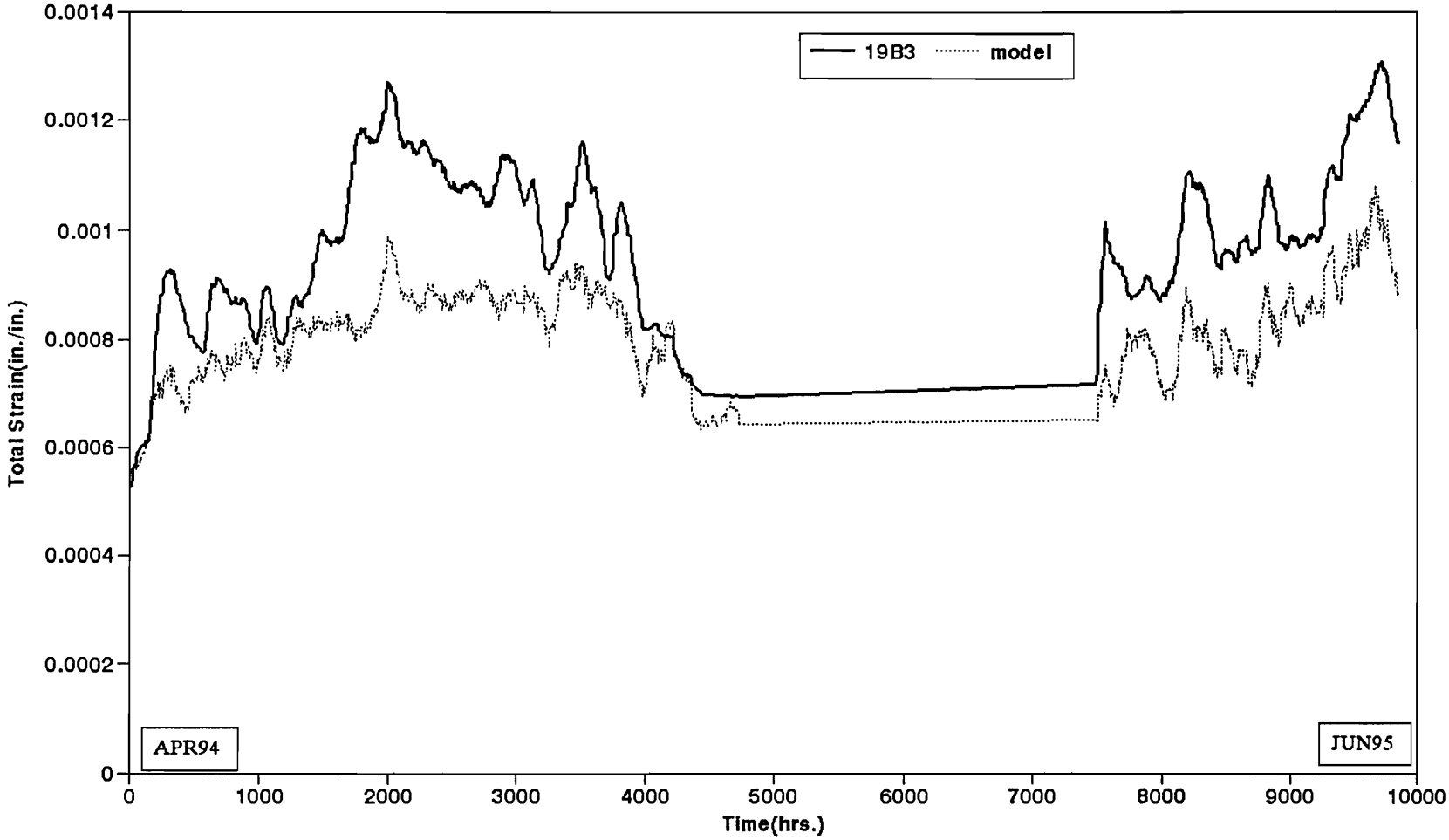

Figure 6-22 Four-Element Model Prediction for 19B3

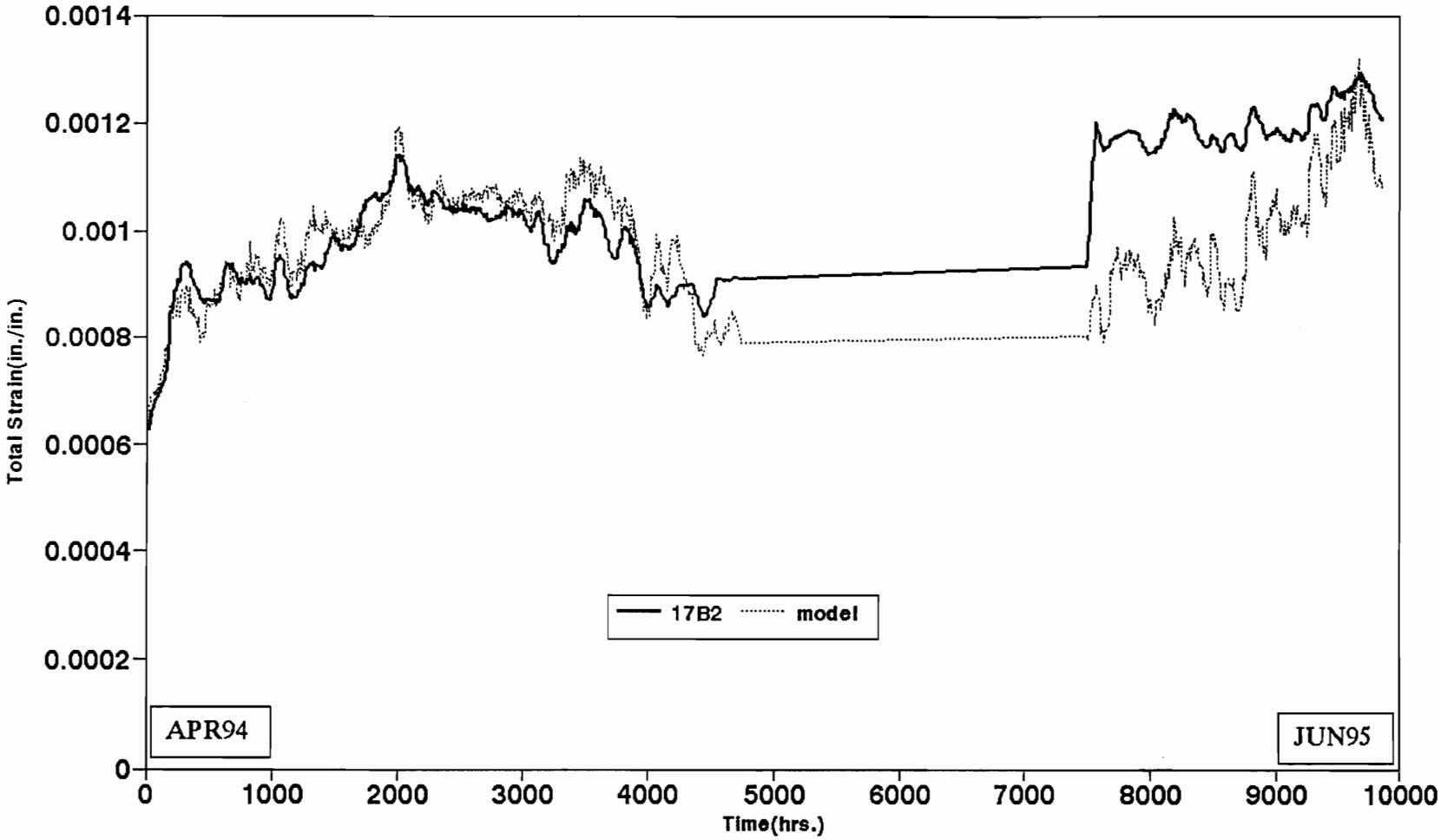

Figure 6-23 Four-Element Model Prediction for 17B2

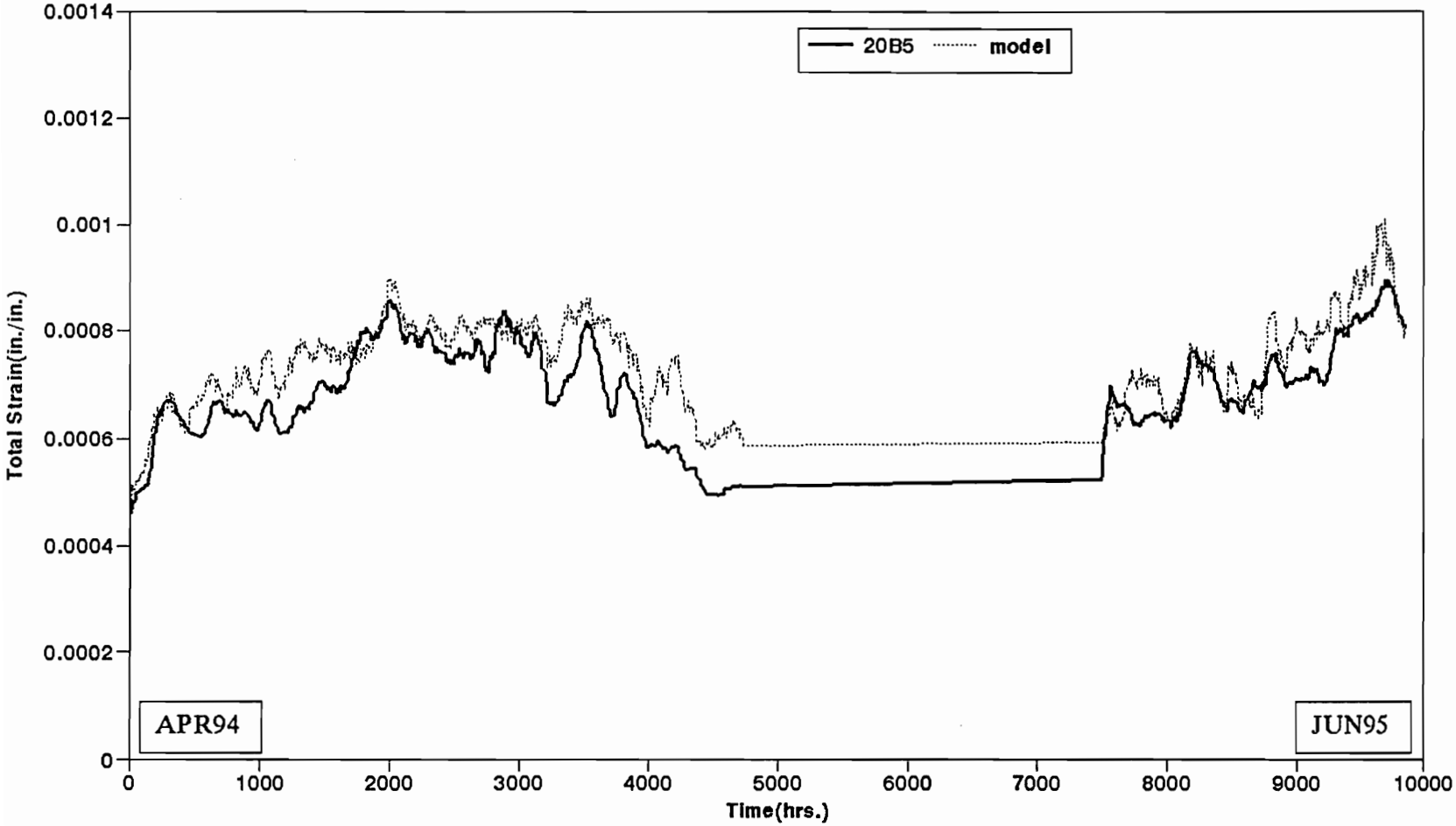

Figure 6-24 Four-Element Model Prediction for 20B5

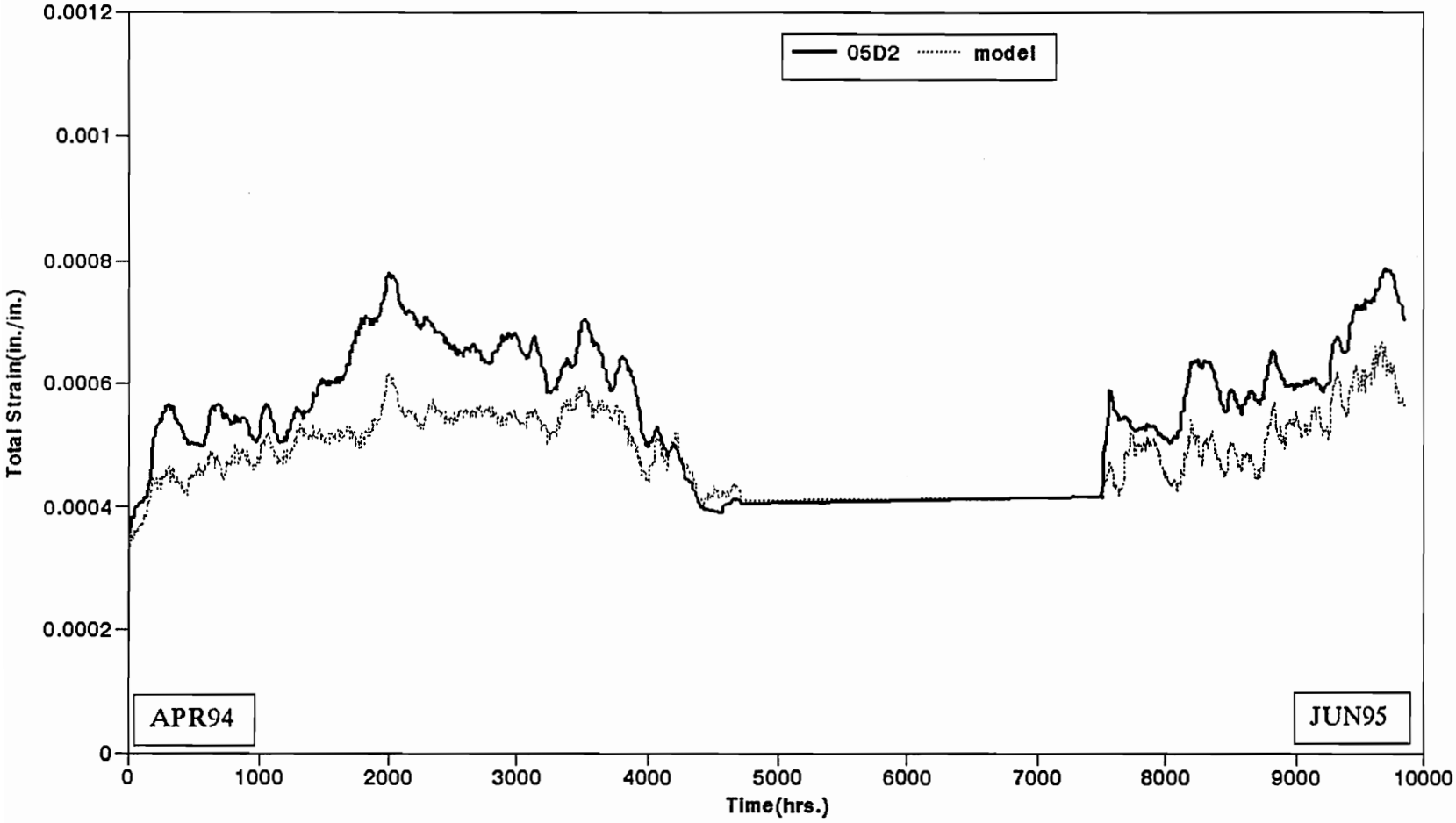

Figure 6-25 Four-Element Model Prediction for 05D2

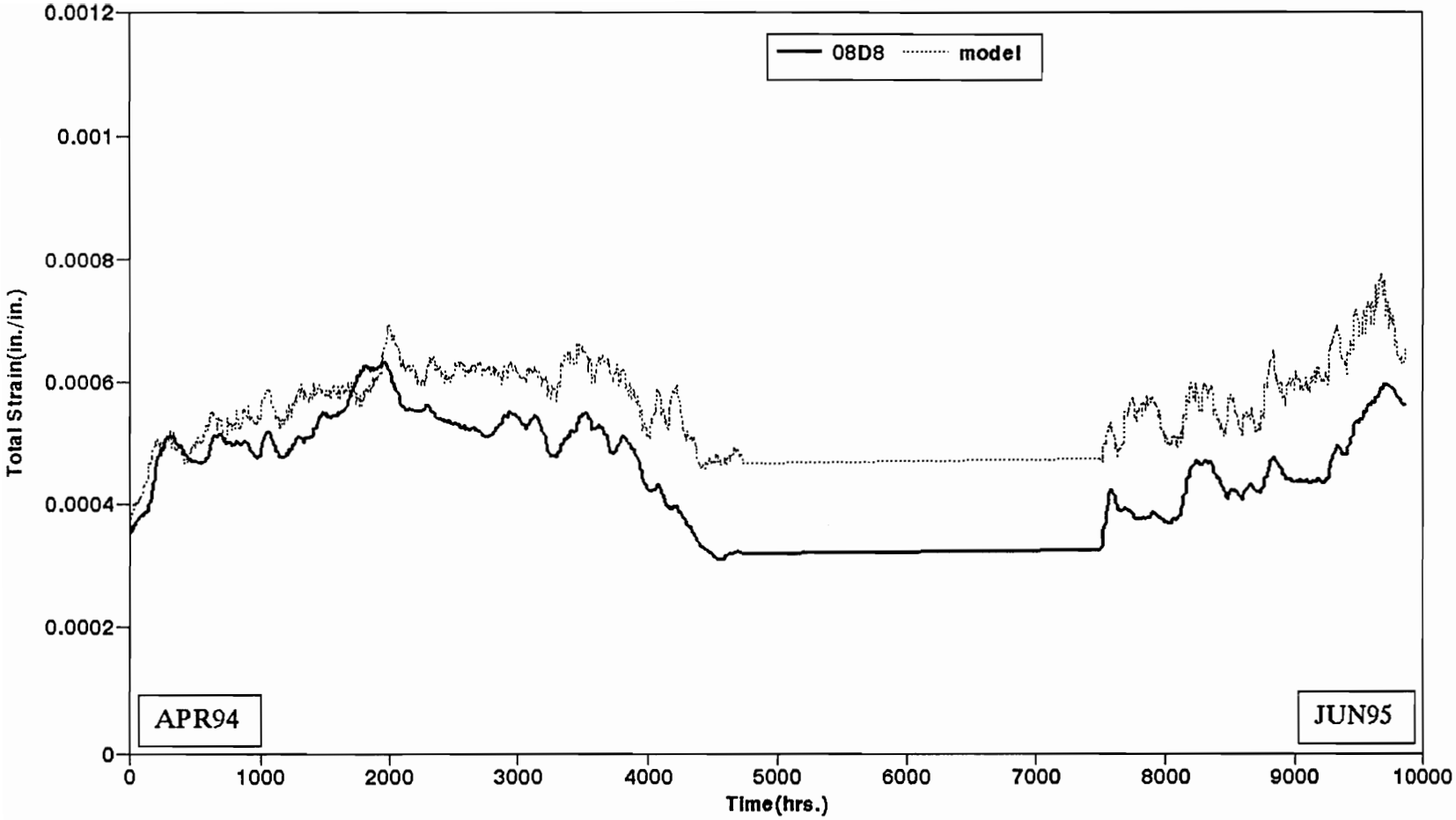

Figure 6-26 Four-Element Model Prediction for 08D8

5,000 hours. The reason could be that the model parameters are determined using the first 5,000 hour data only.

However, the model does not seem to predict creep strain of specimen 04A5 very well. Figure (6-12) shows that the experimental creep strain of 04A5 is much larger than the predicted strain using the model, although both curves have similar fluctuations. There are two possible reasons for this. One could be an error from MOE measurement, which is related to the MOE factor, Q, in the model. The other reason could be the defects in the specimen. It has been previously discussed and shown in Table (3-1) that the specimen, 04A5, has critical edge knots within the load span, which reduce the mechanical properties of the specimen, and cause more creep strain.

The four model parameters, K_c, K_k, μ_k, and μ_v must be positive based on their physical meanings. Since relative temperature, α, may be positive as the temperature is above 20° C, and negative as the temperature is below 20°C, it is possible for equations (5-3) to (5-6) to produce negative results, i.e., K_c, K_k, μ_k, and μ_v could be negative. Based on the model constants, q_1-q_8, listed in Table (5-2), the value of the four model parameters, K_c, K_k, μ_k, and μ_v will remain positive if air temperature is below 153° C. That is to say that the four model parameters in this study will remain positive under normal natural environmental conditions.

6.8 Empirical Model Prediction

Figure (6-27) shows both the predicted creep curve using the modified power law, equation (5-8), and the experimental creep curve of the reference

specimen, 07D5. Figures (6-28) to (6-45) show the predicted creep curve for all other specimens. In addition to the phenomenon that the predicted creep changes faster than the experimental creep, which has been explained in Section 6.7, it is also observed that the MOE has the same effects on the creep strain as it does on the total strain. In general, the predicted creep strain using the modified power law may quantitatively represent the experimental creep strain for every specimen. The MOE factors, Q, in the power law are the same as those in the four-element model.

Again, the model does not seem to predict creep strain of the specimen, 04A5. It has been discussed in Section 6.7 that the major reasons for the difference between the experimental creep strain and the predicted creep strain for the specimen, 04A5, are possible MOE measurement error and the specimen defects.

6.9 Predicted Data vs. Experimental Data

A computer program (Statgraphics 1991), was used to statistically compare the predicted creep data and the experimental data. The experimental data of the reference specimen, 07d5, and the predicted data using both the four-element model and the power law are imported into the program. The predicted data is statistically compared with the experimental data using the two sample tool in the program. The hypothesis tests shown in both Table (6-2) and Table (6-3), indicate that the predicted data using the four-element model is not significantly different from the experimental data, and the predicted data using the empirical model is

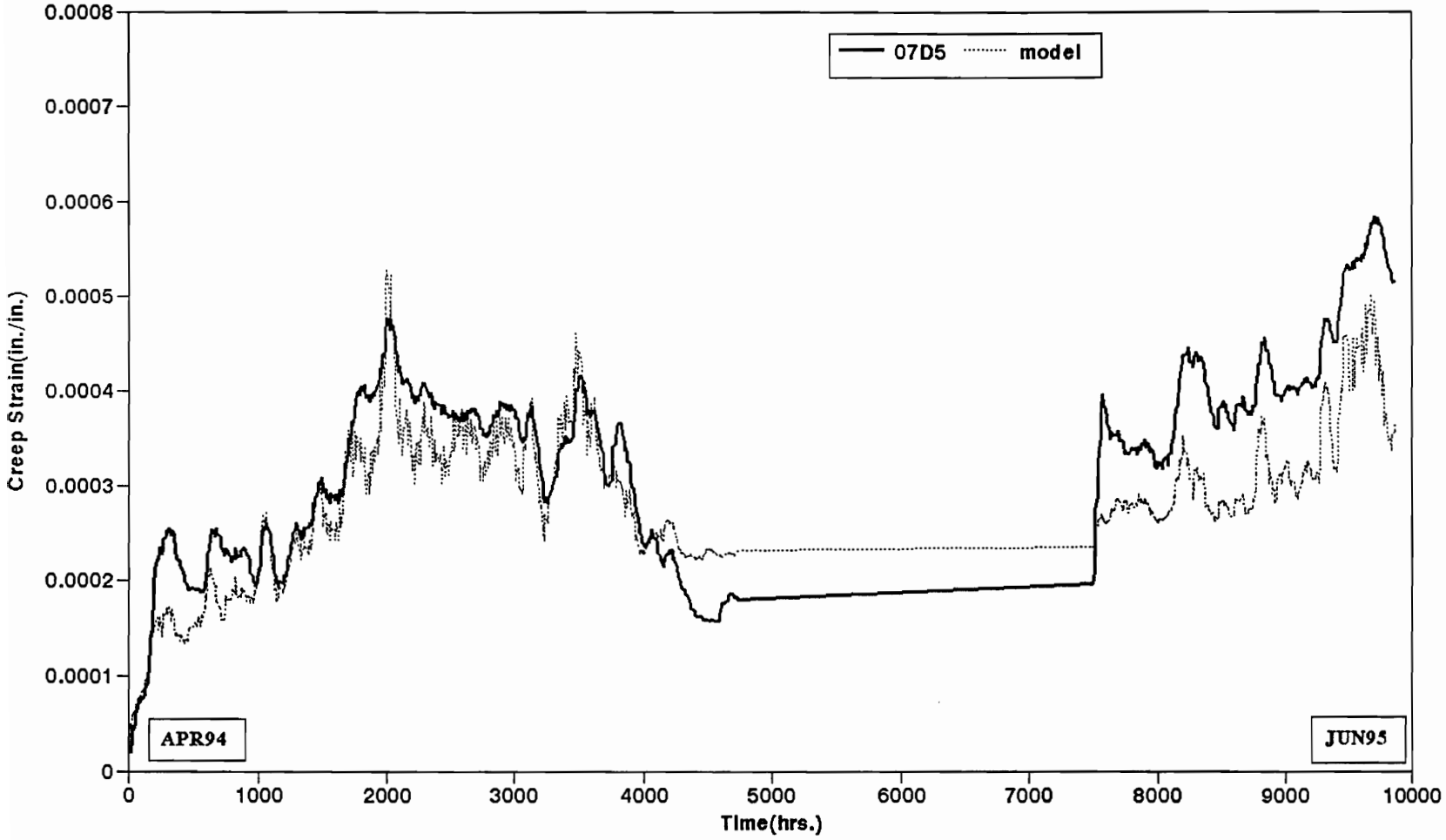

Figure 6-27 Empirical Model Prediction for Reference Beam 07D5

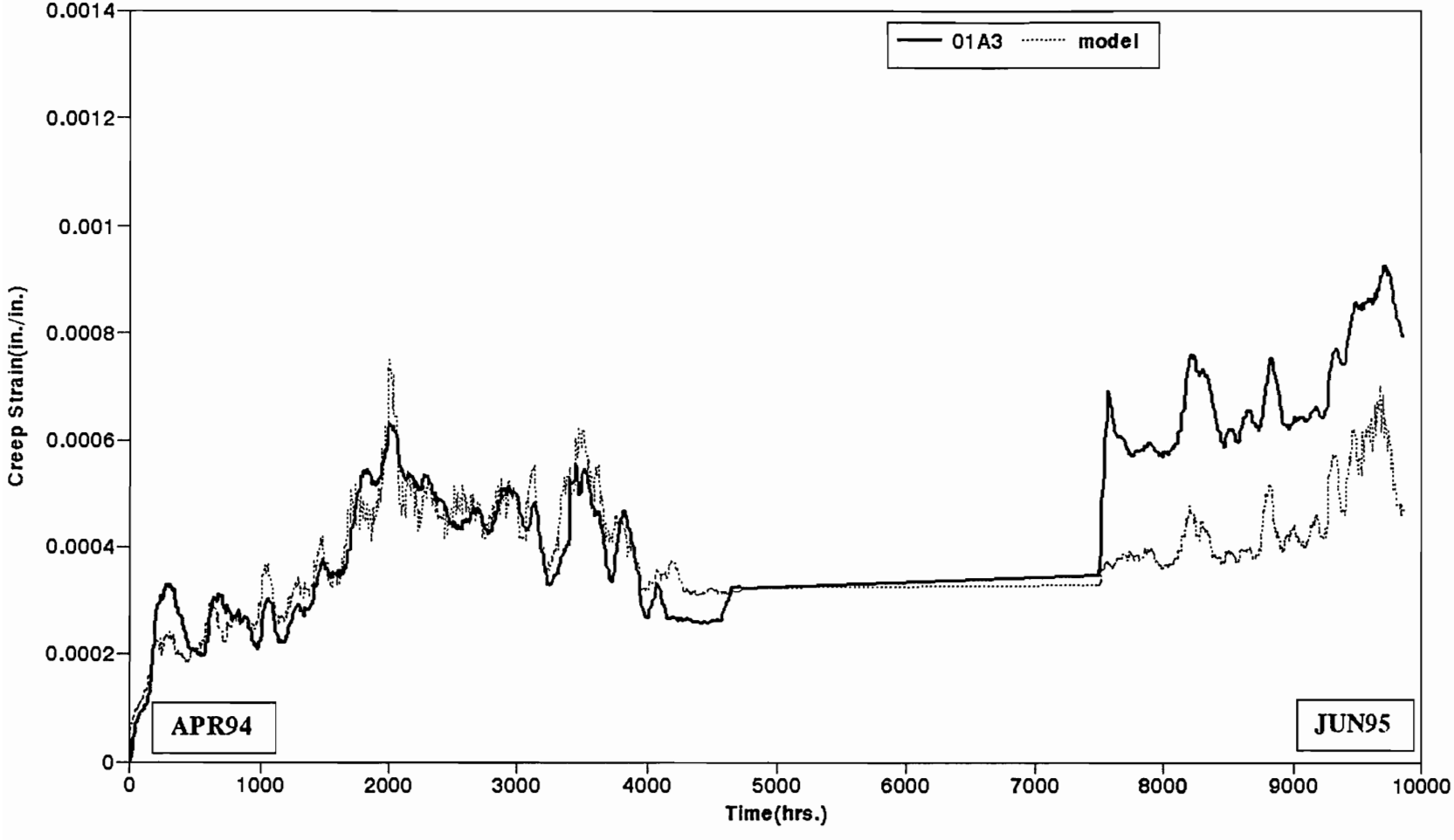

Figure 6-28 Empirical Model Prediction for 01A3

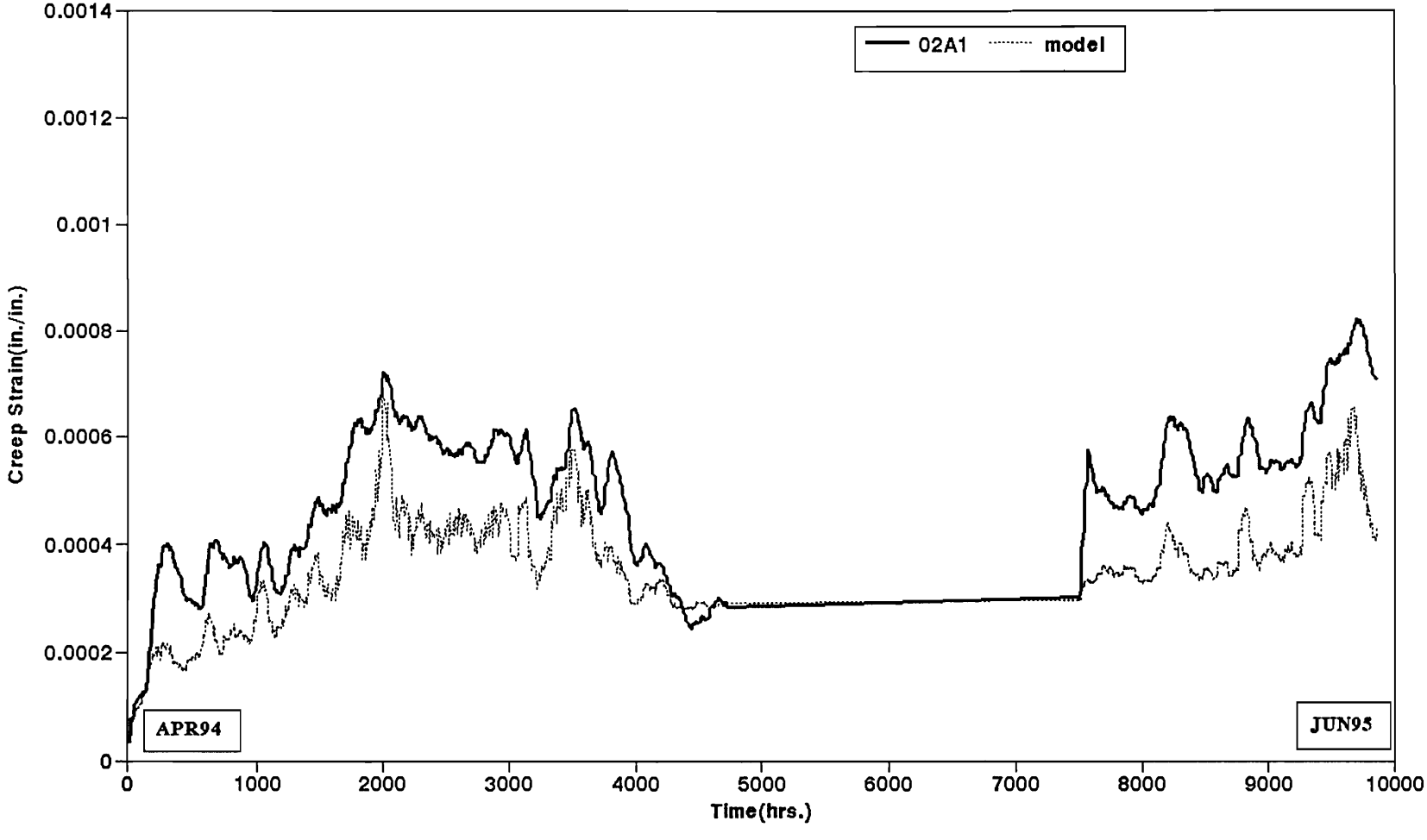

Figure 6-29 Empirical Model Prediction for 02A1

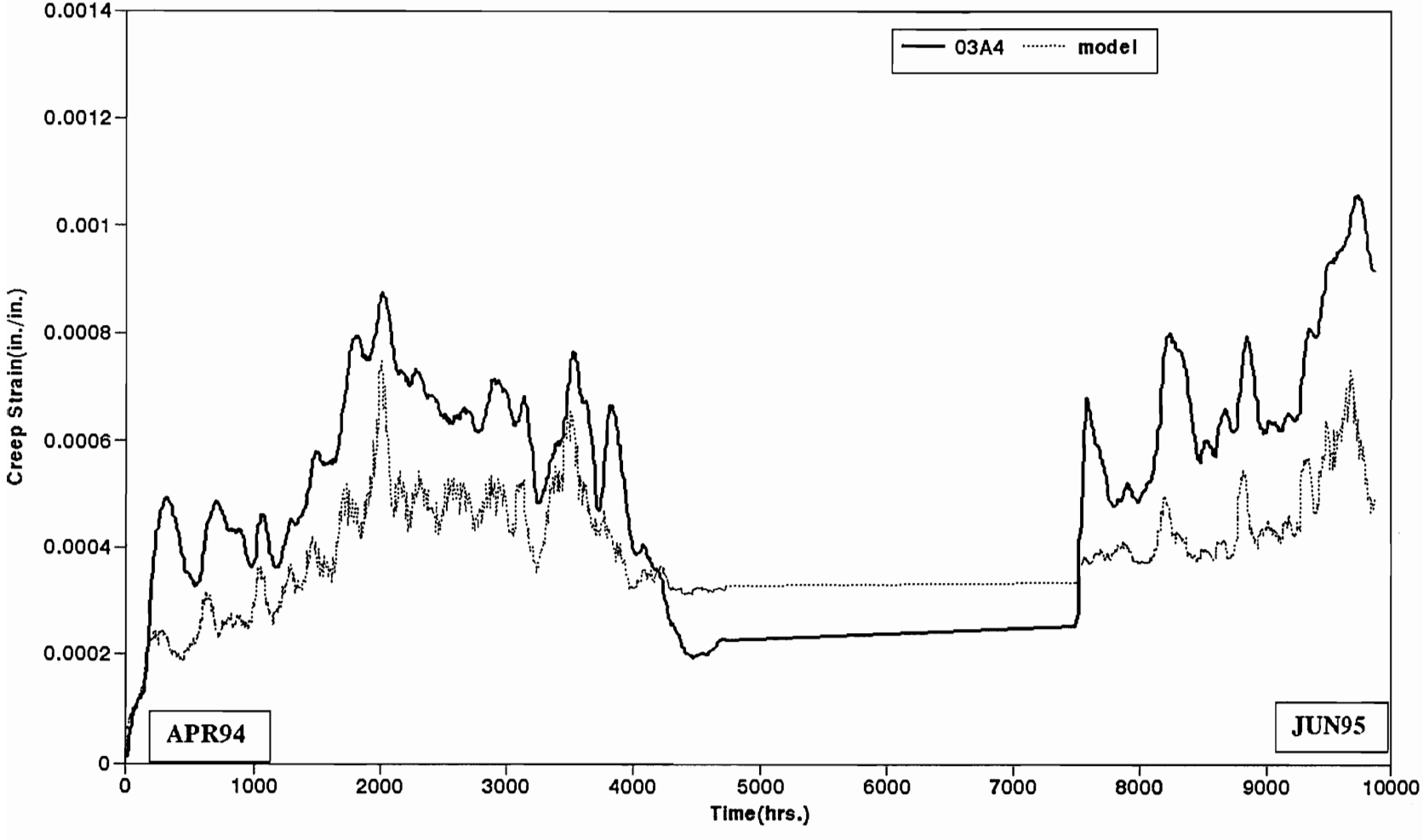

Figure 6-30 Empirical Model Prediction for 03A4

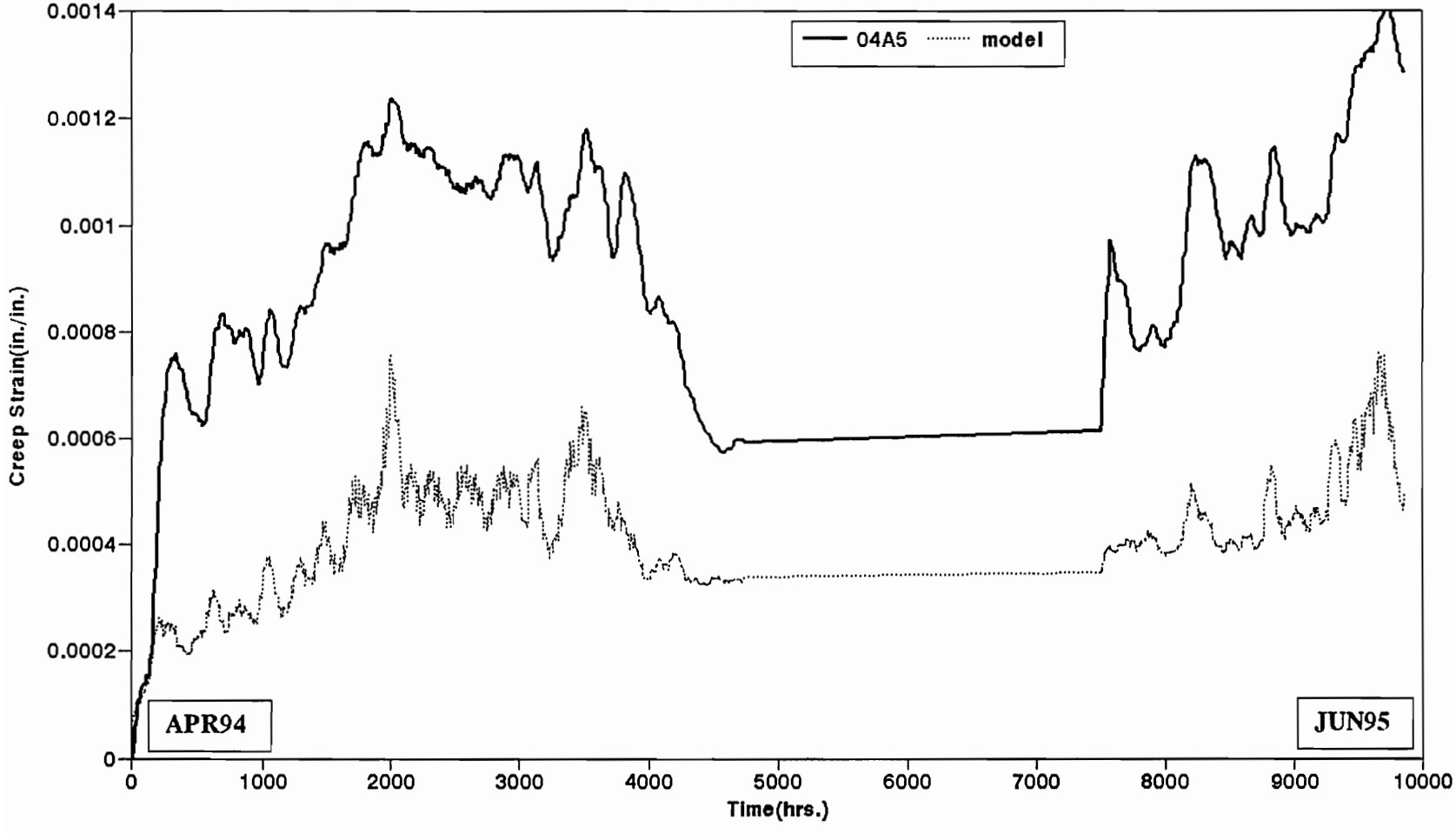

Figure 6-31 Empirical Model Prediction for 04A5

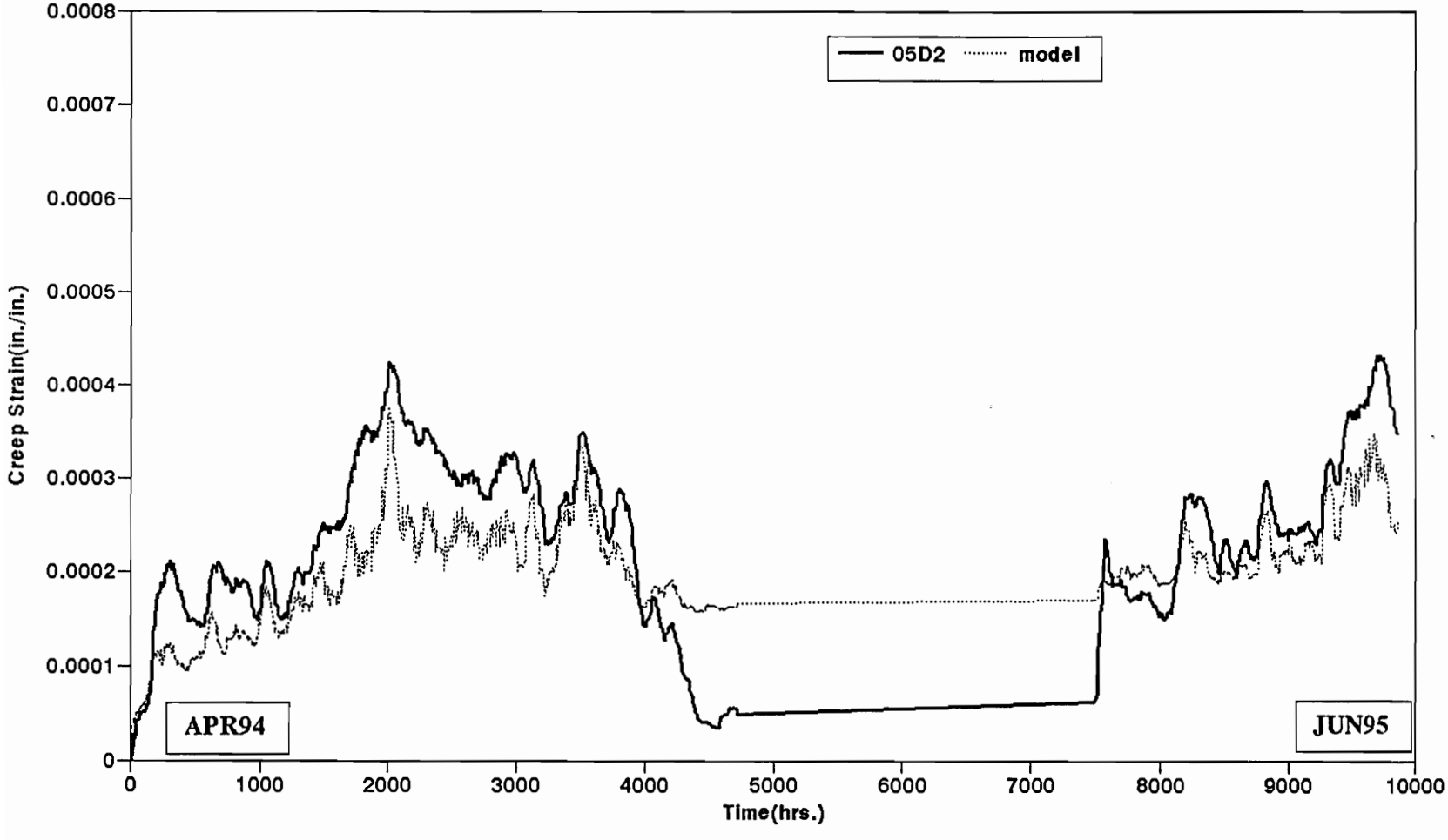

Figure 6-32 Empirical Model Prediction for 05D2

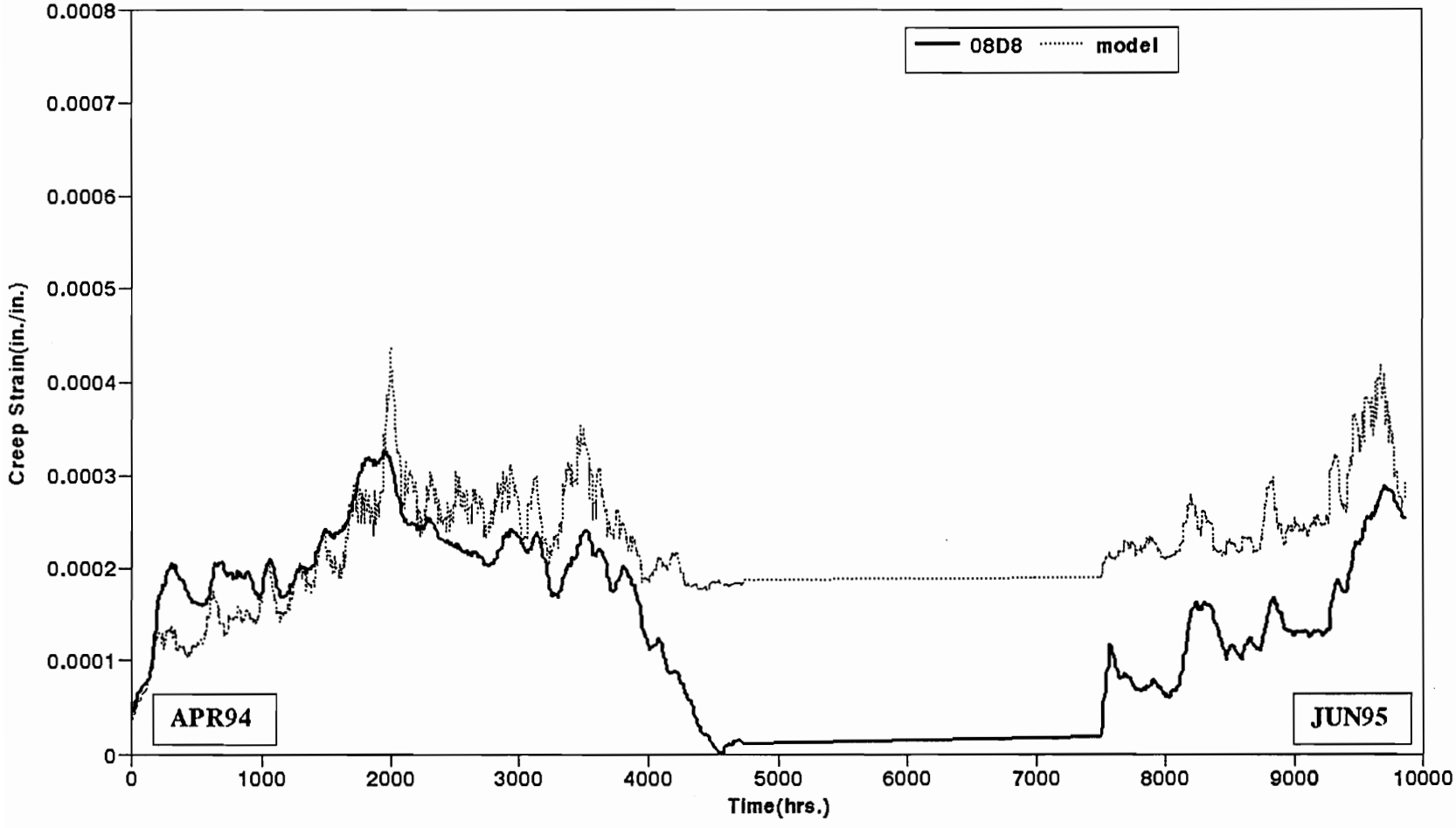

Figure 6-33 Empirical Model Prediction for 08D8

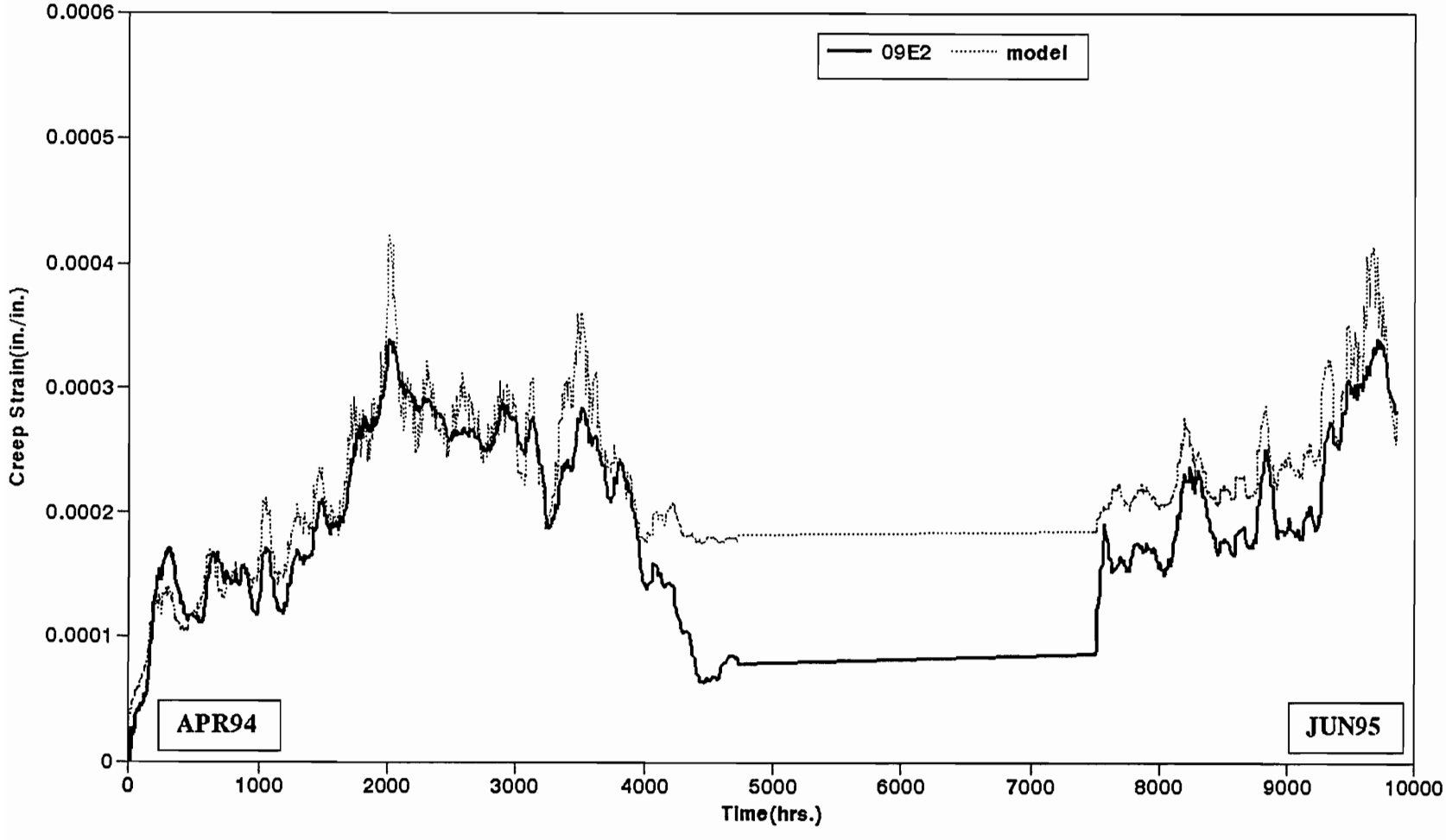

Figure 6-34 Empirical Model Prediction for 09E2

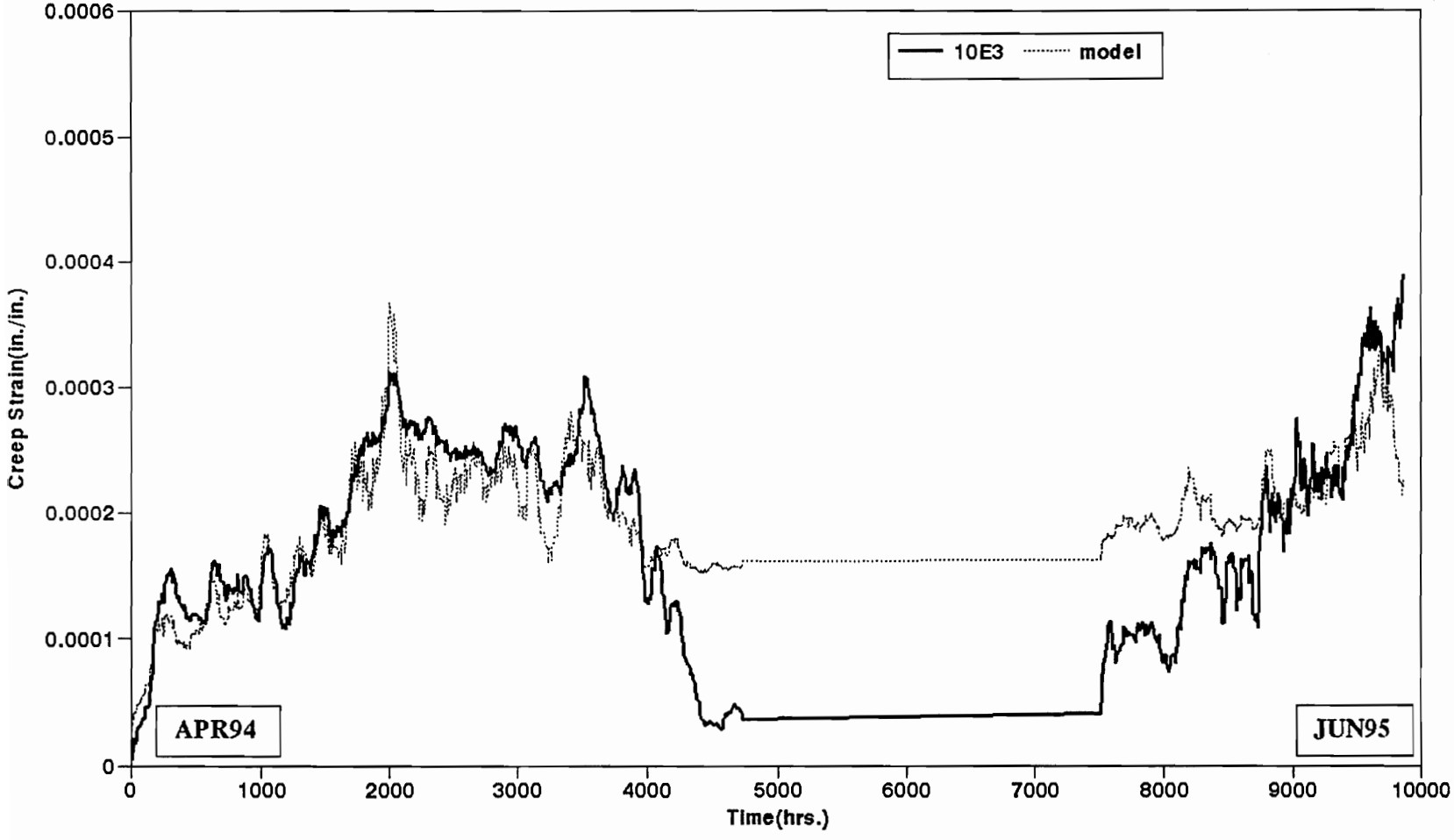

Figure 6-35 Empirical Model Prediction for 10E3

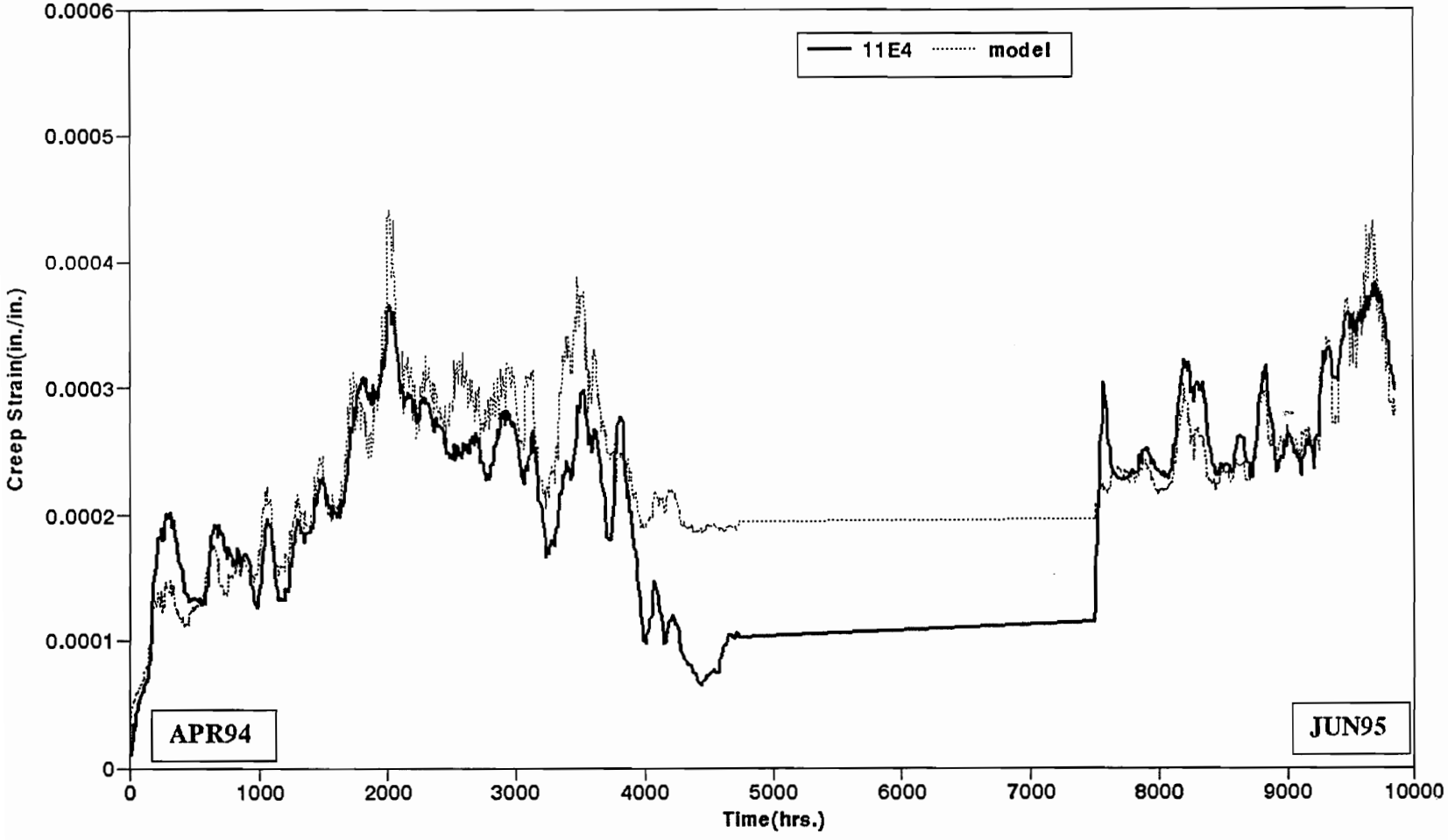

Figure 6-36 Empirical Model Prediction for 11E4

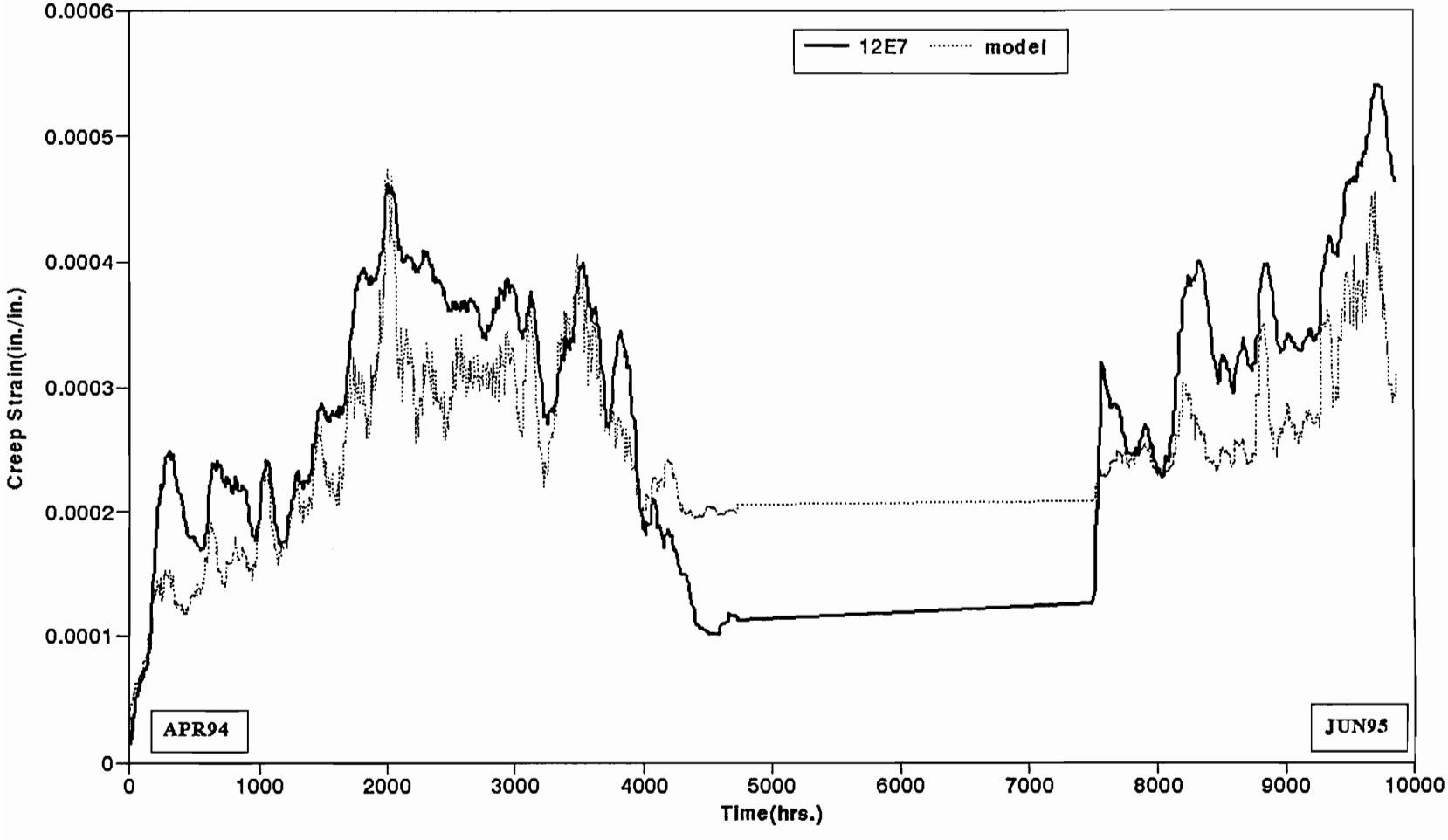

Figure 6-37 Empirical Model Prediction for 12E7

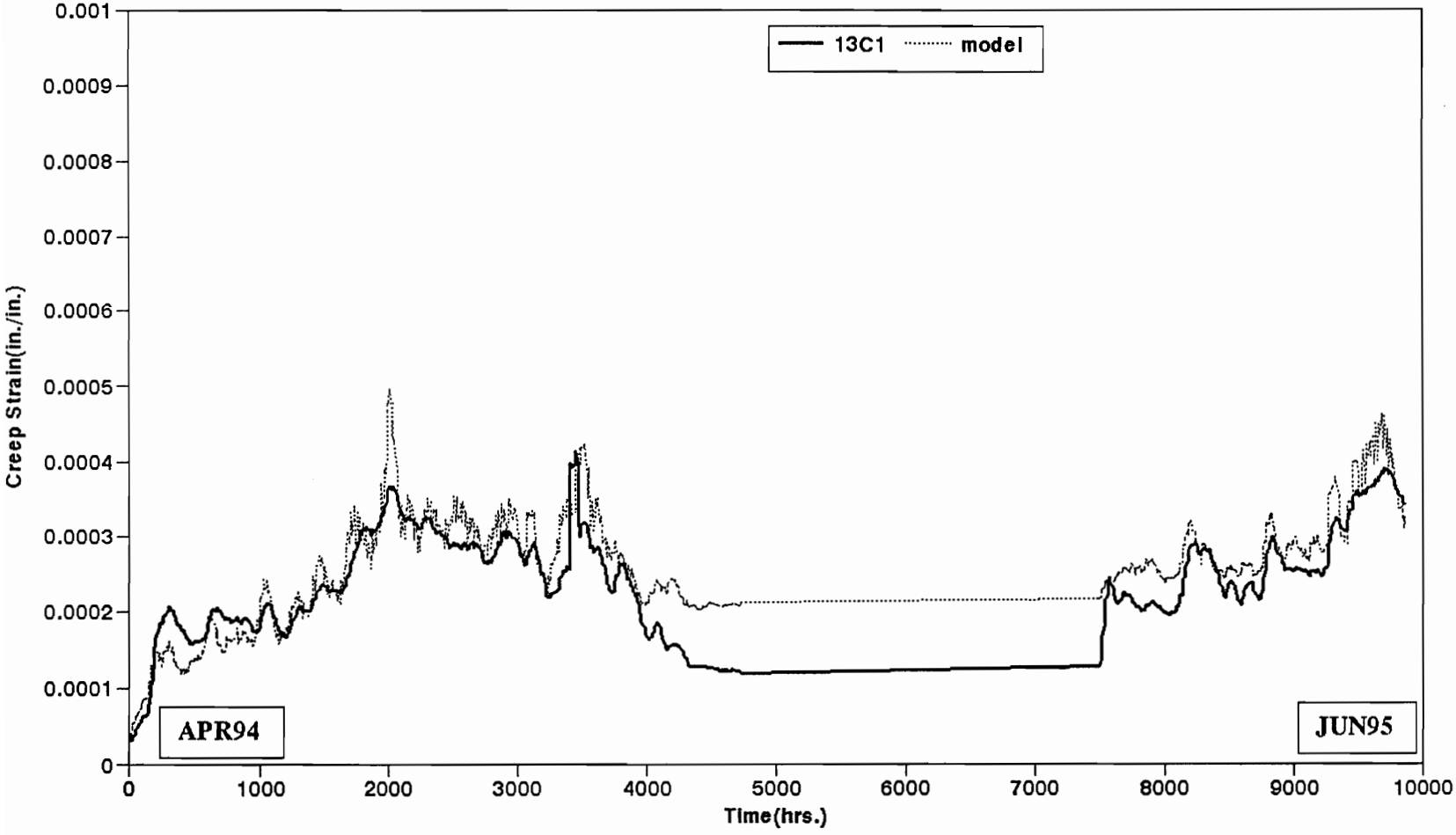

Figure 6-38 Empirical Model Prediction for 13C1

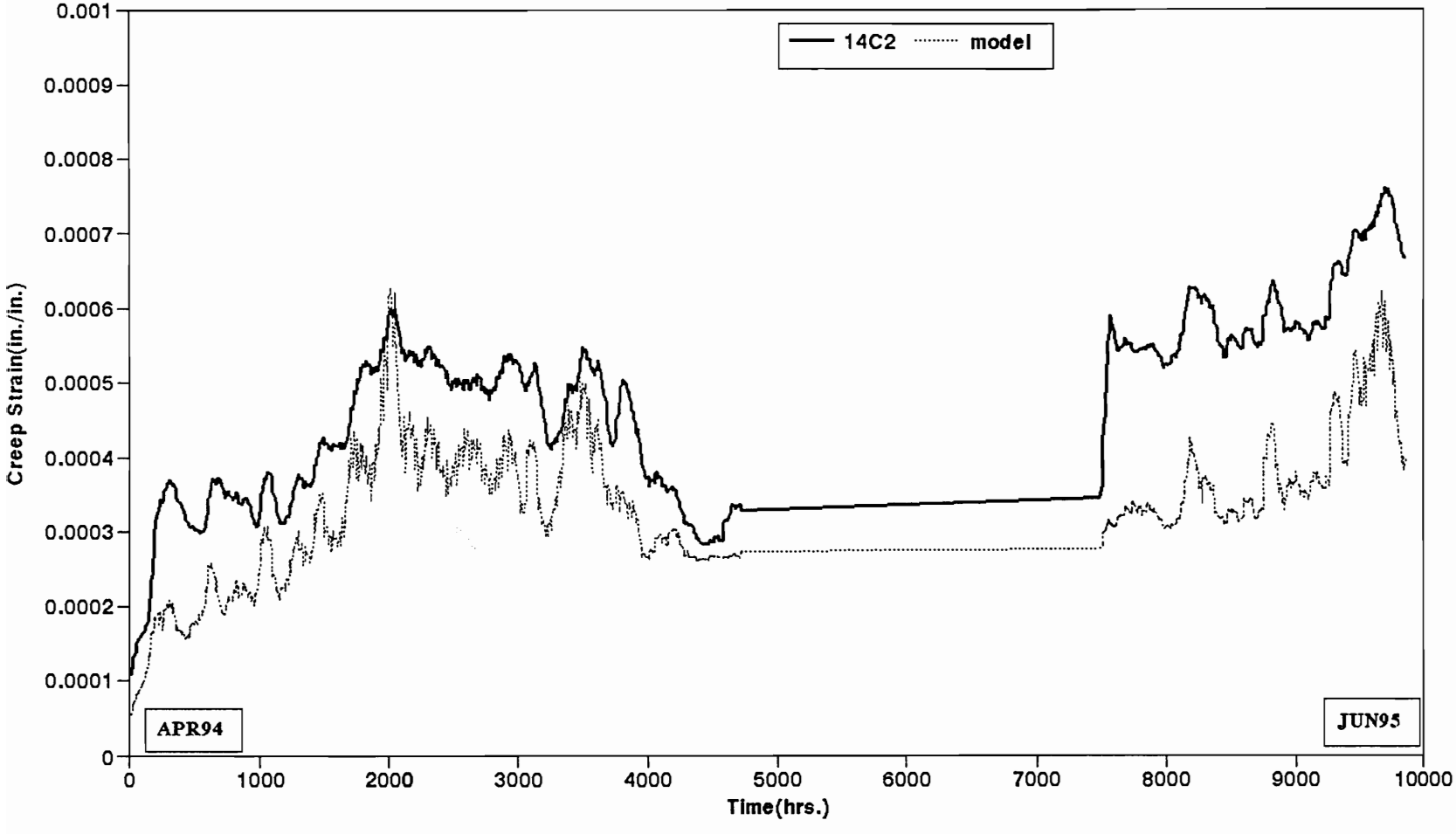

Figure 6-39 Empirical Model Prediction for 14C2

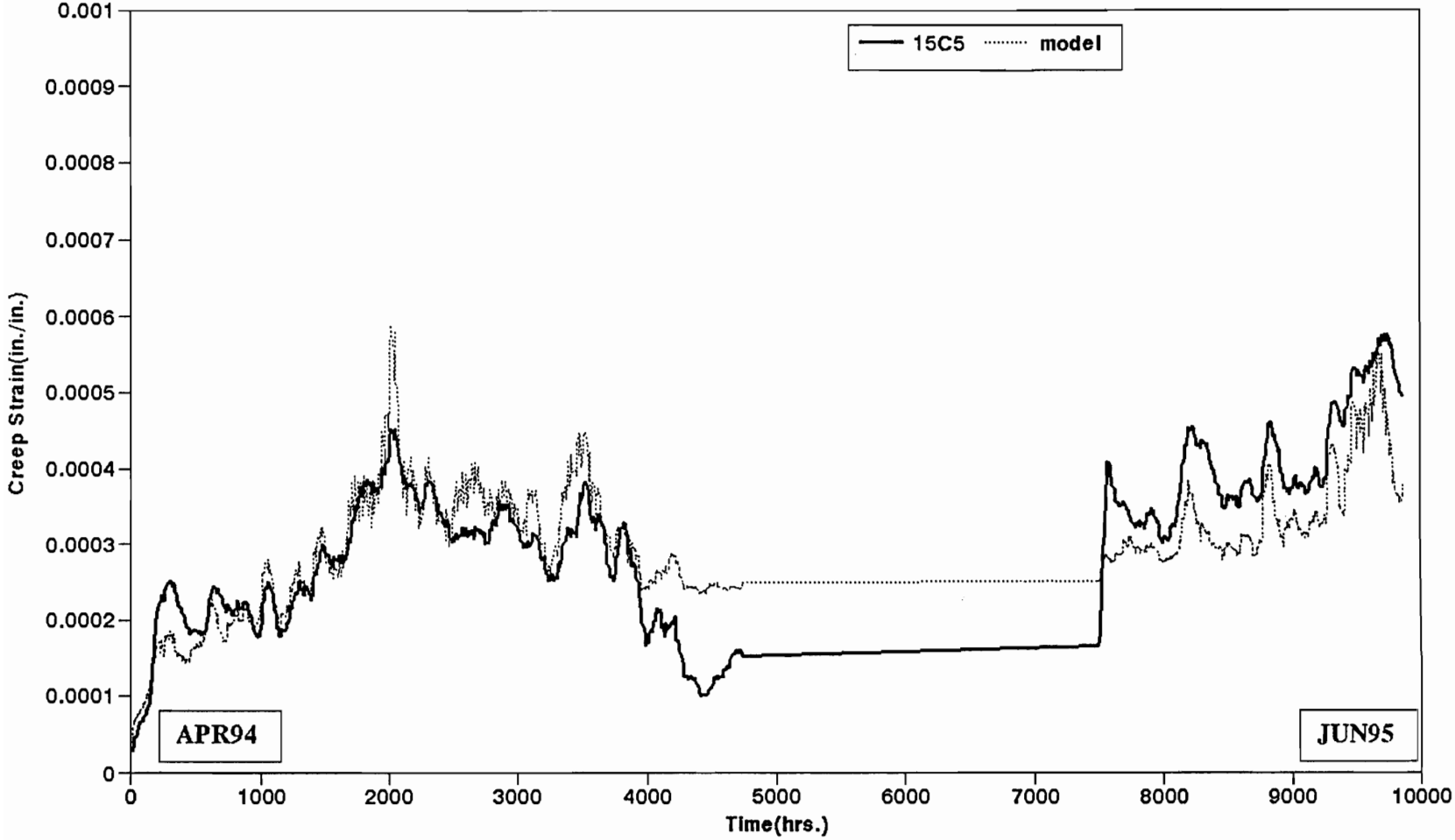

Figure 6-40 Empirical Model Prediction for 15C5

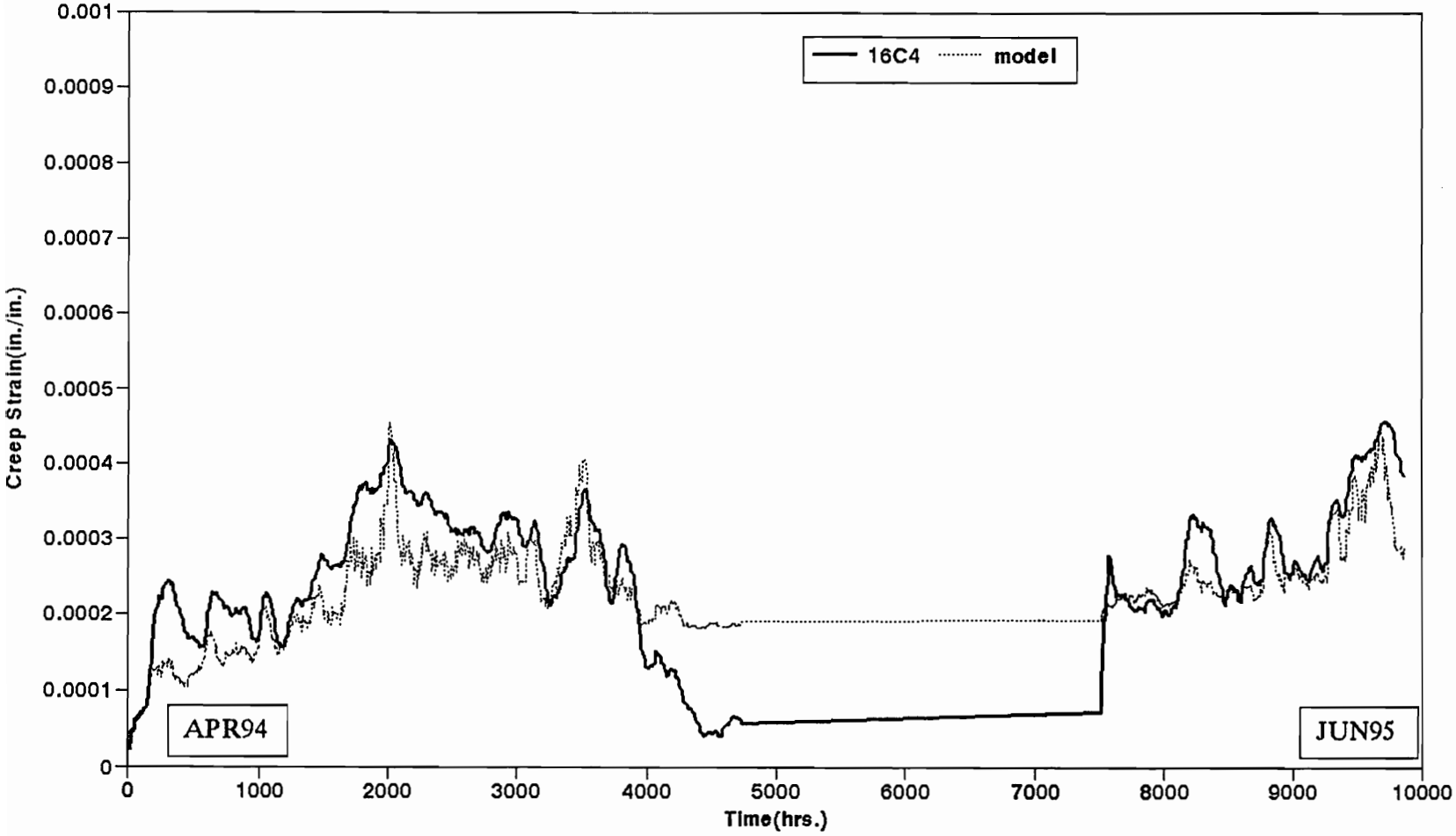

Figure 6-41 Empirical Model Prediction for 16C4

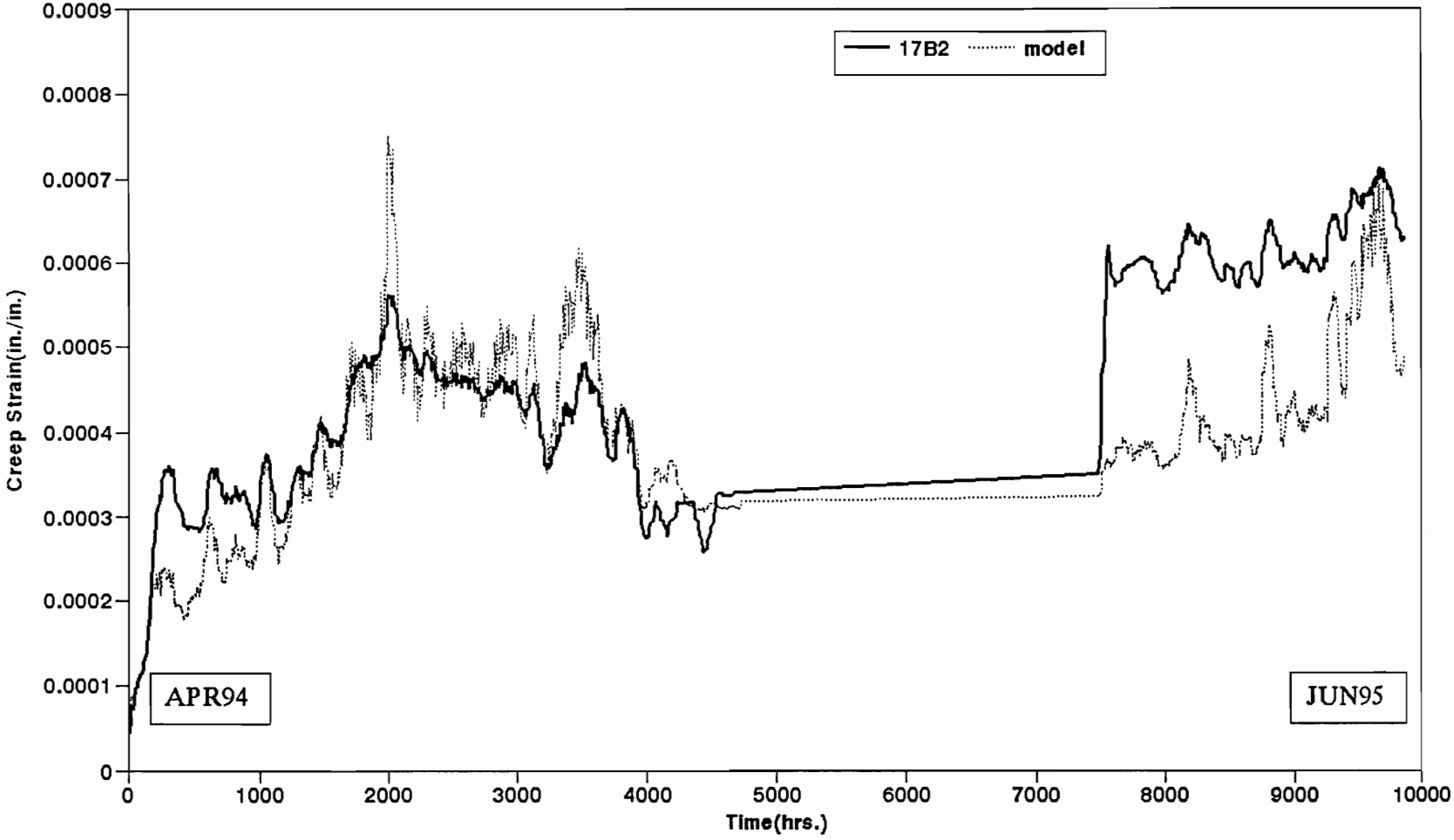

Figure 6-42 Empirical Model Prediction for 17B2

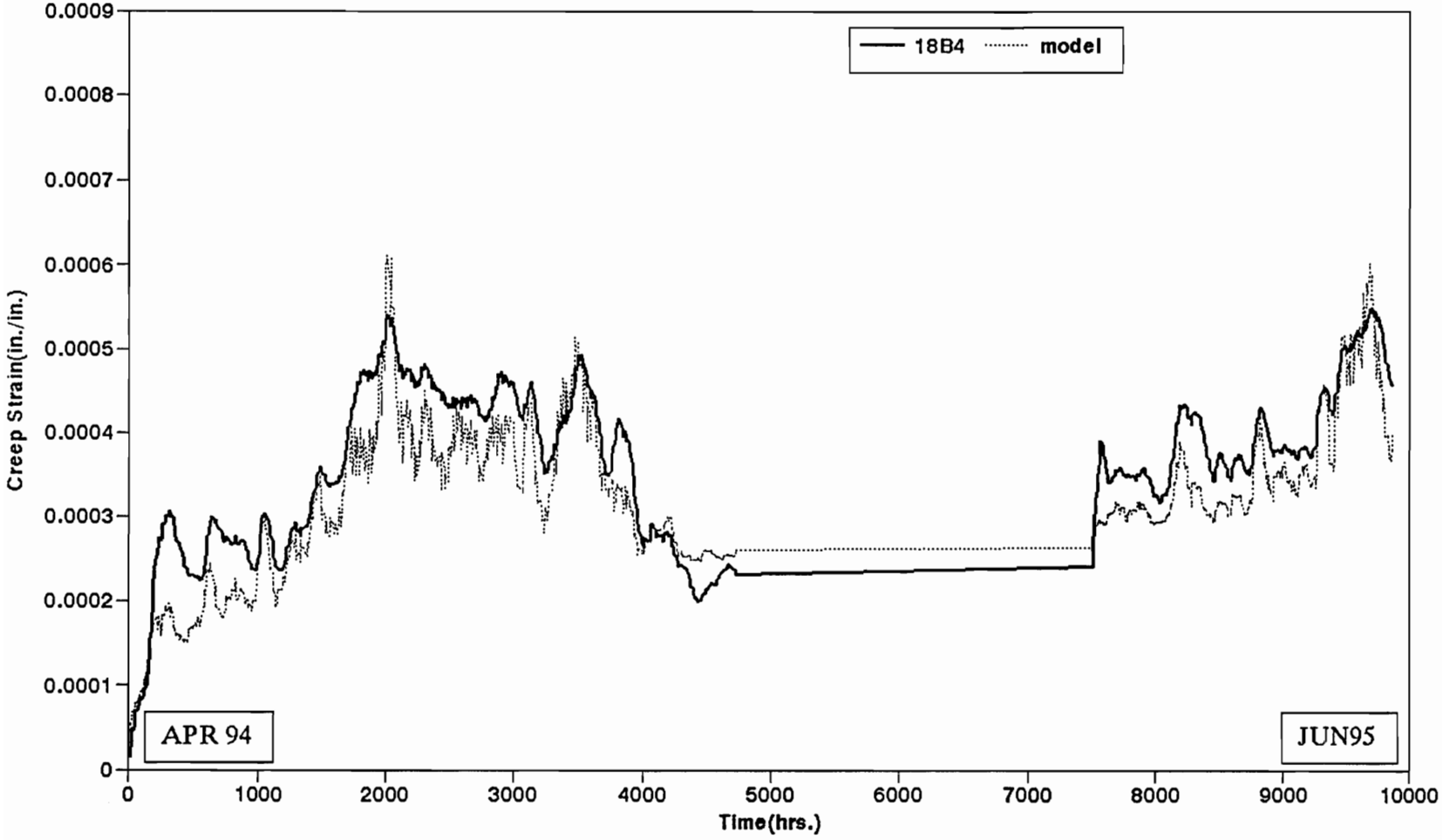

Figure 6-43 Empirical Model Prediction for 18B4

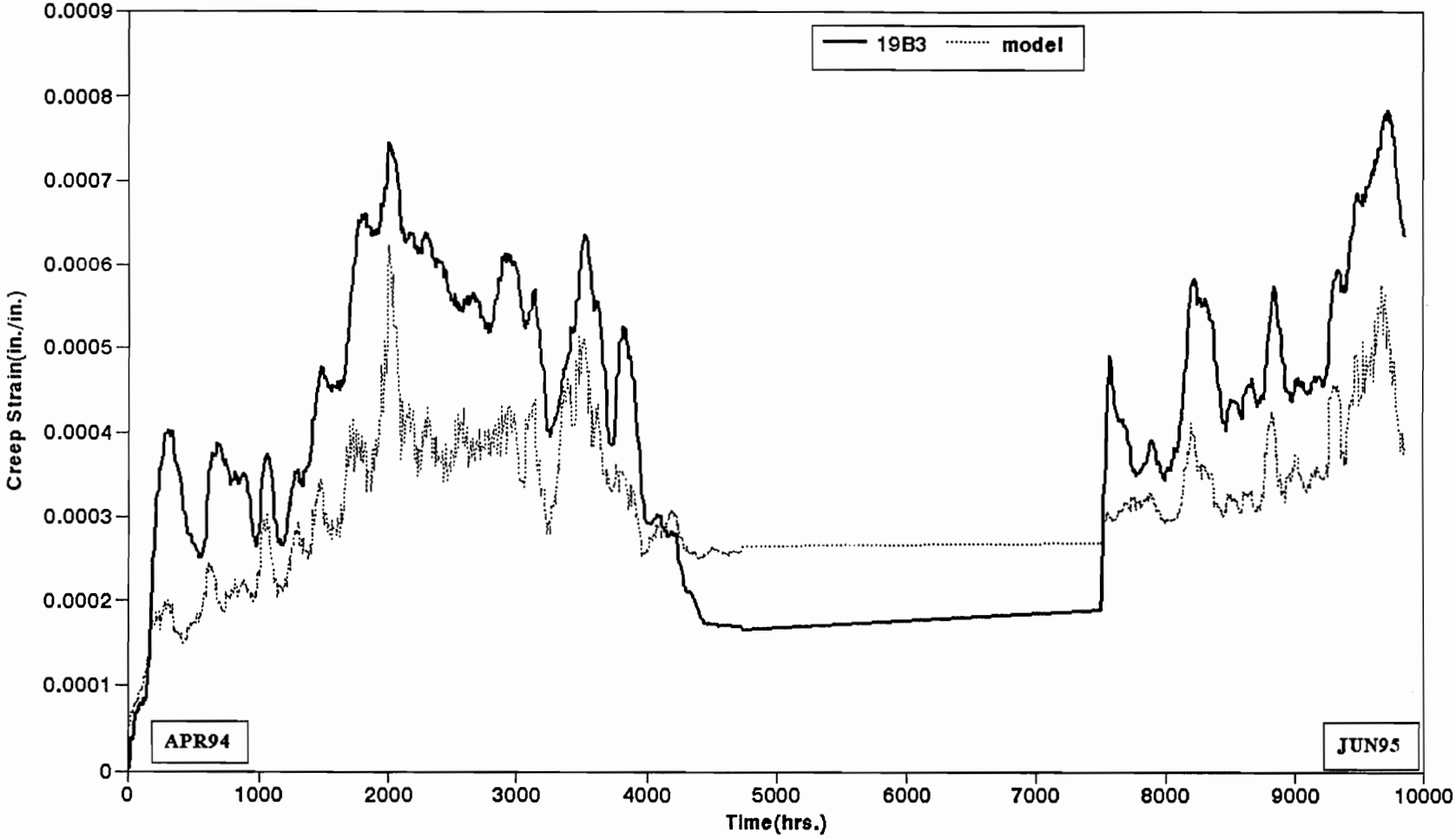

Figure 6-44 Empirical Model Prediction for 19B3

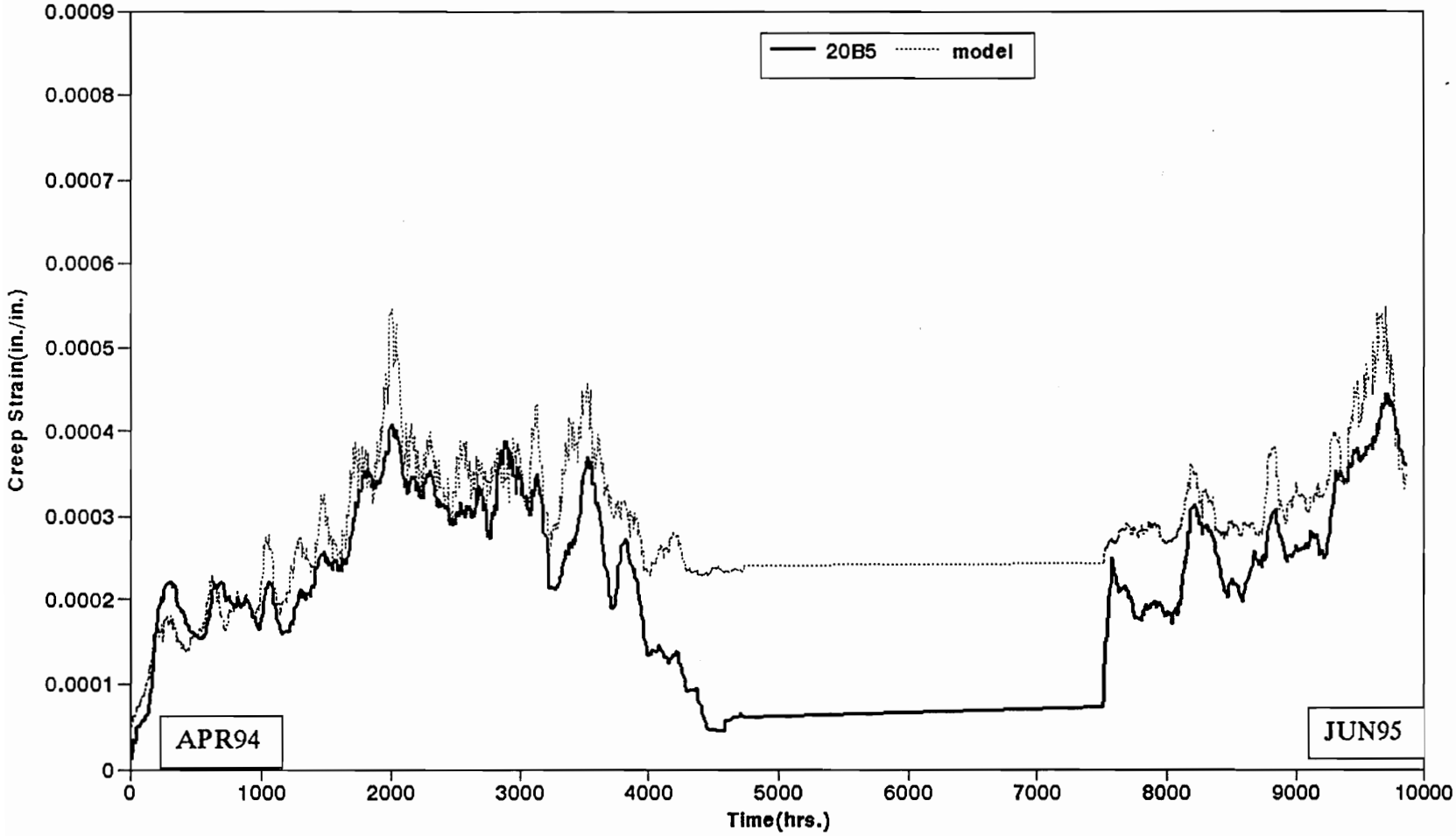

Figure 6-45 Empirical Model Prediction for 20B5

significantly different from the experimental data. Therefore, The four-element model, equation (5-1), is the better model to predict the creep behavior of structural lumber in a natural environment.

Table 6-2 Two-Sample Analysis Results (Experiment vs. Four-Element)

Sample	Experiment	Four-Element	Pooled
Number of Observations	796	796	1592
Mean	7.13×10^{-4}	7.08×10^{-4}	7.11×10^{-4}
Variance	9.30×10^{-9}	1.22×10^{-8}	1.08×10^{-8}
Standard Deviation	9.64×10^{-5}	1.11×10^{-4}	1.04×10^{-4}
Median	7.14×10^{-4}	7.09×10^{-4}	7.11×10^{-4}
Difference Between Means	5.18×10^{-6}		
95% Confidence Interval for DBM (Equal Variables) Smp1-Smp2 (Unequal Variables)	 -5.02×10^{-6} -5.02×10^{-6}	 1.54×10^{-5} 1.54×10^{-5}	 1590 D.F. 1561.1 D.F.
Ratio of Variances	0.76		
Confidence Interval for ROV Smp1/Smp2	0%		
Hypothesis Test for H0 Difference=0 vs. Alt.=NE at Alpha=0.05	Computed t statistic=0.996 Significant Level (P value)=0.319 **So do not reject H0**		

Table 6-3 Two-Sample Analysis Results (Experiment vs. Empirical)

Sample	Experiment	Four-Element	Pooled
Number of Observations	796	796	1592
Mean	2.91×10^{-4}	2.74×10^{-4}	2.83×10^{-4}
Variance	9.30×10^{-9}	1.73×10^{-8}	1.33×10^{-8}
Standard Deviation	9.64×10^{-5}	1.32×10^{-4}	1.15×10^{-4}
Median	2.92×10^{-4}	2.28×10^{-4}	2.51×10^{-4}
Difference Between Means	1.64×10^{-5}		
95% Confidence Interval for DBM (Equal Variables) Smp1-Smp2 (Unequal Variables)	 5.01×10^{-6} 5.01×10^{-6}	 2.77×10^{-5} 2.77×10^{-5}	 1590 D.F. 1457.2 D.F.
Ratio of Variances	0.54		
Confidence Interval for ROV Smp1/Smp2	0%		
Hypothesis Test for H0 Difference=0 vs. Alt.=NE at Alpha=0.05	Computed t statistic=2.828 Significant Level (P value)=4.68×10^{-3} **So reject H0**		

VII. SUMMARY

Based on the analysis of the fourteen-month data from the creep experiment, it may be concluded that creep deformation can be much larger than elastic deformation, depending upon stiffness of the beams.

Fridley's five-element creep model does not predict creep behavior of structural lumber in a natural environment. Because of minimal change in moisture content in the specimens, the mechano-sorptive element in five-element model did not contribute to creep strain of structural lumber under the natural environmental conditions of this study. That is, the normally exhibited mechano-sorptive strain caused by a significant moisture content change in wood under a controlled environment does not exist, when wood is subjected to natural weather conditions, and the mechano-sorptive creep strain is likely the shrinking and swelling on the surfaces of the beam.

Fluctuations of creep strain follow variations in air temperature, and creep strain is larger for low MOE specimens than for high MOE ones. Temperature fluctuations and edge-wise MOE are considered to be two major effects in modelling. In addition, the differences of creep strain between each specimen could also be produced by different stress levels (percentage of ultimate strength) applied on each specimen. Both a four-element model and a power law model were developed to predict the creep strain of structural lumber in a natural environment. The four-element model is statistically equivalent to the experimental data, however, the empirical model is not.

It is recommended for further study that creep behavior be simulated using the four-element model under random varying load levels, and natural environmental conditions. A data base for creep factor, the ratio of creep strain and elastic strain, under the random conditions, can be established afterwards. It is always valuable for wood designers to compare those creep factors recommended by either NDS or ASTM with those in the data base, in order to produce safer and more economic designs.

BIBLIOGRAPHY

American Society for Testing and Materials 1990 *Standard method of testing for small clear specimens of timber.* Designation 143, Annual Book of ASTM Standards. Vol. 04.09.

Armstrong, L.D. and R.S.T.Kingston 1962 *The effect of moisture content changes on the deformation of wood under stress.* Austr.J. of Appl. Sci. 13(4):257-276.

ASCE 1990 *Minimum design loads for buildings and other structures.* (ASCE 7-88), American Society of Civil Engineers, NY.

Bach, L.and R.E. Pentoney 1968 *Nonlinear mechanical behavior of wood.* For.Prod.J. 18(3):60-66.

Bazant, Z.P. 1985: *Constitutive equation of wood at variable humidity and temperature.* Wood Sci. Technol. 19:159-177.

Bhatnagar, N.S. 1964 *Creep of wood in tension parallel to grain.* Holz als Roh- und Werkstoff. 22(8):296-299.

Bodig, J. and B.A. Jayne 1982 *Mechanics of wood and wood composites.* Van Nostrand Reinhold Co. Chap. 5.

Burns, P.J. 1993 *Using Quattro Pro 5.0.* by Que Corporation, Carmel, IN USA.

Campbell Scientific, Inc. HMP35C Temperature/RH Probe Instruction Manual, Revision: Feb. 15, 1993.

Clouser,W.S. 1959 *Creep in small wood beams under constant bending load.* Report No.2150, U.S. Dept. of Agric. Forestry Service, Forest Products Lab., Madison, Wis.

Davidson, W.Robert 1962 *The influence of Temperature on Creep in Wood.* Forest Products Journal. 12(8):377-381.

Findley, W.N., J.S. Lai and K.Onaran 1976 *Applied mathematics and mechanics: Creep and relaxation of nonlinear viscoelastic materials.* North-Holland Pub. Co. Chap. 1 and Chap. 5.

Fridley, K.J. 1990 Load-duration behavior of structural lumber: Effect of mechanical and environmental load histories. Dissertation for PhD at Auburn University.

Fridley, K.J., R.C. Tang and L.A. Soltis 1990a *Thermal effects on load-duration behavior of lumber. Part 1. Effect of constant temperature.* Wood and Fiber Sci. 21(4):420-431.

Fridley, K.J., R.C. Tang and L.A. Soltis 1990b *Thermal effects on load-duration behavior of lumber. Part 2. Effect of cyclic temperature.* Wood and Fiber Sci. 22(2):204-216.

Fridley, K.J., R.C. Tang and L.A. Soltis 1991 *Moisture effects on load-duration behavior of lumber. Part 1. Effect of constant relative humidity.* Wood and Fiber Sci. 23(1):114-127.

Fridley, K.J., R.C. Tang and L.A. Soltis 1992a *Hygrothermal effects on mechanical properties of lumber.* Journal of structural engineering. 118(2):567-581.

Fridley, K.J., R.C. Tang and L.A. Soltis 1992b *Moisture effects on load-duration behavior of lumber. Part 2. Effect of cyclic relative humidity.* Wood and Fiber Sci. 24(1):89-98.

Fridley, K.J., R.C. Tang, L.A. Soltis and Chai H. Yoo 1992c *Hygrothermal effects on load-duration behavior of structural lumber.* Journal of structural Engineering. 118(4):1023-1038.

Fridley, K.J., R.C. Tang and Lawrence A. Soltis 1992d *Creep behavior model for structural lumber.* Journal of Structural Engineering. 118(8):2261-2277.

Fridley, K.J. 1992e *Designing for creep in wood structures.* Forest Products Journal.42(3):23-28.

Gerhards,C.C. 1985 *Time-dependent bending deflections of Douglas-fir 2 by 4's.* Forest Products Journal. 35(4):18-26.

Gerhards,C.C. 1988 *Effect of grade on load duration of douglas-fir lumber in bending.* Wood and Fiber Sci. 20(1):146-161.

Gerhards, C.C. 1991 *Bending creep and load duration of Douglas-fir 2 by 4s under constant load.* Wood and Fiber Sci. 23(3):384-409.

Gressel, P. 1984 *Prediction of long-term deformation behavior from short-term creep experiments.* Holz als Roh-und Werkstoff. 42:293-301.

Grossman, P.U.A. and Kingston 1954 *Creep and stress relaxation in wood during bending.* Australian J.Appl.Sci. 5(4):403-417.

Handbook of Chemistry and Physics 1989-1990. 70TH edition. CRC Press, Inc., Boca Raton, Florida.

Hoffmeyer, P. and R.W. Davidson 1989 *Mechano-sorptive creep mechanism of wood in compression and bending.* Wood Sci. Technol. 23:215-227.

Hoffmeyer, P. 1990 *Failure of wood as influenced by moisture and duration of load.* Doctoral Dissertation. College of Environmental Science and Forestry, SUNY, N.Y. USA

Hoffmeyer, P. 1993 *Non-linear creep caused by slip plane formation.* Wood Sci. Technol. 27: 321-335

Holzer, S.M., J.R. Loferski, D.A. Dillard 1989 *A review of creep in wood: concepts relevant to develop long-term behavior predictions for wood structures.* Wood and Fiber Sci. 21(4):376-392.

Hoyle, J.R., Jr., Michael C.Griffith and Rafik Y.Itani 1985 *Primary creep in douglas-fir beams of commercial size and quality.* Wood and Fiber Sci. 17(3):300-314.

Hoyle, J.R., Jr.,Rafik Y.Itani and J. Jeckard 1986 *Creep of douglas fir beams due to cyclic humidity fluctuations.* Wood and Fiber Sci. 18(3):468-477.

Kassimal, A. 1993 *Structural Analysis*, PWS-Kent Publishing Company, Boston.

King, E.J.,Jr. 1961 *Time-dependent strain behavior of wood in tension parallel to grain.* For.Prod.J. 11(3):156-165.

Kingston, R.S.T. and L.D. Armstrong 1951 *Creep in initially green wooden beams.* Austr.J. of Appl.Sci. 2(2):306-325.

Leicester, R.H. 1971 *A rheological model for mechano-sorptive deflections of beams.* Wood Sci. Technol. Vol.5, p.211-220.

Lu, W. and R. W. Erickson 1994 *The effects of directed diffusion on the mechano-sorptive behavior of small redwood beams.* Forest Products J., 44(1):8-14.

Mårtensson A. 1994 *Mechano-sorptive effects in wooden material.* Wood Science and Technology, 28:437-449.

Mårtensson A. 1995 *Creep behavior of structural timber under varying humidity conditions.* Journal of Strucural Engineering, Vol.120, No.9:2565-2581.

Mohager, S. and T.Toratti 1993 *Long term bending creep of wood in cyclic relative humidity.* Wood Sci. Technol. 27:49-59.

Molinski, W. and J.Raczkowski 1988 *Creep of wood in bending and non-symmetrical moistening. Holz als Roh-und Werkstoff.* 46:457-460.

Mukudai, J. 1983a *Evaluation on non-linear viscoelastic bending deflection of wood.* Wood Sci. Technol. 17:39-54.

Mukudai, J. 1983b *Evaluation of linear and non-linear viscoelastic bending loads of wood as a function of prescribed deflections.* Wood Sci. Technol. 17:203-216.

Mukudai, J. and S.Yata 1986 *Modeling and simulation of viscoelastic behavior (tensile strain) of wood under moisture change.* Wood Sci. Technol. 20:335-348.

Mukudai, J. and S.Yata 1987 *Further modeling and simulation of viscoelastic behavior(bending deflection) of wood under moisture change.* Wood Sci. Technol. 21:49-63.

Mukudai, J. and S.Yata 1988 *Verification of Mukudai's mechano-sorptive model.* Wood Sci. Technol. 22:43-58.

NDS 1991 *The National Design Specification for Wood Construction.* National Forest and Paper Association. Washington DC.

OMEGA Engineering , Load cell calibration certificate, Date: Feb. 17, 1994.

Panshin, A.J. and Zeeuw, C. de 1970 *Textbook of wood technology.* third edition, McGraw-Hill Book Company.

Pentoney, R.E. and Davidson, R.W. 1962 *Rheology and the study of wood.* For. Prod.J.12:243-248.

Philpot, T.A. and D.V. Rosowsky 1992. Effect of creep on the performance and serviceability reliability of wood, Part I, II. CE-STR-92-11, 36. School of Civil Eng., Purdue Univ., West Lafayette, Ind.

Pozgaj, A. 1982 *Deformation of wood during creep flexural load in an outdoor climate.* Holztechnologie, 23(1):36-40.

Raczkowski, J. 1969 *Effect of moisture content changes on the creep behavior of wood.* Holz-Roh-Werkstoff. 27(6):232-237.

Ranta-Maunus, A. 1975 *The Viscoelasticity of wood at varying moisture content.* Wood Sci. and Technol. Vol.9, p.189-205.

Ranta-Maunus, A. 1990 *Impact of mechano-sorptive creep to the long-term strength of timber.* Holz als Roh-und werks. 48:67-71.

SAS NLIN, SAS User's Guide 1979 edition, SAS Institute Statistical Analysis System, SAS Institute, Inc., Cary, N.C.

Schaffer, E.L. 1972 *Modeling the creep of wood in a changing moisture environment.* Wood and Fiber 3(4):232-235.

Schniewind, A.P. and J.D.Barrett 1972 *Wood as a linear orthotropic viscoelastic material.* Wood.Sci.&Technol. 6:43-57.

Senft, J.F. and S.K.Suddarth 1971 *An analysis of creep-inducing stress in Sitka spruce.* Wood Fiber 2(4):321-327.

Statgraphics, version 5 1991 STSC, Inc., Rockville, MD.

Szabo, T. and G. Ifju 1970 *Influence of stress on creep and moisture distribution in wooden beams under sorption conditions.* Wood Sci. 2(3):159-167.

Toratti, T. 1992 *Creep of timber beams in a variable environment.* Dissertation of PhD, Lab. of Structural Engn. & Buld Physics, Helsinki University of Tech, Helsinki.

Western woods use book 1973 *Design bending members.* Western Wood Products Association, Portland, Oregon.

Wood Handbook-wood as an engineering material 1987 USDA. Forest Service, Forest Products Lab. Agriculture handbook No.72.

Ylinen, A. 1965 *Prediction of the time-dependent elastic and strength properties of wood by the aid of a general nonlinear viscoelastic rheological model.* Holz als Roh-und Werkstoff. 23:193-196.

APPENDICES

Appendix A: Programs for 21X Data Logger

The following are the two programs for the 21X data logger used in collecting data for the creep experiment. The short term program is used only for the very first hour of data collection, when the interval between the two readings is one second. After that, the long term program is used, as the interval period is one hour.

Program: Creep in natural environment **(long term)**

Flag Usage: Output flag

Input Channel Usage: 1, 7, 8 differential; 5, 6 single-ended

Excitation Channel Usage: CH1: AM32, 2: LC, 3: Temp, 4: RH

Continuous Analog Output Usage:

Control Port Usage: 1: Am32

Pulse Input Channel Usage:

Output Array Definitions: Day, H:M:S, 20 Deflections, Temperature, Relative Humidity, Surface Temperature

```
*      1      Table 1 Programs
 01:   3600   Sec. Execution Interval
 01:   P30    Z=F (for CAO)
   01: 5000   F
   02: 27     Z  Loc :
02:    P21    Analog Out
   01: 1      CAO Chan (5000mV EX for defl. sensors)
```

02: 27 mV Loc

03: P20 Set Port (enable AM32, clock pulse on)

01: 1 Set high (5V)

02: 1 Port Number

04: P87 Beginning of Loop

01: 0 Delay

02: 20 Loop Count

05: P22 Excitation with Delay (clock pulse advances switch inside AM32)

01: 1 EX Chan

02: 1 Delay w/EX (units = .01 sec)

03: 0 Delay after EX (units = .01 sec)

04: 5000 mV Excitation

06: P2 Volt (DIFF)

01: 1 Rep

02: 5 5000 mV slow Range

03: 1 IN Chan

04: 1-- Loc :

05: 1 Mult

06: 0.0000 Offset

07: P95 End

08: P20 Set Port (disable AM32, clock pulse off)

01: 0 Set low

02: 1 Port Number

09: P2 Volt (DIFF) (load cell)

01: 1 Rep

02: 2 15 mV slow Range

03: 2 IN Chan

04: 21 Loc :

05: 2.8967 Mult

06: 0.0000 Offset

10: P11 Temp 107 Probe

01: 1 Rep

02: 5 IN Chan (single-ended)

03: 3 Excite all reps w/EXchan 3

04: 22 Loc : (air temperature)

05: 1 Mult

06: 0.0000 Offset

11: P4 Excite, Delay, Volt (SE)

01: 1 Rep

02: 5 5000 mV slow Range

03: 6 IN Chan (single-ended)

04: 4 Excite all reps w/EXchan 4

05: 15 Delay (units .01sec)

06: 5000 mV Excitation

07: 23 Loc : (RH)

08: .1 Mult

09: 0.0000 Offset

12: P17 Panel Temperature

01: 28 Loc :

13: P14 Thermocouple Temp (DIFF)

01: 2 Reps (number of thermocouple)

02: 1 5 mV slow Range

03: 7 IN Chan

04: 1 Type T (Copper-Constantan)

05: 28 Ref Temp Loc

06: 24 Loc :

07: 1 Mult

08: 0.0000 Offset

14: P10 Battery Voltage

01: 26 Loc :

15: P92 If time is

01: 0 minutes into a

02: 60 minute interval

03: 10 Set flag 0 (output)

16: P77 Real Time

01: 111 Day, Hour-Minute, Second

17: P70 Sample

01: 26 Rep

02: 1 Loc

18: P End Table 1

* 2 Table 2 Programs

01: 0.0000 Sec. Execution Interval

01: P End Table 2

* 3 Table 3 Subroutines

01: P End Table 3

* 4 Mode 4 Output Options

01: 1 (Tape OFF) (Printer ON)

02: 2 Printer 9600 Baud

* A Mode 10 Memory Allocation

01: 28 Input Locations

02: 64 Intermediate Locations

* C Mode 12 Security

01: 00 Security Option

02: 0000 Security Code

Input Location Assignments (with comments):

Key:

T = Table Number

E = Entry Number

L = Location Number

T: E: L:

1: 6: 1: Loc :

1: 9: 21: Loc :

1: 10: 22: Loc : (air temperature)

1: 11: 23: Loc : (RH)

1: 13: 24: Loc :

1: 14: 26: Loc :

1: 1: 27: Z Loc :

1: 12: 28: Loc :

Program: Creep in natural environment **(short term)**

Flag Usage: Output flag

Input Channel Usage: 1, 7, 8 differential; 5, 6 single-ended

Excitation Channel Usage: CH1: AM32, 2: LC, 3: Temp, 4: RH

Continuous Analog Output Usage:

Control Port Usage: 1: Am32

Pulse Input Channel Usage:

Output Array Definitions: Day, H:M:S, 20 Deflections, Temperature, Relative Humidity, Surface Temperature

* 1 Table 1 Programs

01: 1 Sec. Execution Interval

01: P30 Z=F (for CAO)

01: 5000 F

02: 27 Z Loc :

02: P21 Analog Out

01: 1 CAO Chan (5000mV EX for defl. sensors)

02: 27 mV Loc

03: P20 Set Port (enable AM32, clock pulse on)

01: 1 Set high (5V)

02: 1 Port Number

04: P87 Beginning of Loop

01: 0 Delay

02: 20 Loop Count

05: P22 Excitation with Delay (clock pulse advances switch inside AM32)

01: 1 EX Chan

02: 1 Delay w/EX (units = .01 sec)

03: 0 Delay after EX (units = .01 sec)

04: 5000 mV Excitation

06: P2 Volt (DIFF)

01: 1 Rep

02: 5 5000 mV slow Range

03: 1 IN Chan

04: 1-- Loc :

05: 1 Mult

06: 0.0000 Offset

07: P95 End

08: P20 Set Port (disable AM32, clock pulse off)

01: 0 Set low

02: 1 Port Number

09: P2 Volt (DIFF) (load cell)

01: 1 Rep

02: 2 15 mV slow Range

03: 2 IN Chan

04: 21 Loc :

05: 2.8967 Mult

06: 0.0000 Offset

10: P11 Temp 107 Probe

01: 1 Rep

02: 5 IN Chan (single-ended)

03: 3 Excite all reps w/EXchan 3

04: 22 Loc : (air temperature)

05: 1 Mult

06: 0.0000 Offset

11: P4 Excite, Delay, Volt (SE)

01: 1 Rep

02: 5 5000 mV slow Range

03: 6 IN Chan (single-ended)

04: 4 Excite all reps w/EXchan 4

05: 15 Delay (units .01sec)

06: 5000 mV Excitation

07: 23 Loc : (RH)

08: .1 Mult

09: 0.0000 Offset

12: P17 Panel Temperature

01: 28 Loc :

13: P14 Thermocouple Temp (DIFF)

01: 2 Reps (number of thermocouple)

02: 1 5 mV slow Range

03: 7 IN Chan

04: 1 Type T (Copper-Constantan)

05: 28 Ref Temp Loc

06: 24 Loc :

07: 1 Mult

08: 0.0000 Offset

14: P10 Battery Voltage

01: 26 Loc :

15: P92 If time is

01: 0 minutes into a

02: .0167 minute interval

03: 10 Set flag 0 (output)

16: P77 Real Time

01: 111 Day, Hour-Minute, Second

17: P70 Sample

01: 26 Rep

02: 1 Loc

18: P End Table 1

* 2 Table 2 Programs

01: 0.0000 Sec. Execution Interval

01: P End Table 2

* 3 Table 3 Subroutines

01: P End Table 3

* 4 Mode 4 Output Options

01: 1 (Tape OFF) (Printer ON)

02: 2 Printer 9600 Baud

* A Mode 10 Memory Allocation

01: 28 Input Locations

02: 64 Intermediate Locations

* C Mode 12 Security

01: 00 Security Option

02: 0000 Security Code

Input Location Assignments (with comments):

Key:

T = Table Number

E = Entry Number

L = Location Number

T: E: L:

1: 6: 1: Loc :

1: 9: 21: Loc :

1: 10: 22: Loc : (air temperature)

1: 11: 23: Loc : (RH)

1: 13: 24: Loc :

1: 14: 26: Loc :

1: 1: 27: Z Loc :

1: 12: 28: Loc :

Appendix B: SAS NLIN Programs and the Results

The following are the SAS NLIN programs and the results for determining the model parameters.

1. Program for K_{k0}, μ_{k0}, and μ_{v0} :

```
options ls=80;
data test;
infile ' avg. prn ';
input t s;
proc nlin;
parms
a=1000000 to 4000000 by 1000000
b=200000000 to 800000000 by 100000000
c=30000000000 to 70000000000 by 10000000000;
model
s=(722 / a) * (1 - exp(- a * t / b)) + 722 * *t / c;
der. a=-722 / a*a+ exp (- a * t / b) * (722 / a*a+722 * t / (a * b) );
der. b=- 722 * t * exp ( - a * t / b ) / b*b;
der. c=-722 * t / c*c;
```

Results of K_{0k}, μ_{k0}, and μ_{v0} :

NOTE: Convergence criterion met.

Non-Linear Least Squares Summary Statistics Dependent Variable S

Source	DF	Sum of Squares	Mean Square
Regression	3	0.00006002715	0. 00002000905
Residual	793	0.00000018311	0. 00000000023
Uncorrected Total	796	0.00006021026	
(Corrected Total)	795	0.00000162161	

Parameter	Estimate	Asymptotic Std. Error	Asymptotic 95 % Confidence Interval	
			Lower	Upper
A	3000000	2.10913884E-9	3000000	3000000
B	600000000	4.4936888E-11	600000000	600000000
C	40000000000	7.0762252E-13	40000000000	40000000000

Asymptotic Correlation Matrix

Corr	A	B	C
A	1	-0.58615444	-0.922917276
B	-0.58615444	1	0.5223854346
C	-0.922917276	0.5223854346	1

2. Program for the four-element model parameters, q_1-q_8 :

```
options ls=80;
data test;
infile 'full7.prn';
input t z s;
proc nlin;
```

```
parms
        a=-.1 to -.9 by -.8  b=-.01 to -.09 by -.08
        c=-.1 to -.9 by -.8  d=-.01 to -.09 by -.08
        q=-.1 to -.9 by -.8  r=-.01 to -.09 by -.08
        u=-.1 to -.9 by -.8  v=-.01 to -.09 by -.08;
model
s=722 / (1350000 * (1+q*z+r*z*z))+722 / (3000000 * (1+a*z+b*z*z)) * (1- exp
(-3000000 * (1+a*z +b*z*z) * t / (600000000 * (1+c*z+d*z*z))))+722 * t /
(40000000000 * (1+u*z+v*z*z));
der.a=-722 * z / (3000000 * (1+a*z+b*z*z)**2)+exp(-3000000 * (1+a*z+b*z*z)
* t / (600000000 * (1+c*z+d*z*z))) * (722 * z / (3000000 * (1+a*z+b*z*z)**2 )
+722 * t * z/ (600000000 * (1+a*z+b*z*z) * (1+c*z +d*z*z)));
der.b=- 722 * z*z / (3000000 * (1+a*z+b*z*z)**2)+exp(-3000000 *
(1+a*z+b*z*z) * t / (600000000 * (1+c*z+d*z*z))) * (722 *z*z / (3000000 *
(1+a*z+b*z*z)**2)+722 * t *z*z / (600000000 * (1+a* z+b*z*z) *
(1+c*z+d*z*z)));
der.c=- 722 * z * t / (600000000 * (1+c*z+d*z*z)**2) * exp(-3000000 *
(1+a*z+b*z*z) * t / (600000000 * (1+c*z+d*z*z)));
der.d=- 722 * z*z * t / (600000000 * (1+c*z+d*z*z)**2) * exp(-3000000 *
(1+a*z+b*z*z) * t / (600000000 * (1+c*z+d*z*z)));
der.q=- 722 * z / (1350000 * (1+q*z+r*z*z)**2);
der.r=- 722 * z*z / (1350000 * (1+q*z+r*z*z)**2);
```

der.u=- 722 * t * z / (40000000000 * (1+u*z+v*z*z)**2);

der.v=- 722 * t * z*z / (40000000000 * (1+u*z+v*z*z)**2);

Results of q_1-q_8 :

where, Q = q_1; R = q_2; A = q_3; B = q_4; C = q_5; D = q_6; U =q_7; V = q_8.

NOTE: Convergence criterion met.

Non-Linear Least Squares Summary Statistics Dependent Variable S

Source	DF	Sum of Squares	Mean Square
Regression	8	0. 00040869621	0. 00005108703
Residual	788	0. 00000307282	0. 00000000390
Uncorrected Total	796	0. 00041176903	
(Corrected Total)	795	0. 00000739246	

Parameter	Estimate	Asymptotic Std. Error	Asymptotic 95 % Confidence Interval Lower	Upper
A	0.40431105	0.2259832752	-0.0392967169	0.847918814
B	4.30426218	0.4670981700	3.3873431037	5.221181252
C	-4.09137638	1.0294953780	-6. 1122876331	-2.070465124
D	12.19630964	2.9630597137	6.3797893852	18.012829904
Q	-0.10962763	0.0507431637	-0.2092370469	-0.010018220
R	-0.11614745	0.0637495276	-0.2412885045	0.008993606
U	-2.12003507	0.1459975535	-2.4066299445	-1.833440195
V	1.31688199	0.1763087347	0.9707859134	1.662978057

Asymptotic Correlation Matrix

Corr	A	B	C	D
A	1	0.6966855703	0.248177675	-0.168686228
B	0.6966855703	1	0.1224456223	-0.154306961
C	0.248177675	0.1224456223	1	-0.062429296
D	-0.168686228	-0.154306961	-0.062429296	1
Q	-0.78129661	-0.414968635	-0.501702997	0.2458586573
R	-0.778984527	-0.69217098	-0.427540246	0.1637477441
U	0.1145818578	-0.160762067	0.3991463262	-0.137357034
V	0.1204802187	0.321890001	-0.286869307	0.0877716392

Asymptotic Correlation Matrix

Corr	Q	R	U	V
A	-0.466331111	-0.410045979	.	.
B	0.3346049643	0.2824279299	.	.
C	-0.256840423	-0.180901493	.	.
D	0.2377634615	0.1615730284	.	.
Q	1	0.9508101342	.	.
R	0.9508101342	1	.	.
U	.	.	.	.
V	.	.	.	.

3. Program for the empirical model parameters, r_1-r_4 :

```
options ls=80;
data test;
infile '07.prn';
input t z s;
proc nlin;
parms a=.1 to .9 by .2 b=.1 to .9 by .2
c=.1 to .9 by .2 d=.1 to .9 by .2;
model
s=.0000598*(1+a*z+b*z**2)*t**.202446*(1+c*z+d*z**2);
der.a=z*.0000598*t**.202446*(1+c*z+d*z**2);
der.b=z**2*.0000598*t**.202446*(1+c*z+d*z**2);
der.c=.0000598*.202446*z*(1+a*z+b*z**2)*(lnt)*t**.202446*(1+c*z+d*z**2);
der.d=.0000598*.202446*z**2*(1+a*z+b*z**2)*(lnt)*t**.202446*(1+c*z+d*z*
*2);
```

Results of r_1-r_4 :

where, A = r_1; B = r_2; C = r_3; D = r_4.

NOTE: Convergence criterion met.

Non-Linear Least Squares Summary Statistics Dependent Variable S

Source	DF	Sum of Squares	Mean Square
Regression	0	0. 00007470561	0. 00000000000
Residual	796	0. 00000000000	0. 00000000000

Uncorrected Total 796 0. 00007470561

(Corrected Total) 795 0. 00000739361

NOTE: The Jacobian is singular.

Parameter	Estimate	Asymptotic Std. Error	Asymptotic 95 % Confidence Interval	
			Lower	Upper
A	0.1000000000	0	0.10000000000	0.10000000000
B	0.3000000000	0	0.30000000000	0.30000000000
C	0.5000000000	0	0.50000000000	0.50000000000
D	0.1000000000	0	0.10000000000	0.10000000000

Asymptotic Correlation Matrix

Corr	A	B	C	D
A	.	.	.	.
B	.	.	.	.
C	.	.	.	.
D	.	.	.	.

Appendix C: Analysis on Metal Expansion and Contraction

A brass bar inside a deflection sensor and a steel frame supporting the sensor will expand or contract due to temperature changes. The brass bar is 8 inch long with one end touching on a wood beam (item 1 in Figure 3-1). The steel frame supporting the deflection sensor (item 2 in Figure 3-1) with two ends attached on the wood beam is 7 foot long in the direction perpendicular to the deflection and 2.5 inch long along the deflection direction. The thermal coefficient of linear expansion is 6.7×10^{-6} in./in.°F for the steel and 10.5×10^{-6} in./in.°F for the brass (Handbook of Chemistry and Physics 1989-1990). In order to find whether the expansion and the contraction made by the metal parts affect the accuracy of deflection measuring, the data base of the reference beam, 07D5, was chosen as an example for the following analysis:

Maximum daily temperature changes and the corresponding deflection changes during the entire experimental period were selected from the data base. The highest daily temperature change is 38.0°F, and the corresponding deflection change is 0.052 inches. During the fourteen months, the lowest daily temperature change is 3.5°F, and the corresponding deflection change is 0.002 inches.

Based on the highest daily temperature change, the elongation of the brass bar is about 0.32×10^{-2} inches, and 0.64×10^{-3} inches for the steel frame along the deflection direction, as well as 0.021 inches for the steel frame in the direction perpendicular to the deflection.

Based on the lowest daily temperature change, the elongation of the brass bar is about 0.29×10^{-3} inches, and 0.59×10^{-4} inches for the steel frame along the deflection direction, as well as 0.20×10^{-2} inches for the steel frame in the direction perpendicular to the deflection.

Only half of the elongation of the brass bar affects the deflection measuring, as one end is free. It is assumed that the steel frame attaches to the wood beam through pins, that is, the distance between one of the pins and the horizontal steel beam is 2.5 inches and is fixed. With the assumption, half of the total elongations of the horizontal steel beam, 0.011 inches for highest daily temperature change and 0.10×10^{-2} inches for lowest daily temperature change, are transferred into vertical elongations (the same direction as deflections) of 0.176 inches and 0.017 inches, respectively.

The sum of maximum elongations caused by both the brass bar and the steel frame, which affect the deflection measurement is about 0.178 inches for the largest daily temperature change and 0.017 inches for the lowest daily temperature change. Compared to the corresponding deflection changes recorded, 0.052 inches for the largest daily temperature change, and 0.002 inches for the lowest daily temperature change, the elongations are significant.

Under the assumption of pin connection with specimens, the steel frame seems to have a significant influence on deflection measurement. However, the steel frame is actually connected with the beam by friction between wood and metal. That is, the two ends of the frame may move in both horizontal and vertical directions when the frame expands or contracts due to temperature changes. This

greatly reduces the influence of thermal expansion and contraction of the steel frame to the deflection measurement.

Therefore, the major influence to the accuracy of deflection measurement is from the brass bar in deflection sensors. It is suggested that the resistance type of deflection sensor is somewhat sensitive to temperature changes, and may be replaced in future creep experiment in an uncontrolled environment. In order to obtain more accurate data in future studies for the deflections, elongations and contractions produced by the brass bar may be calculated using recorded temperature data and be finally deleted from the original deflection data.